

Aus dem Institut für Immunologie der Ludwig-Maximilians-Universität München  
Vorstand: Prof. Dr. Thomas Brocker

# **Rho GTPase Cdc42 controls invariant chain processing and MHC II loading in Dendritic Cells**

Dissertation

zum Erwerb des Doktorgrades der Naturwissenschaften (Dr. rer. nat.)  
an der Medizinischen Fakultät  
der Ludwig-Maximilians-Universität München



vorgelegt von  
**Anna Schulz, geb. Wähe**  
aus Darmstadt

2013

**Gedruckt mit Genehmigung der Medizinischen Fakultät  
der Ludwig-Maximilians-Universität München**

Betreuer: Prof. Dr. Thomas Brocker

Zweitgutachter: Prof. Dr. Patrick A. Baeuerle

Dekan: Prof. Dr. med Dr.h.c. Maximilian Reiser,  
FACR, FRCR

Tag der mündlichen Prüfung: 06.11.2013

# AUTHOR'S DECLARATION

Ich versichere hiermit ehrenwörtlich, dass die vorgelegte Dissertation „Rho GTPase Cdc42 controls invariant chain processing and MHC II loading in Dendritic Cells“ von mir selbständig und ohne unerlaubte Hilfe angefertigt wurde. Ich habe mich dabei keiner anderen als der von mir ausdrücklich bezeichneten Hilfen und Quellen bedient.

Die Dissertation wurde in der jetzigen oder ähnlichen Form bei keiner anderen Hochschule eingereicht und hat auch noch keinen anderen Prüfungszwecken gedient.

Anna Schulz

This work contains results presented in the following publication:

**Schulz, A.** et al. Rho GTPase Cdc42 controls invariant chain processing and MHC II loading in Dendritic Cells. Manuscript in preparation.

This publication was also achieved and will be cited as "Paper I":

Luckashenak, N.\*, **Wähe, A.\***, Breit, K., Brakebusch, C., Brocker, T. 2013. Rho-family GTPase Cdc42 controls migration of Langerhans cells *in vivo*. *J Immunol.* 190:27-35. \*equal contribution

## ABBREVIATIONS

SI Units were applied as described elsewhere.

APC	1. antigen presenting cell 2. allophycocyanin
BDP	F-Bar domain protein
BMDC	bone marrow-derived dendritic cell
BSA	bovine serum albumin
CIITA	MHC class II transactivator
ca	constitutively active
CBA	cytometric bead array
CCR7	chemokine (C-C motif) receptor 7
CCV	clathrin coated vesicle
CD	cluster of differentiation
cDC	conventional dendritic cell
Cdc42	cell division cycle 42
CDE	clathrin dependent endocytosis
cDNA	complementary DNA
cTEC	cortical epithelial cell
CDP	common DC precursor
CFSE	carboxyfluorescein-diacetate-succinimidylester
CIE	clathrin independent endocytosis
CLIP	class II-associated Ii peptide
CMP	common myeloid precursor
ConB	concanamycin B
CP	crossing point
CTL	cytotoxic T lymphocyte
Ctsl	cathepsin L
Ctss	cathepsin S
CytD	cytochalasin D
DAPI	4',6-diamidino-2-phenylindole
dNTP	desoxyribonucleotidtriphosphate
DC	dendritic cell
DMSO	dimethyl sulfoxide

## ABBREVIATIONS

dn	nominant negative
DNA	desoxyribonucleic acid
DTT	dithiothreitol
DQ-OVA	non-fluorescent self-quenched conjugate of OVA
dsRNA	double stranded RNA
ECL	enhanced chemiluminescence
EDAC	1-Ethyl-3-(3-Dimethylaminopropyl)carbodiimide
EDTA	ethylenediaminetetraacetic acid
ER	endoplasmic reticulum
FACS	fluorescence activated cell sorter
F-actin	filamentous actin
FCS	fetal calf serum
FITC	fluorescein isothiocyanate
flx	floxed
Flt3L	Flt3 Ligand
for	forward
FSC	forward scatter
GAP	GTPase-activating protein
Gapdh	glyceraldehyde-3-phosphate dehydrogenase
GDI	guanine nucleotide-dissociation inhibitor
GEF	guanine exchange factor
GM-CSF	granulocyte-macrophage colony stimulating factor
GO	Gene Ontology
GTPase	GTP-binding protein
H2-M	H2-M beta 2 chain
HEPES	4-(2-hydroxyethyl)-1-piperazineethanesulfonic acid
Hip1r	Huntingtin interacting protein 1 related
HIV	human immunodeficiency virus
HPRT	hypoxanthine-guanine phosphoribosyltransferase
HRP	horseradish peroxidase
IFN	interferon
Ig	Immunoglobulin
Ii	invariant chain
IL	interleukin
kb	kilobase

## ABBREVIATIONS

kDa	kilo Dalton
ko	knockout
LAMP1	lysosome-associated membrane glycoprotein 1
LatB	latrunculin B
LC	Langerhans cell
LCA	leucocyte common antigen
LC-MSMS	liquid chromatography-tandem mass spectrometry
LPS	lipopolysaccharide
MIIC	MHC II loading compartment
M6pr	mannose-6-phosphate receptor
MACS	magnetic cell sorting
MAPK	Mitogen-activated protein kinase
M-CSF	macrophage colony stimulating factor
mDC	migratory DC
MES	compound 2-(N-morpholino)ethanesulfonic acid
MFI	mean fluorescent intensity
MHC	major histocompatibility complex
MLN	mesenteric lymph node
MT	microtubule
MTOC	microtubule organizing center
MVB	multi vesicular bodies
mRNA	messenger RNA
NF- $\kappa$ B	nuclear factor kappaB
NK cell	natural killer cell
Noco	nocodazole
NP-40	Nonidet (octyl phenoxy polyethoxy ethanol) P-40
OVA	ovalbumin
PBS	phosphate buffered saline
PBMC	peripheral blood mononuclear cell
PCR	polymerase chain reaction
pDC	plasmacytoid dendritic cell
PE	phycoerythrin
PerCP	peridinin-chlorophyll-a protein
qPCR	quantitative PCR
PKC	protein kinase C

## ABBREVIATIONS

PMSF	phenylmethylsulfonyl fluoride
Rac1	Ras-related C3 botulinum toxin substrate 1
rDC	resident DC
rev	reverse
RhoA	transforming protein RhoA
RNA	ribonucleic acid
SA	streptavidin
SDS	sodium dodecyl sulfate
SEM	standard error of the mean
SIINFEKL	OVA <sub>257-264</sub>
SSC	side scatter
TAP	transporter associated with antigen processing
TCR	T cell receptor
T <sub>H</sub> cell	T helper cell
TEMED	tetramethylethylenediamin
TGF- $\beta$	transforming growth factor beta
TGN	trans-Golgi network
TLR	toll like receptor
TNF	tumor necrosis factor
vs.	versus
WASP	Wiskott-Aldrich syndrome protein
wt	wild type

# TABLE OF CONTENTS

AUTHOR'S DECLARATION .....	iii
ABBREVIATIONS .....	v
TABLE OF CONTENTS .....	ix
1 SUMMARY .....	1
2 ZUSAMMENFASSUNG .....	2
3 INTRODUCTION .....	3
3.1 Dendritic cells as antigen presenting cells .....	3
3.1.1 DCs – sentinels of the immune system .....	3
3.1.2 DC maturation .....	4
3.1.3 DC antigen presentation .....	6
3.1.3.1 Uptake of soluble and particulate antigens .....	6
3.1.3.2 Antigen cross-presentation .....	8
3.1.3.3 MHC II antigen presentation: A role for invariant chain .....	9
3.1.3.4 DC - T cell interaction .....	10
3.2 Small Rho GTPase Cdc42 and its cellular functions .....	11
3.2.1 Small Rho GTPases .....	11
3.2.2 Constraints in studying Rho GTPases .....	12
3.2.3 Cdc42 contributes to actin dynamics .....	12
3.2.4 Rho GTPases are targets of bacterial toxins .....	14
3.2.5 Functions of Cdc42 in DCs .....	14
3.3 Aims of the study .....	17
3.3.1 Characterization of a DC-specific knockout for Cdc42 .....	17
3.3.2 Elucidation of the mechanism by which Cdc42 controls MHC II antigen presentation in DCs .....	17
3.3.3 Examination of MHC II loading in DC subsets .....	17
4 MATERIALS AND METHODS .....	18
4.1 Materials .....	18
4.1.1 Antibodies .....	18
4.1.2 Chemicals .....	20
4.1.3 Consumables .....	20
4.1.4 Devices .....	20
4.1.5 Inhibitors .....	21
4.1.6 Media and solutions .....	21
4.1.7 Mouse strains .....	24

## TABLE OF CONTENTS

4.1.8	Fluorescent probes, proteins, peptides and primers .....	24
4.2	Methods.....	25
4.2.1	Cellular and immunological methods.....	25
4.2.1.1	Generation of bone marrow-derived dendritic cells (BMDCs).....	25
4.2.1.2	Flow cytometry – Fluorescence activated cell sorting (FACS).....	25
4.2.1.3	Antigen uptake & presentation .....	26
4.2.1.4	Antigen processing.....	26
4.2.1.5	Inhibitor treatment of cultured cells .....	27
4.2.1.6	Internalization of invariant chain from the cell surface of DCs.....	27
4.2.1.7	Cytometric Bead Array (CBA).....	28
4.2.1.8	Magnetic cell sorting (MACS).....	28
4.2.1.9	Harvesting organs from mice .....	28
4.2.1.10	Isolation of cells from organs.....	29
4.2.1.11	CFSE labeling of T cells.....	29
4.2.1.12	Immunization and adoptive cell transfer.....	30
4.2.2	Molecular biology and biochemical methods .....	30
4.2.2.1	Mouse genotyping.....	30
4.2.2.2	RNA isolation and complementary DNA (cDNA) synthesis .....	31
4.2.2.3	Quantitative PCR (qPCR) .....	31
4.2.2.4	Preparation of lysates for Western blot .....	32
4.2.2.5	SDS Page and Western blot.....	33
4.2.2.6	Western blot quantification.....	34
4.2.3	Quantitative proteomics and data analysis .....	34
4.2.3.1	Quantitative proteomics .....	34
4.2.3.2	Label-free quantification.....	34
4.2.3.3	Web-based evaluation of identified proteins .....	35
4.2.4	Statistical analysis.....	35
5	RESULTS.....	36
5.1	Cdc42 maintains DC functions critical for the induction and control of immune responses.....	36
5.1.1	A novel DC-specific knockout for Cdc42.....	36
5.1.2	Phenotype of Cdc42-ko BMDCs.....	37
5.1.3	Cdc42 is required for uptake, but not processing of soluble antigen ...	40
5.1.4	Cdc42-ko DCs fail to induce proper immune responses to OVA-specific T cells.....	42

5.2	The proteome of Cdc42-ko BMDCs .....	44
5.2.1	An unbiased proteomics screen.....	44
5.2.2	Pathways affected upon Cdc42 removal.....	45
5.2.3	Cdc42-ko DCs show abnormalities in lysosomal protein composition...	47
5.3	Cdc42 controls invariant chain (Ii) processing and thus, MHC II loading in an actin-dependent manner .....	49
5.3.1	Confirmation of the proteomics screen: Cdc42-ko DCs lack lysosomal proteases .....	49
5.3.2	The lack of Cathepsin S in Cdc42-ko BMDCs causes an MHC II loading defect by inhibiting Ii processing .....	50
5.3.3	Functional actin dynamics are required for both lysosomal integrity and Ii degradation .....	53
5.3.4	Cdc42 acts via the Arp2/3 complex on the actin cytoskeleton, with no impact on Ii processing .....	58
5.3.5	BMDCs defective for clathrin-mediated vesicle budding secrete mature CtSI into culture supernatants.....	61
5.3.6	Summary of processes affected upon Cdc42 knockout with implications for MHC II loading .....	63
5.4	Phenotype of Cdc42-ko mice .....	64
5.4.1	DC subsets in spleen and lymph nodes of Cdc42-ko mice.....	64
5.4.2	Antigen presentation of OT-II peptide is impaired <i>in vivo</i> .....	64
5.4.3	DC subsets in Cdc42-ko mice differentially regulate Ii expression.....	66
6	DISCUSSION.....	68
6.1	Cdc42 controls DC-mediated immunity .....	68
6.2	Loss of Cdc42 affects actin dynamics and vesicle trafficking .....	74
6.3	MHC II loading requires Cdc42 and a functional actin network .....	75
6.4	<i>In vivo</i> DC subsets differentially regulate MHC II loading .....	81
6.5	Conclusion & Outlook .....	83
7	APPENDIX .....	85
7.1	Gene Ontology (GO) term analyses .....	85
8	REFERENCES.....	89
9	CURRICULUM VITAE .....	I
10	PUBLICATIONS .....	III
11	ACKNOWLEDGMENTS.....	IV

# 1 SUMMARY

Cell division cycle 42 (Cdc42) is a member of the Rho GTPase family and has pivotal functions in actin organization, cell migration and proliferation. Furthermore, Cdc42 has been shown to regulate dendritic cell (DC) functions critical for the initiation and control of immune responses. For example, there is evidence that Cdc42 plays a role in antigen uptake, migration and the control of T cell stimulation. However, as constraints for most of these studies, Cdc42 has been studied using dominant negative and constitutively active mutants with possible unspecific effects on other members of the Rho GTPase family like Rac1 and RhoA. Thus, the actual contribution of Cdc42 to these processes might not have been fully addressed. Here we used a LoxP/Cre-recombinase approach to knock out Cdc42 selectively in DCs. Using bone-marrow derived dendritic cells (BMDCs) we confirm that Cdc42 contributes to antigen uptake and the presentation of whole protein antigen. Furthermore, we demonstrate that pre-processed antigenic peptides are inefficiently presented by Cdc42-ko DCs, as Cdc42 regulates intracellular levels of lysosomal proteases required for invariant chain (Ii) processing and thus, specifically MHC II loading. As a result, Ii was not efficiently degraded in Cdc42-ko BMDCs and accumulated on the surface of these cells in an actin-dependent manner, possibly as a result of misrouting of lysosomal contents into culture supernatants. Our results propose that Cdc42 controls an actin-dependent mechanism, which regulates MHC II loading, antigen presentation and thus, DC-mediated immunity.

This study is important for understanding basic mechanisms in DCs required for the initiation of adaptive immune responses. Cdc42 is required for efficient antigen presentation and therefore crucial to efficiently eliminate pathogens. Understanding how Cdc42 contributes to antigen presentation might lead to new therapeutic strategies to manipulate DC function in fighting infections, diseases and tumors.

## 2 ZUSAMMENFASSUNG

*Cell Division Cycle 42* (engl., Cdc42) reguliert die Polymerisierung von Aktin, die Migration und die Proliferation von Zellen. In dendritischen Zellen reguliert Cdc42 unter Anderem die Aufnahme von Antigenen, deren Transport von der Peripherie zu drainierenden lymphatischen Organen, sowie die T Zell-Aktivierung. Dadurch spielt Cdc42 eine wichtige Rolle bei der Initiierung und Kontrolle von Immunantworten.

In vorangegangenen Arbeiten wurde Cdc42 vornehmlich unter Zuhilfenahme von Proteinmutanten studiert, die in der Zelle eine Aktivierung von Cdc42 unterdrückten oder konstitutiv aktiv vorlagen. Da diese Mutanten möglicherweise nicht ausschließlich Cdc42, sondern auch andere Rho GTPasen, wie z.B. Rac1 und RhoA beeinflussen, entschieden wir uns für einen spezifischen *knockout*, der ein Fehlen von Cdc42 in dendritischen Zellen verursacht.

Unter Verwendung von Cdc42-defizienten aus dem Knochenmark differenzierten dendritischen Zellen, konnten wir *in vitro* zeigen, dass Cdc42 sowohl bei der Aufnahme von Antigenen, als auch bei deren Präsentation zu CD4<sup>+</sup> und CD8<sup>+</sup> T Zellen eine Rolle spielt. Interessanterweise war in Cdc42<sup>-/-</sup>-dendritischen Zellen auch die MHC Klasse II-abhängige Präsentation von bereits prozessierten Peptiden vermindert, als Folge einer Fehlsortierung der für die Beladung von MHC Klasse II benötigten lysosomalen Proteasen: Cdc42-defiziente dendritische Zellen zeigten eine unvollständige Prozessierung der *Ia antigen-associated invariant chain* (engl., Ii) von MHC Klasse II, wodurch der Austausch von Antigenen auf MHC Klasse II nicht effizient stattfinden kann. Ii gebundene MHC Klasse II Moleküle akkumulierten somit in einem Aktin-abhängigen Mechanismus an der Zelloberfläche von Cdc42-defizienten dendritischen Zellen- mit Auswirkungen auf die Beladung und somit die MHC Klasse II-abhängige Präsentation von Antigenen und somit die Effizienz der Immunantwort.

Diese Ergebnisse zeigen, dass Cdc42 benötigt wird, um auf exogene Antigene zu reagieren und eine effiziente adaptive Immunantwort einzuleiten. Somit ist Cdc42 möglicherweise notwendig um Pathogene effizient zu bekämpfen. Cdc42-regulierte Prozesse könnten demnach von essentieller Bedeutung für die Bekämpfung von Infektionen, Krankheiten und auch Tumore durch dendritische Zellen sein.

## 3 INTRODUCTION

### 3.1 Dendritic cells as antigen presenting cells

#### 3.1.1 DCs – sentinels of the immune system

Dendritic cells (DCs) are professional antigen presenting cells (APC) with pivotal roles for the induction of both adaptive and innate immune responses. Their competence is based primarily on their ability to capture and present antigens to T cells, thereby regulating T cell functions in immunity and tolerance (reviewed in (1-3)). Depending on the nature of environmental stimuli, DCs “decide” between triggering immunity by stimulating immunogenic T cells and NK cells, and tolerance by inducing deletion, anergy or regulatory T cell (Treg) differentiation.

DCs originate from a common myeloid precursor (CMP) in the bone marrow that becomes committed to the DC lineage upon encountering a combination of the cytokines granulocyte-macrophage colony stimulating factor (GM-CSF), macrophage colony stimulating factor (M-CSF), Flt3 Ligand (Flt3L) and transforming growth factor beta (TGF- $\beta$ 1) (reviewed in (4)). This common DC precursor (CDP) gives rise to precursors of conventional DCs (cDCs) termed pre-DCs and plasmacytoid DCs (pDCs) in the bone marrow. Both, pre-DCs and pDCs leave the bone marrow, enter the blood stream and seed lymphoid organs such as spleen, lymph nodes and Peyer’s patches, where they differentiate into one of the multiple DC subsets (5-7), based on the tissue-specific expression of cytokines and transcription factors. Whereas cDCs are very effective in antigen capture and presentation, pDCs have a limited potential to present extracellular tissue antigens and function mainly in producing large amounts of type I interferons in response to viruses (reviewed in (8)). However, most DCs share a high expression of the integrin CD11c, but may differ in expression levels of major histocompatibility complex (MHC) II or co-stimulatory molecules CD80 and CD86.

DCs comprise multiple subsets with distinct localizations throughout the body (9), sampling the environment for both self and foreign antigens whilst developing functional specifications due to environmental stimuli, such as cytokines. Tissue-resident DCs enter lymphoid tissues as pre-DCs released from the bone marrow and differentiate inside the tissues. Migratory DC subsets localized in peripheral

non-lymphoid tissues act as sentinels of the immune system and migrate directionally via the lymphatic vessels into the T cell area of lymph nodes to initiate immune responses (10, 11). Tissue-resident DCs, on the other hand, acquire antigens from migratory DCs, or by sampling blood or lymph and are key players in producing cytokines and priming T cells (12).

Half of the DCs present in lymph nodes are resident DCs, the other half migratory DCs that, in the absence of infection, migrate spontaneously through the lymphatic vessels. Depending on the local distribution, lymph nodes drain different organs and tissues and therefore contain specialized migratory DC subsets. For example, cutaneous lymph nodes drain the skin and therefore include migratory DC subsets such as Langerhans cells (CD11c<sup>+</sup>MHC II<sup>+</sup> expressing Langerin and EpCam) residing in the epidermis, Langerin<sup>+</sup> dermal DCs (MHC II<sup>+</sup>CD103<sup>+</sup>Langerin<sup>+</sup>) or Langerin<sup>-</sup> dermal DCs (MHC II<sup>+</sup>CD103<sup>-</sup>Langerin<sup>-</sup>), the latter two both residing in the dermis of the skin (13). Mesenteric lymph nodes (MLN), on the other hand, drain the gut and contain migratory DC subsets originating from the lamina propria that can be characterized based on the expression of CD11b and CD103 (CD11c<sup>+</sup>MHC II<sup>+</sup>CD103<sup>+</sup>CD11b<sup>-</sup> or CD11b<sup>+</sup> DCs) (14).

Mouse spleens, as opposed to lymph nodes, are exclusively comprised of blood-derived, resident DCs. Splenic DCs subsets can be distinguished based on the expression of CD4 and CD8 $\alpha$  (CD4<sup>+</sup> and CD8<sup>+</sup> DCs and double-negative DCs) and have distinct, cell type-specific functions. Depending on the nature of antigen specific pathways of entry are triggered in these splenic DC subsets that lead to the induction of CD8<sup>+</sup> or CD4<sup>+</sup> T cell responses. The induction of CD8<sup>+</sup> T cell responses involves the presentation of exogenously derived antigens on MHC I molecules, a process termed cross-presentation (reviewed in (15)). CD4<sup>+</sup> T cell responses, on the other hand, require the presentation of exogenously derived antigens in the context of MHC II (reviewed in (12)).

### 3.1.2 DC maturation

DCs residing in tissues are of an immature phenotype expressing low amounts of surface MHC I, MHC II and costimulatory molecules (e.g. CD86) and have a high potential to take up antigen. However, upon migration to draining lymph nodes

DCs mature and develop their full potential to activate T cells. DC maturation is a signaling switch typically turned on upon microbial or viral-derived external stimuli, such as lipopolysaccharide (LPS), CpG DNA or dsRNA (16). However, DC maturation can also be triggered by pro-inflammatory cytokines, such as tumor necrosis factor alpha (TNF $\alpha$ ) and interleukin 1 beta (IL-1 $\beta$ ) or ligation of CD40 and a variety of noninflammatory, pathogen-unrelated stimuli (16, 17).

Besides triggering both nuclear factor kappaB (NF- $\kappa$ B) activation and the production of pro-inflammatory cytokines, the “activation” of DCs leads to substantial changes of cell shape, mediated by rearrangements of the actin cytoskeleton. These changes include a shut down of the cell’s potential to take up antigens via macropinocytosis, pinocytosis and receptor-mediated endocytosis. However, a recent publication challenged the belief that all mechanisms of endocytosis are affected upon DC maturation by showing that uptake via the CD205 receptor (DEC-205) was still functional in LPS-treated, mature BMDCs (18). DC maturation also includes the transport of antigen-loaded MHC I as well as MHC II molecules to the cell surface for recognition by T cells (17) (reviewed in (16)). MHC II antigen presentation in mature DCs is accompanied by a downregulation of transcription of the transcriptional coactivator of MHC II genes, the MHC class II transactivator (CIITA). Additionally, the formation of MHC II-peptide complexes in lysosomal compartments is downregulated due to a decreased endosomal pH within the endocytic system, as a result of an increased assembly of a proton pump (for references, see (6)). MHC II-peptide complexes are translocated to the plasma membrane and cell surface MHC II, which is constantly recycling on immature DCs, is stabilized at the plasma membrane as a result of decreased ubiquitination of the MHC II  $\beta$  chain (19).

Besides the regulation of MHC expression, DC maturation also includes the upregulation of B7 family members on DCs, which include CD80 and CD86 and provide co-stimulation. Additionally, DCs produce and secrete pro-inflammatory cytokines such as IL12 and interferon alpha (IFN $\alpha$ ) that constitute additional signals to prime T cells (2). All these processes contribute to fully enable DCs as potent inducers of adaptive immune responses.

### 3.1.3 DC antigen presentation

DCs are capable of different strategies to present self- and foreign antigens to T cells, thereby inducing tolerogenic or immunogenic immune responses. Endogenous antigens are loaded onto MHC I molecules, whereas exogenously derived antigens are presented by the classical MHC II antigen pathway. Besides these two “classical” antigen presentation pathways two “non-classical” pathways also exist, which include the presentation of exogenously derived antigens on MHC I molecules (cross-presentation) (20) and autophagy of cytosolic components for presentation on MHC II (21).

In order to present exogenously derived antigens, DCs need to take up, process and load these antigens onto MHC I as well as MHC II molecules. This chapter’s focus will be on the mechanisms involved in MHC I- or MHC II-dependent presentation of exogenously derived antigens by DCs contributing to an adaptive, immunogenic immune response.

#### 3.1.3.1 Uptake of soluble and particulate antigens

Immature DCs constitutively sample their environment using three major routes of antigen uptake: clathrin-independent endocytosis (CIE), clathrin-dependent endocytosis (CDE) and phagocytosis. Whereas CIE and CDE are mechanisms required for fluid-phase uptake, phagocytosis mediates the uptake of large particulate antigens, e.g. dead cells. All pathways of antigen entry into cells are

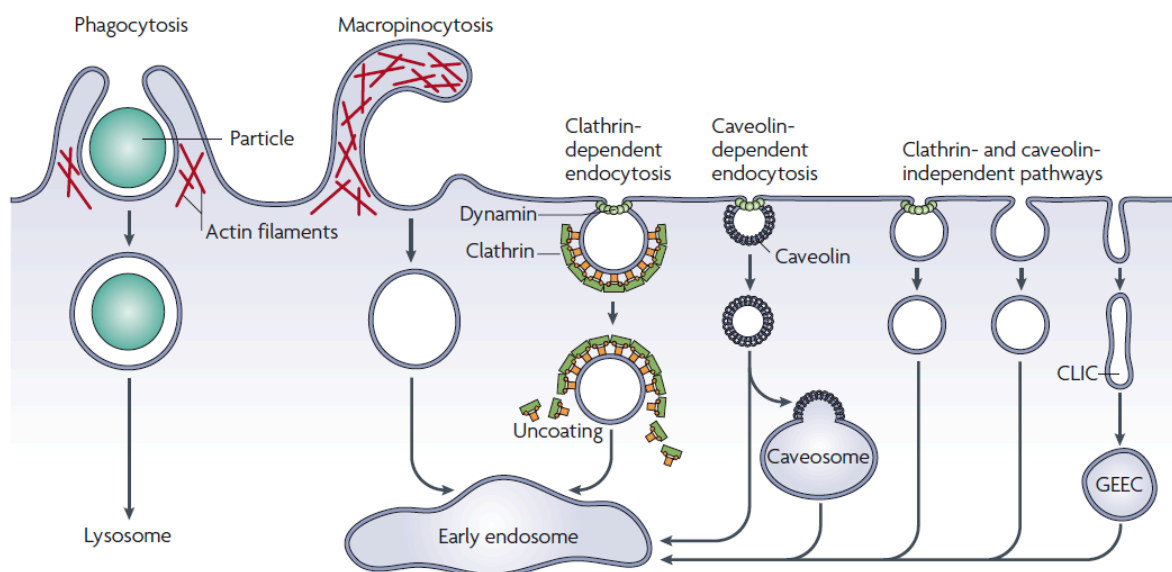


**Figure 1: Pathways of entry into cells.**

CLIC, tubular intermediates of clathrin and dynamin-independent carriers; GEEC, glycosyl phosphatidylinositol-anchored protein enriched early endosomal compartments. Figure from Mayor & Pagano, 2007 (22).

summarized in Figure 1 (figure from (22), also reviewed in (23)). For this study relevant pathways will be described in the following section.

### **Uptake of soluble antigens**

Both CDE and CIE constitute mechanisms for fluid-phase entry into cells. The latter includes macropinocytosis, pinocytosis and mechanisms dependent or independent of caveolin and/or dynamin (summarized in Figure 1).

The majority of soluble antigens are taken up by clathrin-independent macropinocytosis, a mechanism during which DCs form protrusions, thereby engulfing large amounts of the fluid phase. This process is highly actin-dependent: active actin polymerization at the site of entry is required to mechanically push the plasma membrane. Macropinocytosis is constitutively active in immature DCs and is shut down upon DC activation. However, this uptake mechanism is rather unspecific and results in the acquisition of large volumes of surrounding fluid. A variation of this process, pinocytosis allows for small volume fluid-phase uptake. A prominent example for macropinocytosis is ovalbumin (OVA) uptake by DCs, a model antigen, which does not trigger a specific pathway of entry.

DCs can also capture antigens through receptor-engagement followed by the internalization of these receptor-bound antigens (reviewed in (24)). Depending on the receptor triggered, this process can be either clathrin-dependent or clathrin-independent; the latter constitutes a minor route for some selective receptors including Wnt and Notch receptors (reviewed in (25)). However, CDE is the major pathway, by which receptor-engaged antigens are internalized. After formation of a clathrin coat surrounding parts of the plasma membrane, receptors are sequestered into these structures and then trigger the recruitment of accessory proteins required for membrane bending, vesicle formation and vesicle budding. Proteins involved in CDE include plasma-membrane deforming F-Bar proteins (FCHo), actin-nucleating proteins (e.g. neutral Wiskott-Aldrich syndrome protein (N-WASP)), proteins that connect the emerging vesicle with the pre-existing actin lattice (e.g. Huntingtin interacting protein 1 related (Hip1r)) and finally proteins that actively nucleate actin filaments (e.g. the actin related protein-2/3 (Arp2/3)

complex and cell division cycle 42 protein (Cdc42)) to mechanically separate the vesicle from the plasma membrane (26).

Interestingly, clathrin-mediated vesicle budding also takes place at the trans-Golgi network (TGN), where it serves to supply the endosomal system with lysosomal proteases in a mannose-6-phosphate receptor (46kDa M6pr)- and actin-dependent manner. M6pr-mediated clathrin-dependent vesicle budding is required for antigen presentation, since it constitutes the major route of protease exit from the TGN (27). Lysosomal proteases that travel in an M6pr-dependent manner are for example cathepsins, required for the processing of antigens as well as MHC II maturation, as described in chapter 3.1.3.3.

### **Uptake of particles and cells**

DCs are not only capable of fluid-phase uptake, but can also take up of large particles ( $>0.5 \mu\text{m}$ ), such as dead or dying cells, environmental debris or pathogenic bacteria. This process is termed phagocytosis and includes an extensive reshaping of the plasma membrane and active actin polymerization at sites of entry. Phagocytosis can either be FC-receptor-mediated (here the cell “reaches” for particles by forming protrusions) or complement-mediated (here particles “sink” into cells) and may also take place inside the cell (autophagy) to engulf cytosolic material, organelles and microorganisms (all reviewed in (28)). In adaptive immunity, DC phagocytosis is important for the acquisition of bacterial antigens that are presented to immunogenic T cells required for pathogen clearance. Receptor engagement triggered by bacteria induces the production of pro-inflammatory cytokines and chemokines that direct adaptive immunity towards local and systemic responses.

### **3.1.3.2 Antigen cross-presentation**

As opposed to classical, direct MHC I presentation of endogenous antigens, antigen cross-presentation provides the presentation of exogenously derived antigens in the context of MHC I, which may include immune complexes, bacteria, parasites as well as cellular antigens. Antigen-loaded MHC I complexes are recognized by naïve  $\text{CD8}^+$  T cells, contributing to activation, expansion and differentiation of these T cells into effectors including cytotoxic T lymphocytes (CTL). CTL are capable of destroying virus-infected cells, tumor cells or APCs infected with intracellular parasites. The term cross-priming refers to antigen cross

over from a donor cell to the host APC, which then initiates MHC I-restricted CTL priming.

The mechanism of antigen cross-presentation has been extensively reviewed (20, 29, 30). In brief, antigens are internalized into specialized compartments dedicated to the generation of MHC I restricted peptides. These compartments can be phagosome-endoplasmic reticulum (ER) hybrid compartments (for references, see (20)) and generally feature a basal pH. In these compartments, endocytosed proteins are either proteolytically degraded, or exported to the cytosol for degradation by the proteasome, followed by transporter associated with antigen presentation (TAP)-dependent re-import into the vesicle. The peptides are loaded onto either newly synthesized MHC I molecules originating from the ER, or recycling MHC I complexes re-internalized from the plasma membrane, followed by transport of peptide-loaded MHC I complexes to the cell surface.

### 3.1.3.3 MHC II antigen presentation: A role for invariant chain

Apart from cross-presentation, DCs use a mechanism termed MHC II antigen presentation to present exogenously derived antigens in the context of MHC II to CD4<sup>+</sup> T cells.

Figure 2 summarizes the basic pathway of MHC II loading (from (31)). In brief, a trimer of MHC II  $\alpha$ - and  $\beta$ -chains assembles in the ER with the assistance of three

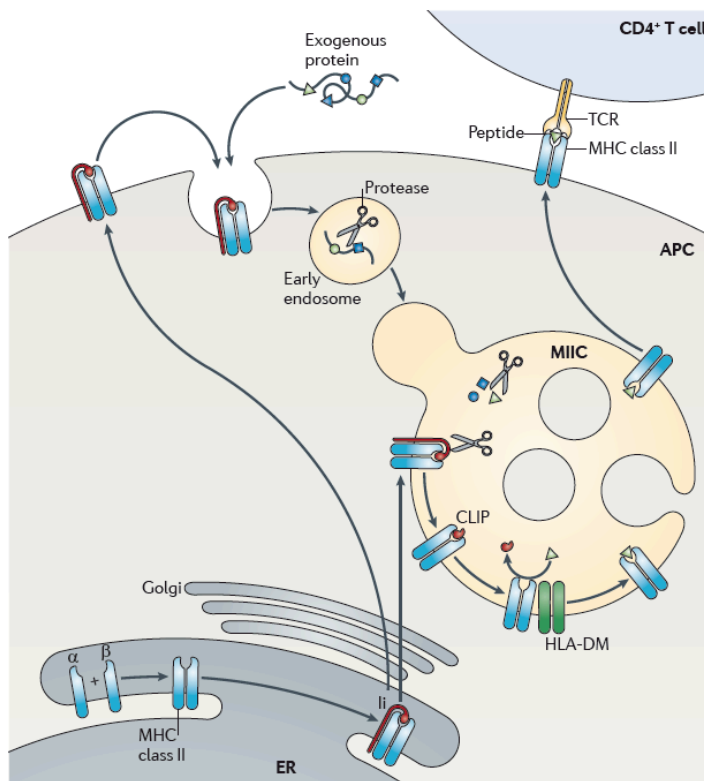


**Figure 2: The basic MHC class II antigen presentation pathway.**

For description, see text. ER, endoplasmic reticulum; APC, antigen-presenting cell; MIIC, MHC II loading compartment; TCR, T cell receptor; Ii, invariant chain. Figure from Neeffjes et al., 2011 (31).

invariant chain (Ii) molecules. This Ii-MHC II heterotrimer travels through the Golgi to the MHC class II loading compartment (MIIC), a process mediated by two dileucine sorting motifs in the N-terminal of Ii (32-34). Ii-MHC II is transported either directly to the MIIC, or via the plasma membrane followed by rapid re-internalization. Along the endocytic route, Ii is processed until only the class II-associated Ii peptide (CLIP) occupies the MHC II binding groove, which in the MIIC can be exchanged for the antigenic peptide by the chaperone H2-M (HLA-DM in humans). Ii processing proceeds from C-terminal to N-terminal direction, giving rise to degradation intermediates of different sizes that will be introduced in chapter 5.3.2 in more detail. "Mature", peptide-loaded MHC II molecules are then transported from the MIIC to the plasma membrane, where peptides are presented to CD4<sup>+</sup> T cells.

The soluble, lysosomal proteases cathepsin S (Ctss) and cathepsin L (Ctsl) are key players in Ii processing and thus MHC II loading (35-40). However, activity of these two proteases varies between cell types and it may only be noted here that Ctss is the major protease in DCs that conducts the final step in Ii degradation.

The nature of lysosomes is important for MHC II antigen presentation, because these compartments supply the MIIC with proteases required for Ii as well as antigen processing. Supply of lysosomes with soluble proteases such as cathepsins is M6pr-dependent (41, 42), whereas lysosomal membrane proteins like lysosome-associated membrane glycoprotein-1 (LAMP-1) are transported in an M6pr-independent manner (for a review in lysosome biogenesis, see (27)). However, both pathways depend on clathrin-mediated vesicle budding (see chapter 3.1.3.1). Cathepsins leave the TGN as precursors and are processed into their mature forms upon decreasing pH as they travel along the endocytic route. Endosomal acidification depends on the V-ATPase proton pump, which translocates protons into the endosomal lumen. M6pr translocate from these acidifying endosomes and are recycled back to the TGN. Resulting lysosomes lack M6pr, are rich in lysosomal membrane proteins and have a pH below five (43), ready to provide their lytic functions.

#### **3.1.3.4 DC - T cell interaction**

DC-T cell interaction includes the formation of an immunological synapse that includes MHC-T cell receptor (TCR) engagement (termed signal 1) in the absence or presence of costimulation (termed signal 2). Depending on the type of effector

function, DCs deliver an additional signal (termed signal 3), which determines T cell differentiation. For example, IL-12 secretion as a third signal promotes either T<sub>H</sub>1-cell or CTL development (2). Which kind of response is triggered, depends on the DC's maturation status regarding the expression of costimulatory molecules CD40, CD80 and CD86, and both its ability to form functional cell-cell contacts and trigger third signal responses, such as secretion of pro-inflammatory cytokines for CTL differentiation. All those mechanisms contribute to the DC's potential to initiate effective immune responses.

## **3.2 Small Rho GTPase Cdc42 and its cellular functions**

### **3.2.1 Small Rho GTPases**

Small guanosine triphosphate-binding proteins (GTPases) are central regulators of a variety of local intracellular events. They act as molecular switches cycling between an active GTP-bound and inactive GDP-bound state. Nucleotide exchange on GTPases is a tightly controlled process that involves different classes of proteins: guanine nucleotide exchange factors (GEFs) promote the exchange of GDP for GTP from these molecules, GTPase-activating proteins (GAPs) increase the intrinsic GTPase activity of their targets, thereby promoting the hydrolysis of GTP back to GDP inducing an inactive GDP-bound state, and guanine nucleotide-dissociation inhibitors (GDIs) that sequester GTPases away from their regulators and targets at their membrane sites of action, by masking their prenyl membrane binding groups (44). Over 150 GTPases have been identified in humans including the Ras, Rab, Arf and Rho family members (45); each member triggering specific signaling cascades tightly controlled through the expression of its effectors in the respective cell types.

Mammalian Rho GTPases comprise a family of 20 intracellular signaling proteins with well-documented functions in regulating the actin cytoskeleton. Active GTP-bound Rho GTPases target downstream effector proteins triggering signaling cascades that lead to the reorganization of the cell's cytoskeleton with implications for vesicle transport, microtubule dynamics, cell polarity and filopodia formation, the latter two required for cell migration. The three most prominent and best-characterized Rho GTPases are Cdc42, Ras-related C3 botulinum toxin substrate 1 (Rac1) and transforming protein RhoA (RhoA). While Cdc42 and Rac1 trigger similar cellular functions using related mechanisms, RhoA often acts as an

antagonist for Cdc42 and Rac1 (46). Multiple functions specific for Cdc42, Rac1 or RhoA have been ascribed including morphogenesis, polarity, movement, and cell division, summarized in a variety of excellent reviews (44, 47-51).

### 3.2.2 Constraints in studying Rho GTPases

Until now, Rho GTPases have mostly been studied using dominant negative (dn) and constitutively active (ca) mutants. Dn-mutants bind GEFs, thereby blocking their activity required for nucleotide exchange on endogenous GTPase proteins. Ca-mutants, on the other hand, are GTP-bound mutants that cannot hydrolyze GTP and therefore remain constitutively active. Limitations of these approaches rely on the nature of most GEFs targeting more than one Rho GTPase: inactivating one GEF could lead to inhibition of more than one Rho GTPase (46). Besides these mutants, bacterial toxins have been used to target and thereby inactivate endogenous Rho GTPases, unfortunately comprising a similar lack of specificity (52). The recent availability of various Rho GTPase knockout mice provides a better means to study the functions of selected GTPases in more detail- and also provides new insights for their *in vivo* functions (reviewed by (44, 53). However, a global Cdc42 knockout is embryonic lethal (54).

### 3.2.3 Cdc42 contributes to actin dynamics

Small Rho GTPases, especially Cdc42, are active at the cell periphery close to membranes, where they promote actin polymerization upon external stimuli. Active, GTP-bound Cdc42 has conserved roles in regulating membrane-deformations of different kinds at the plasma membrane; a prominent example is the formation of a lamellipodium at the leading edge of migrating cells. The lamellipodium is an area consisting of branched as well as linear, bundled actin filaments, which push against the plasma membrane, thereby inducing protrusions. Whereas membrane ruffling constitutes a rather mild form of membrane deformations, the formation of filopodia in migrating cells requires stronger forces in form of actin bundles consisting of linear actin filaments connected by cytoskeletal linkers (55).

GTP-bound Cdc42 stimulates effector proteins that act on the actin cytoskeleton, promoting basically either the branching of actin filaments or linear filament growth. The branching, as well as the formation of de-novo actin filaments is mediated by Cdc42-dependent activation of N-WASP and WASP, which then recruit the Arp2/3 complex promoting nucleation and elongation of branched

actin networks (56, 57). Arp2/3-dependent actin polymerization contributes to membrane ruffling, a process by which a cell builds up membrane tension and increases its surface area in order to produce delimited membrane protrusions (51). Linear actin polymerization, as opposed to actin branching, requires Cdc42-signaling via formins (58), which are protein dimers surrounding barbed ends of filaments, thereby preventing the recruitment of capping proteins. Both mechanisms of Arp2/3-mediated actin branching and the formin-dependent linear polymerization of filaments are effects that occur downstream of Cdc42 signaling. A protein kinase C (PKC $\alpha$ )- and Src kinase-dependent signaling cascade upstream of Cdc42 leads to the formation of ring-like cell protrusions mediating cell-extracellular matrix interactions called podosomes (59).

Besides contributing to the general shape of cells in the steady state, these mechanisms also play critical roles for the reorganization of intracellular contents that occur upon extracellular stimuli. Cell polarization for example is a Cdc42-dependent process (60), in which cells have to asymmetrically reorganize their contents in order to react upon certain stimuli. Cell polarity is important for asymmetric cell division, directed cell migration, or the directed flow of proteins or organelles along microtubules towards a certain location, e.g. the immunological synapse. The latter requires microtubule-organizing center (MTOC) reorientation, which is highly actin- as well as Cdc42-dependent (61).

Intracellular protein transport in animal cells involves long-range vesicle transport along microtubules that originate from the MTOC and point towards the cell membrane, or short-range transport along filamentous actin (F-actin) filaments randomly oriented in the cytoplasm. Examples of motors that mediate traffic on microtubules are for example dynein, a minus-end oriented protein that mediates vesicle transport to the cell center (62), or kinesins, plus-end directed motor proteins that mediate outward transport (63). The only microtubule-independent protein that is suitable for long-range transport on actin-filaments is myosin, which however, has only very short tracks at its disposal. This classical textbook knowledge has recently been extended based on the finding that there was also long-range vesicle transport on actin tracks detectable that, furthermore was formin-dependent (64), indicating a possible role of Cdc42 in this mechanism. In brief, vesicles themselves recruit actin-nucleating factors Spire-1, Spire-2 and

Formin-2 that build up short actin filaments surrounding the vesicle surface. These short filaments connect the vesicle to the pre-existing actin network and initiate vesicle movement toward the cell surface in a Myosin-Vb-dependent manner (64).

Besides these intracellular movements, vesicle formation is also important at the cell surface of APCs, such as DCs. It serves in acquisition of extracellular contents such as nutrients and involves membrane deformation, vesicle formation and scission followed by transport along the endocytic route. Depending on the mode of “sampling” different types of signaling cascades induce the recruitment of Rho GTPases (51).

### **3.2.4 Rho GTPases are targets of bacterial toxins**

Due to their potential in reorganizing the actin cytoskeleton, it is not surprising that Rho family members have become targets of numerous bacterial toxins (reviewed in (65, 66)). The coherent mechanism of these toxins relies in the activation or deactivation of Rho GTPases, inducing local actin polymerization events (e.g. at the plasma membrane) facilitating bacterial entry into non-phagocytic cells, or disrupting cytoskeleton dynamics required for APC motility, thereby promoting local bacterial cell invasivity. Many mechanisms involve the Rho GTPases Rac1, Cdc42 and RhoA with downstream signaling on the actin cytoskeleton and a variety of virulence factors have been identified that differentially regulate their activities (reviewed in (65) and (67)). Therefore, the mechanisms of action of Rac1, Cdc42 and RhoA remain important to fully understand their functions in DC biology upon encounter of pathogens.

### **3.2.5 Functions of Cdc42 in DCs**

Until now, Cdc42 function has mostly been studied in non-hematopoietic cell lines using either mutant proteins or bacterial toxins. A global Cdc42 knockout is embryonic lethal (54). Therefore, Cdc42 function in DCs could only be studied *in vitro* by modulating Cdc42 activity in bone-marrow derived DCs (BMDCs). The following section briefly summarizes previous findings of how Cdc42 regulates cell shape, antigen acquisition and presentation.

#### **Filopodia and podosome formation**

The best-studied function of Cdc42 involves its regulation of the actin cytoskeleton, which is summarized in chapter 3.2.3. Actin dynamics are important

for general DC morphology and APC function. More specifically, dendrite morphology plays a role in the periphery for acquisition of antigens and DC migration, and in lymph nodes to maximize contact with T cells. Interestingly, a role of Cdc42 could be identified in the dendrite morphology of peripheral blood mononuclear cell (PBMC)-derived DCs and their adhesion capacity to fibronectin-coated surfaces using mutant proteins (68). Whereas DCs deficient for Cdc42 activity showed strong retraction of dendrites, acceleration of Cdc42 activity caused strong DC spreading due to actin polymerization at active sites. The loss of Cdc42 function lead to a disruption of F-actin structures and diffuse intracellular localization of broke filaments. Another study in mature human Langerhans cell (LC)-type DCs showed that depletion of functional Cdc42 resulted in a loss of both filopodia and lamellipodia (69). This study also indicated a role of active Cdc42 during both DC activation and MHC I surface expression. A developmental regulation of Cdc42 in DCs has been proposed in several publications (discussed in chapter 6.1.).

A study using human PBMC-derived DCs established a role of Cdc42 in podosome formation, and the formation of important adhesion structures at the leading edge of migrating cells. DCs transfected with a dn-Cdc42 mutant showed an increase in cell polarity accompanied with a loss of filopodia in migrating cells (70). This study also showed that overexpression of Cdc42 in mature DCs lead to an extension of filopodia formation, which was, furthermore, WASP and Arp2/3-dependent.

### **Endocytosis and antigen presentation**

Besides the formation of large protrusive structures, Cdc42 also mediates small changes in membrane dynamics with an impact on antigen acquisition and presentation. Shurin and colleagues confirmed a function for Cdc42 in adhesion, endocytosis and antigen presentation using BMDCs (71). The authors extensively characterized these cells transfected with a dn-Cdc42 mutant, showing that DCs in the absence of functional Cdc42 protein showed reduced adhesion on polylysine slides, no role for motility using a transwell system and a reduced capacity to take up dextran and present an OVA-derived peptide to CD4<sup>+</sup> T cells. In human LC-derived DCs the loss of Cdc42 function was associated with an impaired capacity

to stimulate CD8<sup>+</sup> T cells (69), probably due to low MHC I expression and costimulation of transduced mature DCs.

DC endocytosis was already earlier shown to be dependent on Cdc42 function using immature BMDCs: Garrett and colleagues (72) identified a role of Cdc42 in macropinocytosis, receptor-mediated endocytosis and pinocytosis. Furthermore, they found that DC activation was accompanied with a shutdown of endocytosis, caused by a downregulation of Cdc42 activity.

Altogether these studies point towards a contribution of Cdc42 in DCs in regulating processes required for basic APC functions like antigen acquisition, migration and antigen presentation. However, due to their usage of dn- or ca-mutants of Cdc42, several of these studies lack specificity and mechanistic details required to understand how Cdc42 specifically contributes to DC-mediated immunity.

### **3.3 Aims of the study**

#### **3.3.1 Characterization of a DC-specific knockout for Cdc42**

In order to avoid caveats due to an unspecific targeting of mutant proteins or toxins (see 3.2.2) we used a novel knockout mouse that conditionally lacks Cdc42 expression only in CD11c<sup>+</sup> cells, thereby leaving other Rho GTPases in DCs, and other cell types in the mouse unaffected.

We first aimed to characterize DCs derived from these mice (termed Cdc42-ko) with respect to cell surface expression of immune molecules required for APC function. Furthermore, we wanted to study the functional consequences of Cdc42 removal on important APC functions such as endocytosis, antigen acquisition and T cell stimulation in Cdc42-ko DCs, in order to investigate the role of specifically Cdc42 for these processes.

#### **3.3.2 Elucidation of the mechanism by which Cdc42 controls MHC II antigen presentation in DCs**

Based on the finding that Cdc42-ko BMDCs failed to induce CD4<sup>+</sup> T cell responses, we aimed to elucidate the specific contribution of Cdc42 to MHC II antigen presentation. In order to get an unbiased overview of pathways affected upon Cdc42 removal, we wanted to investigate the proteome composition of Cdc42-ko BMDCs using proteomics. More specifically, we aimed to identify factors responsible for MHC II antigen presentation that might be affected upon Cdc42 knockout. Given the role of Cdc42 in regulating actin dynamics, we aimed to study the contribution of the actin cytoskeleton to MHC II loading by chemically disrupting actin filaments. Furthermore, we wanted to identify a Cdc42-dependent mechanism that regulates actin dynamics involved in MHC II loading, in order to define the specific contribution of Cdc42 for this process.

#### **3.3.3 Examination of MHC II loading in DC subsets**

Additionally, we aimed to study selected *in vivo* DC subsets of wild type (wt) and Cdc42-ko mice with respect to MHC II loading and investigate their potential to fully activate CD4<sup>+</sup> T cells when pulsed with pre-processed OVA peptide.

With this study we want to further expand the knowledge about the regulation of MHC II antigen presentation of exogenously derived antigens and describe the role of Cdc42 in adaptive immunity *in vivo*.

## 4 MATERIALS AND METHODS

Materials are listed in alphabetical order. Methods are subdivided into cellular/immunological methods, biochemical methods and proteomics and within these subdivisions listed as they appear in the results section. Company headquarters are listed at first mention only.

### 4.1 Materials

#### 4.1.1 Antibodies

**Table 1: Antibodies used for flow cytometry.**

Specificity (anti-mouse)	Conjugate	Clone	Supplier
CD3e	PerCP	145-2C11	Becton, Dickinson & Co. (BD), Franklin Lakes, NJ, USA
CD4	PE, PerCP	CK1.5, RM4-5	BD
CD8a	APC-Cy7, PE, PerCP53-6.7		BD
CD11b	PE	M1/70	BD
CD11c	APC, Biotin, Pe-Cy5.5, Pe-Cy7	N418, HL3	eBioscience, San Diego, CA, USA, BD
CD16/CD32	Purified		BD
CD19	PerCP-Cy5.5	1D3	BD
CD40	APC	1C10	eBioscience
CD44	FITC	IM7	BD
CD62L	APC	MEL-14	BD
CD74	FITC	ln-1	BD
CD86	PE	GL1	BD
CD90.1	APC, PerCP	HIS51, OX-7	eBioscience, BD
CD103	PE	M290	BD
CD107a (LAMP-1)	FITC, PE	eBio1D4B	eBioscience
F4/80	Biotin, PE	BM8	eBioscience
H2-K <sup>b</sup> (MHC I)	FITC, PE	AF6-88.5	BD

The table continues on the next page.

Specificity (anti-mouse)	Conjugate	Clone	Supplier
I-A <sup>b</sup> (MHC II)	Alexa Fluor®647, Biotin, FITC	AF6-120.1, 25-9-17	BD, BioLegend
MHC class II	FITC	15G4	Santa Cruz Biotechnology, Santa Cruz, CA, USA
V $\alpha$ 2 TCR	FITC	B20.1	BD
V $\beta$ 5.1/5.2 TCR	PE	MR9-4	BD
anti-mouse IgG1	APC	X56	BD
anti-mouse IgG2a	Alexa Fluor®647	MOPC-173	BioLegend
anti-mouse IgG1	FITC	-	Santa Cruz

Streptavidin conjugates were purchased from BD (SA-PerCP) and eBiosciences (SA-Pe-Cy7). Dead cell exclusion DAPI and LIVE/DEAD® Violet Dead Cell Stain were purchased from Invitrogen (Life Technologies, Paisley, UK).

**Table 2: Unconjugated Antibodies used for Western blot.**

Specificity	Clone	Isotype	Supplier
$\beta$ -Actin	Polyclonal	Rabbit IgG	Cell Signaling Technology, Danvers, MA, USA
Cathepsin D	Polyclonal	Goat IgG	R&D Systems, Minneapolis, MN, USA
Cathepsin L	Polyclonal	Goat IgG	R&D
Cathepsin S	Polyclonal	Goat IgG	Acris Antibodies GmbH, Herford, Germany
CD107a (LAMP-1)	1D4B	Rat IgG	BioLegend
CD74 (Ii)	ln-1	Rat IgG	BD
Cdc42	11A11	Rabbit IgG	Cell Signaling
Gapdh	14C10	Rabbit IgG	Cell Signaling
Hip1R	44/Hip1R	Mouse IgG	BD
Rac1	ARC03	Mouse IgG	Cytoskeleton, Inc., Denver, CO, USA
RhoA	67B9	Rabbit IgG	Cell Signaling
$\beta$ -Tubulin	9F3	Rabbit IgG	Cell Signaling

Anti-rat horseradish peroxidase (HRP) was purchased from Cell Signaling. Anti-rabbit, anti-goat and anti-mouse HRP were purchased from Jackson ImmunoResearch Laboratories (West Grove, PA, USA).

#### 4.1.2 Chemicals

Unless stated otherwise, chemicals were purchased from Merck (Darmstadt, Germany), Roth (Karlsruhe, Germany) or Sigma-Aldrich (St. Louis, MO, USA).

#### 4.1.3 Consumables

Cell strainer (100  $\mu$ M, BD), disposable syringe 1 and 5 ml (Braun, Melsungen, Germany), disposable syringe filter 0.2+0.45  $\mu$ m (Nalgene Nunc Int., Rochester, NJ, USA), disposable injection needle 26 Gx1/2" (Terumo Medical Corporation, Tokyo, Japan), reaction container 1.5 ml und 2 ml (Eppendorf, Hamburg, Germany), reaction tube 5 ml (BD), reaction tube 15 ml und 50 ml (Greiner, Frickenhausen, Germany).

Other materials and plastic wares were purchased from BD, Nunc (Wiesbaden, Germany) and Greiner.

#### 4.1.4 Devices

Analytic scale (Adventurer, Ohaus Corp., Pine Brooks, NJ, USA), automatic pipettors (Integra Biosciences, Baar, Switzerland), bench centrifuge (Centrifuge 5415 D, Eppendorf, Hamburg, Germany), cell counter (Coulter Counter Z2, Beckman Coulter, Krefeld, Germany), centrifuge (Rotixa RP, Hettich, Tuttlingen, Germany), chemical scale (Kern, Albstadt, Germany), Coulter counter Z2 instrument (Beckman Coulter), flow cytometer (FACSCantoII and FACS Aria, BD), incubator (Hera cell, Heraeus Kendro Laboratory Products, Hanau, Germany), laminar airflow cabinet (Heraeus), magnetic stirrer (Ika Labortechnik, Staufen, Germany), Optimax® developing machine (Protec Medical Systems), pH-meter (Inolab, Weilheim, Germany), pipettes (Gilson, Middleton, WI, USA), Polymax 1040 platform shaker (Heidolph, Schwabach, Germany), power supply (Amersham Pharmacia, Piscataway, NJ, USA), radiographic cassette 18x14 cm (Siemens), real-time PCR machine (CFX96 Real Time System, BIO-RAD), tank transfer system (BIO-RAD), Thermocycler PCR-machine (Biometra, Goettingen, Germany), vacuum pump (KNF Neuberger, Munzingen, Germany), vortex-

Genie2 (Scientific Industries, Bohemia, NY, USA), water bath (Grant Instruments Ltd., Barrington Cambridge, UK).

#### 4.1.5 Inhibitors

Cytochalasin D and Nocodazole were purchased from Sigma-Aldrich; Gö 6983, Latrunculin B and SMIFH2 were purchased from Calbiochem EMD Millipore (Billerica, MA, USA) and Concanamycin B and CK-548 delivered from Enzo (Lörrach, Germany). Pitstop 2 was purchased from Abcam (Cambridge, UK).

#### 4.1.6 Media and solutions

**Table 3: Cell culture media used in this study.**

All media supplementing solutions were purchased from Gibco (Invitrogen, Carlsbad, CA, USA) or PAN-Biotech (Aidenbach, Germany).

Medium	Supplementing solutions
BMDC medium	Iscove's Modified Dulbecco's Medium (IMDM, Sigma-Aldrich) 500 mM $\beta$ -mercaptoethanol 2 mM glutamine 100 U/ml penicillin 100 $\mu$ g/ml streptomycin 10 % FCS (heat inactivated) 20 ng/ml GM-CSF
DC medium	RPMI 1640 + glutamine (PAA, Pasching, Austria) 500 mM $\beta$ -mercaptoethanol 100 U/ml penicillin 100 $\mu$ g/ml streptomycin 10 % FCS (heat inactivated) 20 ng/ml GM-CSF

**Table 4: Buffers and solutions.**

All buffers and solutions were prepared using double distilled water.

Buffers and Solutions	Composition
ACK	8.29 g NH <sub>4</sub> Cl 1 g KHCO <sub>3</sub> 37.2 mg Na <sub>2</sub> EDTA H <sub>2</sub> O ad 1 l pH 7.2-7.4 adjusted with HCl sterilized by 0.2 µm filtration
PBS	150 mM NaCl 10 mM Na <sub>2</sub> HPO <sub>4</sub> 2 mM KH <sub>2</sub> PO <sub>4</sub> pH 7.4 adjusted with 5 N NaOH
PBS (cell culture)	Dulbecco's PBS without Ca <sup>2+</sup> /Mg <sup>2+</sup> (PAA)
FACS buffer	PBS 2 % FCS 0.01 % NaN <sub>3</sub>
MACS buffer	PBS 0.5 % FCS
10x Gitocher buffer	670 mM Tris, pH 8.8 166 mM ammonium sulfate 65 mM MgCl <sub>2</sub> 0.1 % Gelatin
5x Cresol red buffer	250 mM KCL 50 mM Tris /HCL pH 8.3 43 % glycerol 2 mM Cresol-red 7.5 mM MgCl <sub>2</sub>
50x TAE buffer	242 g Tris 57.1 ml 100 % acetic acid 100 ml 0,5 M EDTA (pH 8.0), H <sub>2</sub> O ad 1 l
SDS running buffer	192 mM Glycin 25 mM Tris 0.1 % SDS

The table continues on the next page.

## MATERIALS AND METHODS

Buffers and Solutions	Composition
Transfer buffer	192 mM Glycin 25 mM Tris 20 % Methanol 0.002 % SDS
“Stripping” buffer	62.5 mM Tris pH 6.7 adjusted with HCL 100 mM $\beta$ -mercaptoethanol 2 % SDS
PBST	PBS 0.05 % Tween-20
5x SDS sample buffer	50 % Glycerin 250 mM Tris pH 6.8 adjusted with HCL 500 mM DTT 10 % SDS 0.5 % bromphenol blue
NP-40 cell lysis buffer	50 mM Tris pH 8.0 adjusted with HCL 150 mM NaCl <sub>2</sub> 1 % NP-40 Protease inhibitor cocktail 1x add 1 mM PMSF before use

**Table 5: Preparation of gels for SDS Page.**

Volumes in brackets apply to the amount required for 2 gels.

Gel	Composition
Resolving gel (12 %)	H <sub>2</sub> O (6.6 ml) 30 % acrylamide mix (8 ml) 1.5 M Tris/HCL, pH 8.8 (5 ml) 10 % SDS (200 µl) 10 % ammonia persulphate (200 µl) TEMED (20 µl)
Stacking gel	H <sub>2</sub> O (2.1 ml) 30 % acrylamide mix (500 µl) 1 M Tris/HCL, pH 6.8 (380 µl) 10 % SDS (30 µl) 10 % ammonia persulphate (30 µl) TEMED (3 µl)

#### 4.1.7 Mouse strains

Cdc42flx-Cre mice (termed Cdc42-ko) were generated by breeding CD11c-Cre<sup>+</sup> mice (73), kindly provided by Boris Reizis (Columbia University, New York, NY), with Cdc42fl/fl mice (74), kindly provided by Cord Brakebusch (University of Copenhagen, Copenhagen, Denmark). OT-I and OT-II mice (expressing a transgenic TCR specific for OVA<sub>257-264</sub> or OVA<sub>323-339</sub>, respectively) and C57BL/6 CD45.1<sup>+</sup> mice were originally obtained from The Jackson Laboratory (Bar Harbor, ME, USA). Mice were bred and maintained in a conventional facility at the Institute for Immunology (Munich, Germany) and used according to protocols approved by the local animal ethics committee.

#### 4.1.8 Fluorescent probes, proteins, peptides and primers

(I) Fluorescent probes: Alexa Fluor<sup>®</sup>647-conjugated OVA (Alexa-OVA), FITC-dextran and Lucifer yellow CH lithium salt were all purchased from Molecular Probes (Invitrogen).

(II) Proteins and Peptides: OVA grade VII (peptide-free) was purchased from Sigma-Aldrich; the peptides SIINFEKL (OVA<sub>257-264</sub>) and P323-339 (OVA<sub>323-339</sub>) were obtained from NeoMPS (Strasbourg, France).

(III) Primers: All oligonucleotides were purchased from MWG-Biotech AG (Ebersberg, Germany). Primer sequences are listed in the respective methods sections.

## 4.2 Methods

### 4.2.1 Cellular and immunological methods

#### 4.2.1.1 Generation of bone marrow-derived dendritic cells (BMDCs)

Primary cultures of immature DCs were generated by culturing bone marrow cells, isolated from femurs and tibiae of mice (see 4.2.1.9 and 4.2.1.10), for 10-14 days in BMDC medium (Table 3) containing 20 ng/ml GM-CSF. Cells were passed at days 3 and 7 and plated at a concentration of  $1.5 \times 10^6$  cells/ml. BMDCs were analyzed by flow cytometry based on the expression of CD11c, MHC II and CD86. Mature BMDCs were obtained by overnight stimulation with 1  $\mu$ g/ml lipopolysaccharide (LPS, Sigma-Aldrich).

#### 4.2.1.2 Flow cytometry – Fluorescence activated cell sorting (FACS)

Flow cytometry is a method used for the evaluation of various characteristics of cells such as cell size (forward scatter, FSC), granularity (side scatter, SSC) and fluorescence intensity. In brief, single cell suspensions are labeled with fluorescent antibodies specific for cell type specific molecular markers and pass by a focused laser beam, which stimulates the fluorophores. The emitted light from the fluorophores can then be detected concomitantly with the scattered light generated by these cells. Thus, this technique can be used to identify distinct cell populations within a heterogeneous mixture of cells. The flow cytometer used in this study was the FACSCanto II (BD) equipped with three lasers (488, 633 and 405 nm). A FACSAria instrument (BD) was used to sort DCs from splenic single cell suspensions based on electrostatic droplet deflection. Data from flow cytometry were analyzed with the FlowJo software (TreeStar, Ashland, OR, USA).

#### Staining of cells with fluorescent antibodies:

Equal numbers of cells were mixed with 100  $\mu$ l of FACS buffer containing specific antibodies of interest and incubated at 4 °C in the dark. After 20 min, cells were washed with 2 ml FACS buffer to remove unbound antibodies (180xg, 4 °C). Biotinylated antibodies were detected in a second step using fluorescent

streptavidin-conjugates. Stained cells were passed over a filter (41  $\mu\text{m}$  mesh, Reichelt Chemietechnik, Heidelberg, Germany) to obtain single cell suspensions.

#### 4.2.1.3 Antigen uptake & presentation

For antigen uptake, immature BMDCs were harvested, resuspended at a concentration of  $1 \times 10^6$  cells/ml in serum-free IMDM containing 5  $\mu\text{g}/\text{ml}$  Alexa-OVA, 1 mg/ml FITC-dextran and 0.5 mg/ml Lucifer yellow and were then incubated at 4  $^{\circ}\text{C}$  or 37  $^{\circ}\text{C}$  for 20 min. Uptake was stopped with 4 washes in ice-cold FACS-buffer. Cells were then stained with fluorescent antibodies and analyzed by flow cytometry. In a second experiment, Alexa-OVA was titrated to visualize how much OVA was taken up by cells that were used for a T cell proliferation assay (Figure 6B). BMDCs at day 13 of culture were incubated with 5, 25 or 125  $\mu\text{g}/\text{ml}$  Alexa-OVA for 3 h and then stimulated with 1  $\mu\text{g}/\text{ml}$  LPS overnight. Cells were then stained with fluorescent antibodies and analyzed by flow cytometry.

Antigen presentation was examined by co-culturing antigen-loaded BMDCs with CFSE-labeled OVA-specific T cells (see 4.2.1.11). For the presentation of whole protein antigen immature BMDCs were pulsed with 5, 25 or 125  $\mu\text{g}$  peptide-free OVA for 3 h, stimulated overnight with 1  $\mu\text{g}/\text{ml}$  LPS. BMDCs were next co-cultured together with T cells in BMDC medium at a DC:T cell ratio of 1:20 in 96-well round-bottom plates for 3 d. For the presentation of pre-processed OVA peptides, BMDCs were first matured overnight in the presence of LPS and incubated with 0.1, 1, 10 and 100  $\mu\text{g}/\text{ml}$  SIINFEKL peptide or 0.01, 0.1, 1 and 10  $\mu\text{g}/\text{ml}$  P323-339 peptide for 3 h. Peptide-loaded BMDCs were washed 3x and subsequently co-cultured with T cells at a DC:T cell ratio of 1:40 with OT-I or OT-II cells for 3 and 4 days, respectively. T cells were stained with fluorescent antibodies and T cell proliferation was examined from CFSE dilution.

#### 4.2.1.4 Antigen processing

BMDCs were incubated with 50  $\mu\text{g}/\text{ml}$  of a non-fluorescent self-quenched conjugate of ovalbumin (DQ-OVA, Molecular Probes) that exhibits fluorescence upon proteolytic degradation. 5  $\mu\text{g}/\text{ml}$  non-degradable Alexa-OVA (see 4.1.8) in the same mix served as positive control for protein uptake. After 15 min uptake, cells were washed with FACS buffer to remove excess antigen and re-incubated at

37 °C for additional 15 min in BMDC medium to allow DQ-OVA processing. Cells were then stained for flow cytometry and analysis was performed gating on CD11c<sup>+</sup>Alexa-OVA<sup>+</sup> cells.

#### 4.2.1.5 Inhibitor treatment of cultured cells

BMDCs were treated with small molecules that specifically inhibit processes required for basic cell functions. These freely membrane permeable molecules were applied to Wt BMDC cultures for 16 h (overnight).

Table 6 lists the inhibitors, their specificities and the final concentrations they were used at.

**Table 6: Inhibitors used in this study.**

Suppliers are listed in chapter 4.1.5.

Inhibitor	Specificity	Final concentration(s)	References
CK-548	Arp3	100, 50, 25, 12.5, 6.25 µM	(75)
Concanamycin B	V-ATPase	2 nM	(76, 77)
Cytochalasin D	Actin cytoskeleton	10 µg/ml	(78)
Gö 6983	Protein kinase C (PKC)	1 µM	(59, 74)
Latrunculin B	Actin cytoskeleton	1 µg/ml	(79, 80)
Nocodazole	Tubulin	30 µM	(81)
Pitstop 2	Clathrin heavy chain	30, 10, 5 µM	(82)
SMIFH2	Formin FH2 domain	10 µM	(83)

#### 4.2.1.6 Internalization of invariant chain from the cell surface of DCs

BMDCs were labeled for surface invariant chain bound to I-A<sup>b</sup> at 4 °C using a purified anti-mouse 15G4 mAb (Santa Cruz). Unbound antibody was removed and cells were allowed to internalize surface proteins in the presence of complete medium at 37 °C, 5 % CO<sub>2</sub>. At the indicated times, cells were transferred to 4 °C and remaining antibodies at the cell surface were detected using a secondary APC rat anti-mouse IgG1 antibody (BD Pharmingen). Cells were analyzed by flow cytometry and relative fluorescence intensity (rFI) values of CD11c<sup>+</sup> cells were calculated as described elsewhere (84) using the following equation:

$$\text{rFI} = [\text{MFI}(\text{specific antibody}) - \text{MFI}(\text{isotype control})] / \text{MFI}(\text{isotype control}).$$

#### 4.2.1.7 Cytometric Bead Array (CBA)

The Mouse Inflammation Kit (BD) was used to quantitatively detect inflammatory cytokines in BMDC culture supernatants. The kit follows the CBA principle, which is analogous to conventional ELISAs, but allows detection of several different proteins in one multiplexed assay. In brief, a mixture of beads coated with capture antibodies specific for IL-6, IL-10, monocyte chemoattractant protein 1 (MCP-1), interferon gamma (IFN- $\gamma$ ), TNF and IL-12p70 proteins was applied to culture supernatants and detected with a secondary, PE-conjugated antibody. Samples including a standard curve were acquired by flow cytometry on a FACSCanto II (BD) instrument and analyzed using the FCAP Array Software v1.0.2 (Soft Flow, BD). Supernatants were used undiluted; LPS-treated BMDC culture supernatants were used as positive control and diluted 1:4. The assay was performed according to the manufacturer's instructions.

#### 4.2.1.8 Magnetic cell sorting (MACS)

MACS is a technique used to enrich cell populations according to their expression of cell type specific surface markers. Two different methods are available: positive and negative selection. For positive selection, magnetic beads are conjugated to monoclonal antibodies (here: anti-mouse CD11c mAb, clone N418) that label cells expressing this specific cell surface marker. After labeling, cells are loaded onto a magnetic column placed in a magnetic field that retains the magnetically labeled cells (here: CD11c<sup>+</sup> cells) on the column. For negative selection, a cocktail of biotin-conjugated monoclonal antibodies that do not bind the cell population of interest itself is applied to the cell suspension. In a second step, labeled cells bind to magnetic beads and are retained in the column and depleted from the cell suspension. Negative selection was applied for CD4<sup>+</sup> or CD8<sup>+</sup> T cell enrichment from splenic cell suspensions. Both the CD11c Microbeads and the CD4<sup>+</sup> T cell isolation kit were purchased from Miltenyi Biotec (Bergisch Gladbach, Germany) and used according to the manufacturer's instructions.

#### 4.2.1.9 Harvesting organs from mice

Mice were sacrificed in a CO<sub>2</sub> gas chamber, fixed with needles on a polystyrene pad, disinfected with 70 % ethanol and cut open. Lymph nodes and spleens were harvested with fine tweezers and kept on ice in PBS. For bone-marrow cultures, hind legs were cut, cleaned of muscle, separated into femurs and tibiae and kept on ice in PBS until use.

#### 4.2.1.10 Isolation of cells from organs

Bone marrow: The terminal parts of femurs and tibiae were cut open and the bone marrow was flushed out with needle and syringe using medium containing 10 % FCS. Red blood cells were lysed for 2 min in ACK buffer and the cell suspension was passed over a cell strainer to remove debris. Cells were subsequently subjected to cell culture, or frozen for future use in BMDC medium supplemented with 10 % extra FCS and 10 % dimethyl sulfoxide (DMSO) at -80 °C.

Spleen and lymph nodes: For isolation of DCs from mouse spleens and lymph nodes, organs were enzymatically digested using a solution containing Liberase CI (0.42 mg/ml) and DNase I (0.2 mg/ml, both Roche, Basel, Switzerland). After a 20 min incubation at 37 °C organs were mechanically disrupted using a pestle (Gerresheimer, Querétaro, México) and passed over a cell strainer to obtain a single cell suspension. Erythrocytes in splenic cell suspensions were lysed for 5 min using ACK and the suspension was again passed over a cell strainer. The single cell suspension was used for flow cytometry, or enriched by MACS (see 4.2.1.8) prior to use.

#### 4.2.1.11 CFSE labeling of T cells

CFSE staining (Carboxyfluorescein diacetate succinimidyl ester, Life Technologies™) is a standard method used for the fluorescent labeling of cells. CFSE is a cell-permeable molecule that diffuses passively into cells and reacts with intracellular amines. It is colorless, but exhibits its fluorescence upon cleavage by intracellular esterases. In this study, CFSE staining was used to determine T cell proliferation. As T cells divide, CFSE fluorescence gets diluted, as the dye is equally distributed between the two daughter cells. This effect results in the typical diagram that is characterized by a peak of non-dividing T cells showing undiluted CFSE fluorescence of high intensity, accompanied by a couple of peaks that are lower for CFSE and represent cell divisions.

For CFSE labeling, purified CD4<sup>+</sup> or CD8<sup>+</sup> T cells (see 4.2.1.6) were resuspended at 10x10<sup>6</sup> cells/ml in pre-warmed PBS containing 0.03 % FCS, and 5 µM CFSE was added while vortexing to ensure a homogenous labeling. Cells were incubated for 10 min at 37 °C and vortexed every 2-3 min to ensure homogeneity of fluorescence. The reaction was stopped by adding an equal volume of pure FCS and cells were washed 3 times to remove unbound CFSE. After the staining

procedure, T cells were counted and co-cultured together with BMDCs (see 4.2.1.3).

#### 4.2.1.12 Immunization and adoptive cell transfer

To investigate the presentation of OVA<sub>323-339</sub> peptide (P323-339) *in vivo*,  $2 \times 10^6$  transgenic CD4<sup>+</sup>CD90.1<sup>+</sup> OT-II cells, isolated from lymph nodes of OT-II mice and enriched by negative selection (MACS), were adoptively transferred intravenously into wt and Cdc42-ko recipients. The next day, mice were challenged with a single dose of 20 µg LPS and 100 µg P323-339 peptide in PBS. After five days, mice were sacrificed and spleens were analyzed for the presence of CD4<sup>+</sup>CD90.1<sup>+</sup> T cells. A no-peptide control was used to exclude any unspecific proliferation of transgenic T cells.

## 4.2.2 Molecular biology and biochemical methods

### 4.2.2.1 Mouse genotyping

#### Table 7: Isolation of genomic DNA and mouse genotyping.

The genotype of Cdc42-ko mice was determined by PCR on genomic DNA isolated from mouse tails. PCR products were analyzed by conventional agarose gel electrophoresis in comparison to a 1 kb ladder (New England Biolabs, Ipswich, MA, USA).

Isolation of genomic DNA from mouse tails	
Isolation of genomic DNA:	1x Gitocher buffer (see Table 4) 0.5 % Triton-X 1 % β-mercaptoethanol 0.4 mg/ml proteinase k H <sub>2</sub> O ad 50 µl 6 h at 55 °C and 95 min at 95 °C
Composition of PCR reaction:	1 µl DNA 6 µl Cresol red buffer with MgCl <sub>2</sub> 100 pM primer for 100 pM primer rev 2.5 mM dNTP mix 5 U/ml PANScript DNA polymerase H <sub>2</sub> O ad 29 µl
Primer sequences and genotyping	
Cdc42 fl/fl PCR:	
Cdc42-for	5'-TCTGCCATCTACACATACAC-3'
Cdc42-rev	5'-ATGTAGTGTCTGTCCATTGG-3'

Products:	300 bp (flx); 160 bp (wt)
PCR program:	
Step 1: 95 °C	2 min
Step 2: 65 °C	30 s - $\Delta$ -1 cycle
Step 3: 75 °C	45 s - back to step 1 (10x)
Step 4: 95 °C	30 s
Table 7 continued:	
Step 5: 55 °C	30 s
Step 6: 72 °C	45 s - back to step 4 (35x)
<hr/>	
Cre PCR:	
Cre-for	5'-GGACATGTTTCAGGGATCGCCAGGCG-3'
Cre-rev	5'-GCATAACCAGTGAAACAGCATTGCTG-3'
Products:	270 bp (Cre); none (wt)
PCR program:	
Step 1: 95 °C	5 min
Step 2: 95 °C	30 s - $\Delta$ -1 cycle
Step 3: 55 °C	30 s
Step 4: 72 °C	45 s - back to step 2 (35x)
Step 5: 72 °C	5 min

#### 4.2.2.2 RNA isolation and complementary DNA (cDNA) synthesis

RNA was isolated from total cells using the RNeasy Mini Kit (Qiagen, Hilden, Germany) according to the manufacturer's instructions. To remove any contaminating DNA, the optional on-column DNase digestion step with RNase-free DNase was included. The concentration of RNA was determined with a NanoDrop instrument (Thermo Fisher Scientific, Waltham, MA, USA). Equal amounts of RNA were then used for cDNA synthesis with the SuperScript® VILO™ cDNA Synthesis Kit (Invitrogen) according to the manufacturer's instructions.

#### 4.2.2.3 Quantitative PCR (qPCR)

qPCR allows simultaneous amplification of cDNA templates and is used to determine the exact quantity of a particulate cDNA and thereby, RNA sequence. qPCR was performed using two different methods, SYBR Green and TaqMan, both based on the detection of a fluorescent reporter molecule that accumulates with each cycle of amplification. In brief, SYBR is a fluorescent dye that

intercalates into any double stranded DNA. TaqMan, on the other hand, makes use of specific fluorescent probes that hybridize with the respective amplification products. The cycle number (crossing point, CP), at which the fluorescence exceeds certain intensity, is then correlated with the initial amount of the relevant template cDNA, which can then be assigned to RNA levels.

For both SYBR Green and TaqMan, 10 ng of cDNA was used per reaction and each sample was measured in technical duplicates on a CFX96 Real Time System (BIO-RAD).

The SYBR Green reaction was performed using the Lightcycler FastStart DNA MasterPLUS SYBR Green I Kit (Roche) according to the manufacturer's instructions using the primers b2M-forward 5'-CAGAAAACCCCTCAAATTC AAGTAT-3' and reverse 5'-AATTCAGTGTGAGCCAGGATATAGA-3' (85). Expression levels were normalized to hypoxanthine-guanine phosphoribosyltransferase (HPRT) (primer sequences see Table 8).

The TaqMan assay was performed with the LightCycler TaqMan Master Kit (Roche) and the Universal ProbeLibrary Set mouse (Roche) according to the manufacturer's instructions using the primers and probes listed in Table 8. Expression levels were normalized to ubiquitin C (UbiC), HPRT or glyceraldehyde-3-phosphate dehydrogenase (Gapdh).

#### **4.2.2.4 Preparation of lysates for Western blot**

Cells dedicated for Western blot were washed once with PBS to remove extracellular proteins, pelleted and resuspended at a concentration of  $1 \times 10^6$  cells per 15  $\mu$ L of Nonidet P-40 (NP-40) cell lysis buffer (see 4.1.5) in the presence of protease inhibitors (Protease Inhibitor Cocktail P8340 and phenylmethylsulfonyl fluoride (PMSF) (both Sigma-Aldrich). Cells were lysed for 15 min on ice, followed by 5 min centrifugation at 2500xg to remove intact nuclei and insoluble cellular debris. Both, total cell lysates and supernatants were quantified using the Quanti-iT™ Protein Assay Kit (Molecular Probes) to determine the exact protein concentration. Equal amounts of protein were then denatured using sodium dodecyl sulfate (SDS) sample buffer (see 4.1.5) at 96 °C for 7 min and further subjected to SDS Page and Western blot.

**Table 8: Primers and fluorescent probes used for TaqMan-based qPCR.**

Gene	Forward primer	Reverse primer	Probe #
Cd40	5'-GAGTCAGACTAATGTCAT CTGTGGTT-3'	5'-ACCCCGAAAATGGTGATG-3'	105
Cd74	5'-CACCGAGGCTCCACCTAA-3'	5'-GCAGGGATGTGGCTGACT-3'	72
Cd86	5'-CCTCCAAACCTCTCAATTT CAC-3'	5'-GGAGGGCCACAGTAACTGAA-3'	12
Cdc42	5'-ACAACAAACAAATTCCCA TCG-3'	5'-TTGCCCTGCAGTATCAAAAA-3'	22
Ctsd	5'-CCCTCCATTTCATTGCAAGA TAC-3'	5'-TGCTGGACTTGTCACTGTTGT-3'	3
Ctsl	5'-ACAGAAGACTGTATGGCAC GAA-3'	5'-GGATCATTCTCATGTTCTTCT CC-3'	25
Ctss	5'-CATCTTTGGAGTGAGCACCA-3'	5'-GCATCCAAAACAGCCATCTTA-3'	92
Gapdh	5'-GGGTTCTATAAATACGGAC TGC-3'	5'-CCATTTTGTCTACGGGACGA-3'	52
H2-Ab1	5'-CACAGGAGTCAGAAAGGAC CTC-3'	5'-GTCAAAACACTCTGAGTCACT GC-3'	25
Hprt1	5'-TCCTCCTCAGACCG CTTTT-3'	5'-CCTGGTTCATCATCGCTAATC-3'	95
Lamp1	5'-CCTACGAGACTGCG AATGGT-3'	5'-CCACAAGAAGTGCCATTTTTTC-3'	110
UbiC	5'-GACCAGCAGAGGCT GATCTT-3'	5'-CCTCTGAGGCGAAGGACTAA-3'	11

#### 4.2.2.5 SDS Page and Western blot

Equal amounts of protein were loaded onto a 12 % SDS gel prepared as described in the Current Protocols in Immunology (Unit 8.9; see also Table 5) and separated by gel electrophoresis for 1.5 h at 80-100 V. PageRuler™ prestained protein ladder (Thermo Scientific, Rockford, IL USA) was loaded as a protein standard. Separated proteins were transferred onto a nitrocellulose membrane (Whatman) using a tank transfer system (BIO-RAD) as described in the Current Protocols in Immunology (Unit 8.10); transfer time was adjusted to 1.5 h at 80 V. Membranes were blocked overnight in PBS supplemented with 0.5 % Tween-20 and 5 % milk.

#### 4.2.2.6 Western blot quantification

After incubation with specific primary and secondary antibodies (see 4.1.1, Table 2), membranes were developed using enhanced chemiluminescence (ECL) Western blotting substrate (PerkinElmer Inc., MA, USA) followed by exposure to Amersham Hyperfilm™ (GE Healthcare). Specific bands were quantified relative to actin, tubulin or Gapdh, as indicated in the figure legends, using the free online tool ImageJ (86) according to Luke Miller's instructions ([www.lukemiller.org/journal/2007/08/quantifying-Western-blots-without.html](http://www.lukemiller.org/journal/2007/08/quantifying-Western-blots-without.html), Image J method version 2, as of December 2012).

### 4.2.3 Quantitative proteomics and data analysis

#### 4.2.3.1 Quantitative proteomics

Quantitative proteomics were performed for two biological replicates in collaboration with Stefan Lichtenthaler's group at the German Center for Neurodegenerative Diseases (DZNE) Munich. Sample preparation for mass spectrometry was done as described (87). In brief, approximately  $20 \times 10^6$  cells were lysed. Lysates were centrifuged at  $10.000 \times g$  to remove insoluble cellular debris. Upon addition of five volumes of 8 M urea, one fifth of the cell lysate was subjected to filter-aided sample preparation (88) and fractionated into 5 fractions using StageTip-based SAX fractionation (87). Two technical replicates of each fraction were measured on a liquid chromatography-tandem mass spectrometry (LC-MS/MS) set-up coupling a Proxeon Easy nLCII (Thermo Fisher Scientific) with in-house packed 15 cm columns (2.4  $\mu\text{m}$  C18 beads) to an linear ion trap LTQ Velos Orbitrap mass spectrometer. A TOP14 method was used for data dependent peptide fragmentation. Data were analyzed by label-free quantification (see below).

#### 4.2.3.2 Label-free quantification

Label-free quantification and analysis of the data was performed using the MaxQuant software suite (version 1.1.1.36) with the integrated Andromeda algorithm for protein identification searching a murine IPI database (version 3.78). Standard settings for the algorithm were used (89, 90). Quantification was performed on the basis of unique peptides: proteins detected with four unique peptides were considered "identified". Differences in protein expression between wt and Cdc42-ko BMDCs were defined as fold-change values Cdc42-ko/wt.

### 4.2.3.3 Web-based evaluation of identified proteins

The data set obtained from the proteomics approach was analyzed using the free online tools listed in Table 9. These tools are databases with different scopes, such as detailed information on single proteins (Uniprot), or lists of proteins that can be grouped under certain keywords (Gene Ontology). Their specifications are listed in the table.

**Table 9: Web pages used to analyze the proteomics data set.**

As of December 2012.

Web page	Description
<a href="http://www.uniprot.org">www.uniprot.org</a>	Protein knowledge base
<a href="http://www.string-db.org">www.string-db.org</a>	Search tool for the retrieval of interacting genes and proteins
<a href="http://www.genome.jp/kegg/pathway.html">www.genome.jp/kegg/pathway.html</a>	Collection of manually drawn pathway maps
<a href="http://www.geneontology.org">www.geneontology.org</a>	Collection of biological terms, for which proteins are grouped according to a biological process, cellular component or molecular function they are associated with

### 4.2.4 Statistical analysis

Significance was determined using the Student's T test and defined as follows: \* $p < 0.05$ , \*\* $p < 0.01$  and \*\*\* $p < 0.001$ . Bar graphs show average  $\pm$  standard error of the mean (SEM) from single or combined experiments as indicated in the figure legends.

## 5 RESULTS

### 5.1 Cdc42 maintains DC functions critical for the induction and control of immune responses

#### 5.1.1 A novel DC-specific knockout for Cdc42

In order to study Cdc42 function in DCs we established a model system that did not require dnCdc42 constructs, thereby preventing unspecific effects caused by these mutants. Moreover, this novel knockout mouse lacks Cdc42 selectively in DCs, leaving other cell types Cdc42-sufficient. Thus, we were able to generate a DC-specific knockout with no constraints regarding the viability of mice, in contrast to a global Cdc42 knockout that was embryonic lethal (54).

We generated Cdc42-ko mice by breeding Cdc42<sup>fl/fl</sup> mice (74) with CD11c-Cre mice (91) (Figure 3A). These mice express Cre recombinase (Cre) under the control of the CD11c promoter and therefore specifically in DCs. Once expressed, Cre binds to LoxP sites, which are integrated into exon 2 of the Cdc42 gene. Cre mediates recombination of LoxP sites, thereby excising a genomic region leading to the expression of non-functional Cdc42 mRNA (Cdc42 mutant).

We first tested the efficiency of the model system by analyzing *in vitro* generated BMDCs of control mice expressing Cre only (termed wt) and Cdc42-ko mice (termed Cdc42-ko) for residual Cdc42 protein and mRNA expression. BMDCs were generated by culturing bone marrow in the presence of GM-CSF, which is a

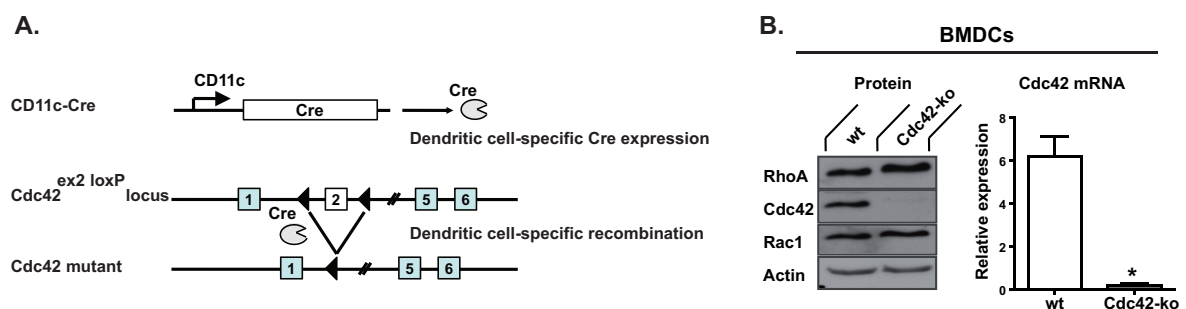


**Figure 3: Cre/LoxP approach to target Cdc42 selectively in DCs.**

(A) The CD11c-promotor driven expression of Cre recombinase (Cre) and the conditional Cdc42 allele. CD11c-Cre recombinase is expressed specifically in DCs under the control of the CD11c promoter. Upon CD11c-Cre mediated recombination, the genomic region between the two LoxP sites is excised, inactivating the Cdc42 gene and resulting in non-functional Cdc42 mRNA (Cdc42 mutant). Figure adapted from Benninger et al., 2007 (73) (B) Western blot analysis of bone marrow-derived dendritic cells (BMDCs) revealed the absence of Cdc42 protein in Cdc42-ko cells. For qPCR, BMDCs were purified by CD11c-MACS prior to RNA isolation. Knockout-specific primers were used that detect only functional Cdc42 mRNA. Results are representative for three independent experiments with similar results.

growth factor required for DC differentiation. A long-term BMDC culture of 10-14 days ensured that after shut down of functional Cdc42 mRNA production residual protein was degraded, generating a complete knockout for both Cdc42 protein and mRNA (Figure 3B). We also analyzed FACS Aria sorted CD11c<sup>+</sup>MHC II<sup>+</sup> spleen DCs out of Cdc42-ko mice for both Cdc42 protein and mRNA where we could detect low amounts of residual Cdc42 protein by Western blot (Paper I, Supplementary Figure S1D), but no functional Cdc42 mRNA in spleen DCs from Cdc42-ko mice (data not shown). Notably, BMDCs (Figure 3B) as well as spleen DCs from Cdc42-ko mice (data not shown), albeit deficient for Cdc42, expressed comparable amounts of RhoA and Rac1, indicating that the expression of these two Rho GTPases was not affected upon Cdc42 knockout.

### 5.1.2 Phenotype of Cdc42-ko BMDCs

In order to study the function of Cdc42 in DCs, BMDCs were used as a model system. BMDCs, generated in the presence of GM-CSF, can be grown in large numbers and facilitate the analysis of DC-functions *in vitro*.

Figure 4A shows representative FACS blots of unstimulated, steady-state wt and Cdc42-ko BMDC cultures (left panel). The purity of DCs (CD11c<sup>+</sup>) cells was typically around 95 % after 10-12 days of culture, the time point at which most of the experiments were performed. Unstimulated BMDCs were defined immature based on their low expression of MHC II and co-stimulatory molecules (e.g. CD86). Stimulated, mature DCs were obtained by culturing BMDCs in the presence of LPS overnight (right panel).

DCs (CD11c<sup>+</sup> cells) were further analyzed based on the expression of several surface markers important for DC function. Histograms show the expression levels of MHC I, MHC II, CD40, CD86, CD80, CD70, chemokine (C-C motif) receptor 7 (CCR7), CD45 and CD11c on wt vs. Cdc42-ko BMDCs (Figure 4B). Bar graphs show a quantification of selected surface markers based on mean fluorescence intensity values (MFI), on unstimulated vs. stimulated Cdc42-ko relative to wt cells (Figure 4C).

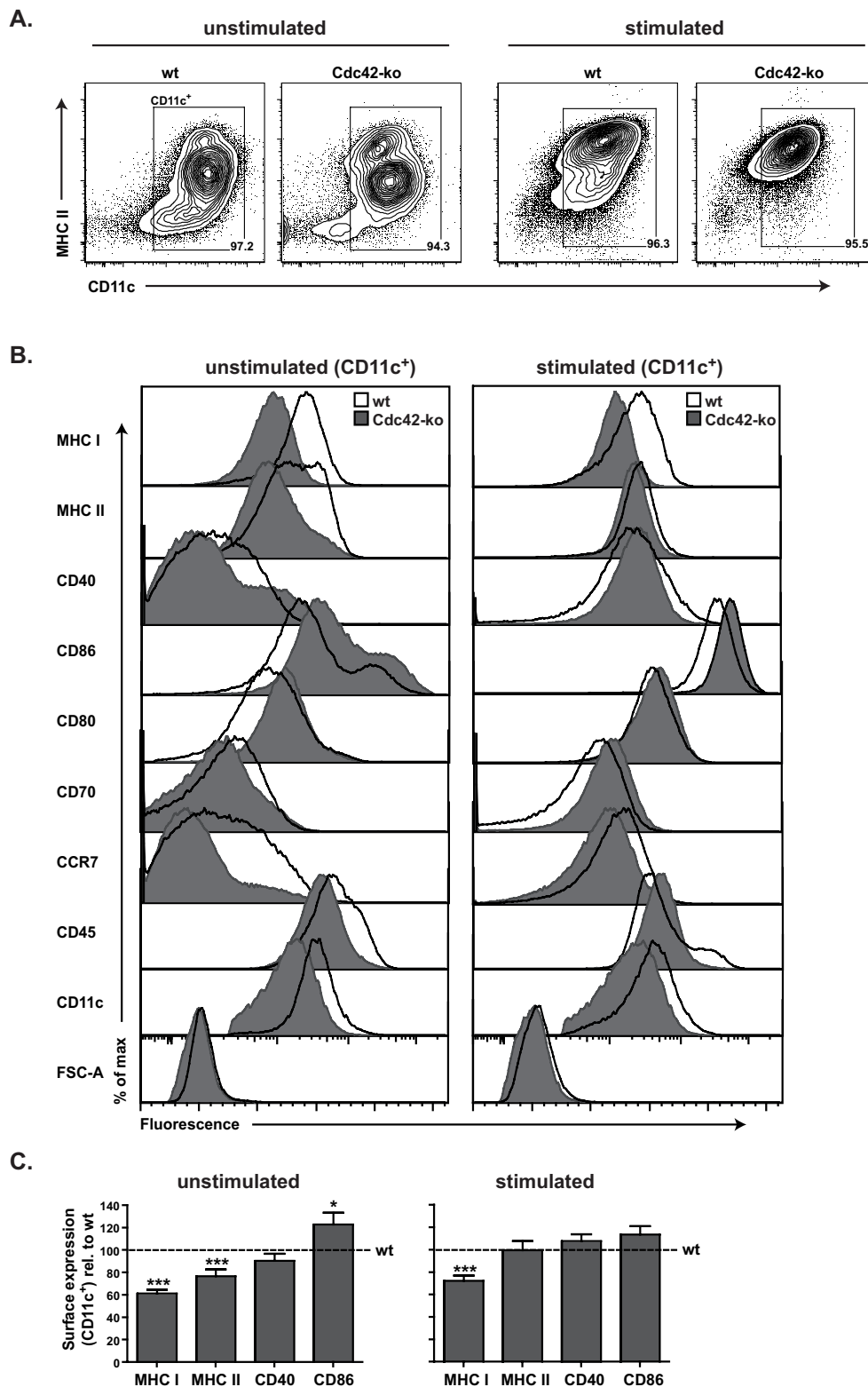


**Figure 4: Phenotype of Cdc42-ko BMDCs.**

(A) Wt and Cdc42-ko BMDCs were analyzed for the expression of CD11c and MHC II. Numbers in FACS blots show DC frequencies for representative wt and Cdc42-ko cultures as frequencies of CD11c<sup>+</sup> cells. Stimulated, mature BMDCs were obtained by overnight treatment with LPS. (B) Histograms show the expression of indicated surface markers on unstimulated and overnight with LPS stimulated CD11c<sup>+</sup> BMDCs. (C) Mean fluorescence intensity values (MFI) for selected surface markers were determined gating on CD11c<sup>+</sup> cells, as shown in B. Bar graphs and statistics show combined data of a minimum of 5 independent experiments with n≥2.

Unstimulated Cdc42-ko BMDCs showed surprisingly low amounts of both cell surface MHC I and MHC II, as compared to wt cells, but normal or higher expression of the co-stimulatory molecules CD40 and CD86 (Figure 4B and C). Interestingly, upon maturation with LPS Cdc42-ko BMDCs were able to upregulate MHC II and co-stimulatory molecules, thereby obtaining a mature phenotype. However, MHC I surface expression stayed low on these mature Cdc42-ko BMDCs, suggesting a function for Cdc42 in MHC I antigen presentation. Further markers evaluated in this manner were CD80 and CD70 (Figure 4B); two proteins that are upregulated at the cell surface upon maturation and play roles in T cell activation. Both were expressed at normal or higher amounts on Cdc42-ko BMDCs, similar to what was observed for the co-stimulatory molecules CD40 and CD86. CCR7, on the other hand, a chemokine receptor required for DC migration, was expressed at very low amounts on unstimulated Cdc42-ko BMDCs and was not properly upregulated in the absence of Cdc42. Similarly, two markers expressed by all DC subtypes, CD45 also known as leukocyte common antigen (LCA) and CD11c, were expressed at slightly reduced amounts on both unstimulated and stimulated Cdc42-ko DCs. Cell size of Cdc42-ko BMDCs, as determined from FSC-A acquisition, a parameter proportional to cell-surface area or size, was slightly reduced (Figure 4B). This phenotype was, however, statistically not significant.

Immature DCs possess a large pool of intracellular MHC I and MHC II, which is redistributed to the cell surface upon maturation (Figure 4B). To investigate, whether the low expression of both MHC I and MHC II on immature Cdc42-ko DCs was due to decreased intracellular protein levels, we performed intracellular FACS analysis. Interestingly, Cdc42-ko DCs showed normal levels of intracellular MHC II, but a low expression of intracellular MHC I, which was, however, statistically not significant (Figure 5A). To evaluate, if this decrease in intracellular MHC I protein expression was due to lower MHC I transcription, we performed qPCR and found normal levels of  $\beta$ 2M (soluble MHC I  $\beta$ -chain) message (Figure 5B) in unstimulated Cdc42-ko cells. H2-Ab1 (MHC II  $\beta$ -chain) mRNA was also expressed at normal amounts in these cells, which indicates that in the absence of Cdc42 both intracellular and surface levels of MHC molecules are most likely regulated post-transcriptionally, at the protein level. However, we did not assess the mRNA expression of the membrane-bound MHC I heavy chain ( $\alpha$ -chain) in this manner.

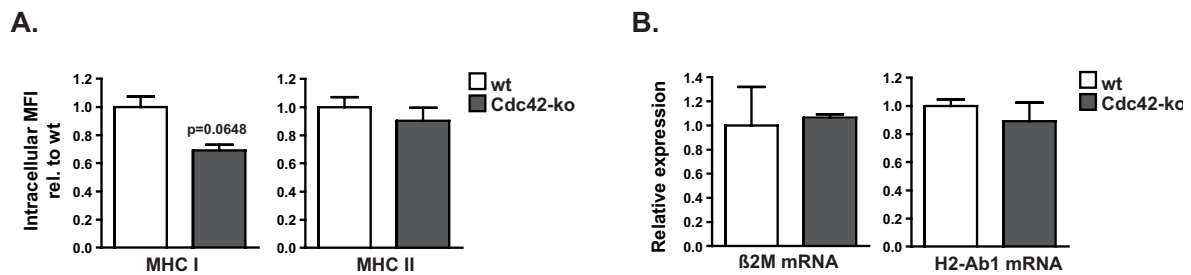


**Figure 5: Both MHC I and MHC II expression on Cdc42-ko BMDCs are regulated on protein level.**

(A) Intracellular FACS analysis of MHC I and MHC II was performed after fixation and permeabilization of wt and Cdc42-ko BMDCs. MFI were calculated gating on CD11c<sup>+</sup> cells. (B) MHC I ( $\beta$ 2M) and MHC II (H2-Ab1) mRNA were measured by qPCR from unstimulated BMDCs that were purified by CD11c positive selection (MACS) prior to RNA isolation. Data show a single experiment (n=2,  $\beta$ 2M) and one representative experiment (n=2) out of three (H2-Ab1) normalized to HPRT or UbiC, respectively.

### 5.1.3 Cdc42 is required for uptake, but not processing of soluble antigen

MHC molecules at the cell surface of DCs are loaded with antigens that are presented to antigen-specific T cells. Both MHC I antigen cross-presentation and MHC II antigen presentation require exogenously derived antigens that have to be actively taken up by the cell. Depending of the nature of antigen, DCs use different routes of uptake that can be addressed using proteins that target different mechanisms: OVA is taken up by both receptor mediated endocytosis and fluid-phase uptake (macropinocytosis), dextran specifically targets mannose-receptor (MR) mediated endocytosis and Lucifer yellow lithium salt enters the cell via its constitutive fluid-phase uptake (pinocytosis).

Thus, we targeted macropinocytosis, MR-mediated endocytosis and pinocytosis in wt vs. Cdc42-ko BMDCs using limiting amounts of the fluorescent proteins Alexa-OVA, FITC-dextran and Lucifer yellow. Interestingly, similar frequencies of Cdc42-ko BMDCs were capable of Alexa-OVA uptake after 20 min of incubation with the antigen (Figure 6A, upper left panel). However, the amount of protein, as observed from MFI (Alexa-OVA) of CD11c<sup>+</sup> cells, was severely reduced in the absence of Cdc42 (Figure 6A, upper right panel). Furthermore, we observed a reduced uptake capacity of Cdc42-ko BMDCs for both FITC-dextran and Lucifer yellow in both frequencies of antigen<sup>+</sup> cells and MFI. These results are in agreement with previously published studies that used BMDCs depleted of functional Cdc42 with help of dominant negative mutants (72).

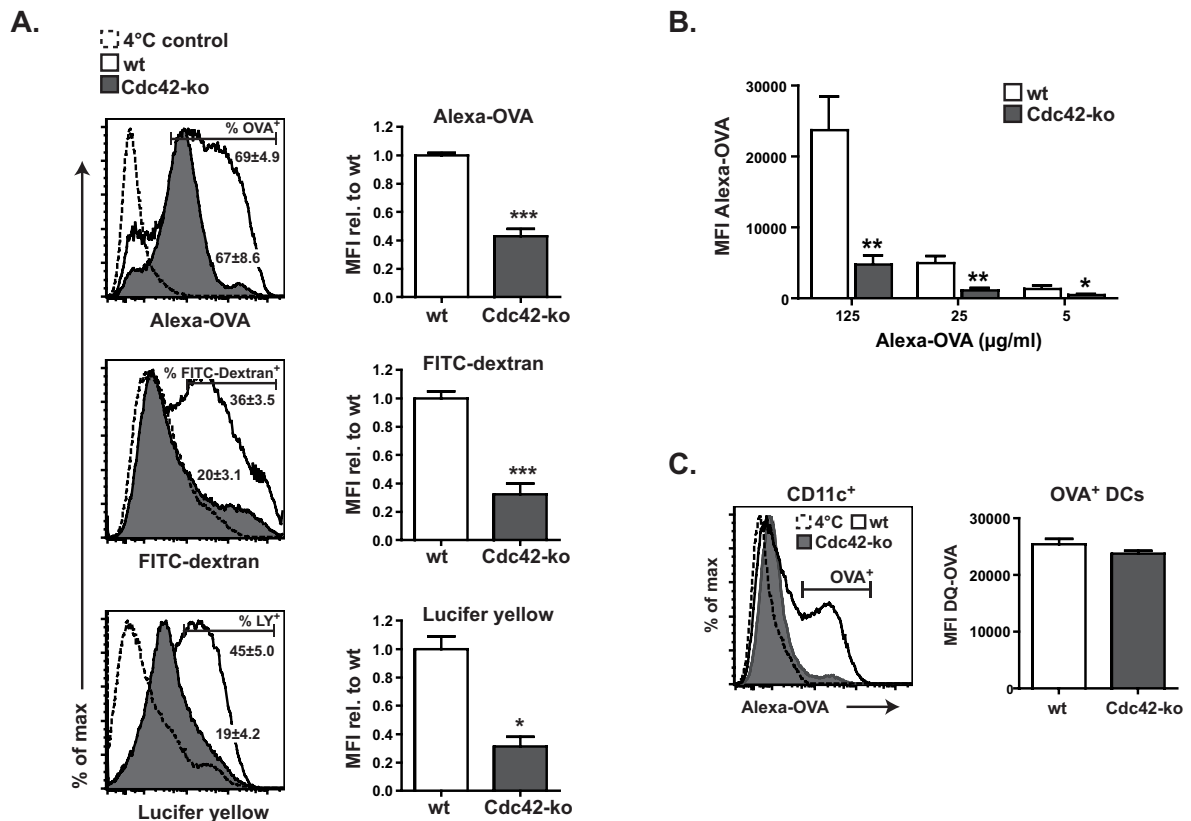


**Figure 6: Cdc42-ko BMDCs fail to take up soluble antigens, but are capable of OVA processing.**

(A) To target macropinocytosis, receptor-mediated endocytosis and pinocytosis, BMDCs were incubated for 20 min with limiting amounts of the fluorescent proteins Alexa-OVA, FITC-dextran and Lucifer yellow. Numbers on FACS blots indicate the frequencies of antigen<sup>+</sup> cells. Diagrams show MFI values gating on CD11c<sup>+</sup> cells. Data are from three independent experiments (n=4). (B) BMDCs were allowed to take up indicated amounts of Alexa-OVA for three hours and matured overnight in the presence of LPS. MFI were obtained gating on CD11c<sup>+</sup> cells. Statistics are from one experiment with n=2 (wt) and n=3 (Cdc42-ko). (C) BMDCs were incubated with Alexa-OVA and DQ-OVA for 15 min. Residual protein was removed from culture supernatants and cells were allowed to process DQ-OVA for 15 min. MFI of DQ-OVA were obtained gating on CD11c<sup>+</sup>Alexa-OVA<sup>+</sup> cells. Data show one experiment (n=2) out of two with similar results.

Next, we tested whether antigen uptake could be rescued in the absence of Cdc42 by increasing antigen concentrations and/or time of antigen uptake. Therefore, wt and Cdc42-ko BMDCs were allowed to take up high amounts of Alexa-OVA for three hours followed by overnight incubation in the presence of LPS, and interestingly neither time, nor large amounts of antigen could increase the amount of Alexa-OVA taken up by Cdc42-ko cells (Figure 6B). After uptake, antigens require processing as a prerequisite for being loaded onto MHC molecules in specialized compartments. Therefore we investigated, whether antigen processing was Cdc42-dependent. We used a non-fluorescent self-quenched conjugate of ovalbumin (DQ-OVA) that exhibits fluorescence upon proteolytic degradation. The amount of processed DQ-OVA was calculated from MFI (DQ-OVA) gating on Alexa-OVA<sup>+</sup> cells. Interestingly, Cdc42-ko BMDCs could process OVA equally

well (Figure 6C) indicating no role for Cdc42 in OVA processing, once the antigen has reached the endocytic system of Cdc42-ko BMDCs.

#### **5.1.4 Cdc42-ko DCs fail to induce proper immune responses to OVA-specific T cells**

Antigen presentation requires antigen uptake, processing and MHC loading followed by the transport of antigen-bound MHC molecules to the cell surface. Once exposed at the plasma membrane, the antigen is presented to antigen-specific T cells. Since Cdc42-ko BMDCs showed a reduced capacity to capture antigens, we investigated MHC I- and MHC II-restricted antigen presentation as a functional consequence for this defect.

To study the presentation of OVA after protein uptake, we pulsed BMDCs with indicated concentrations of peptide-free whole OVA protein (Figure 7A). After three hours of antigen uptake, we induced maturation of DCs by adding LPS to the culture medium. The next day, mature, OVA-loaded BMDCs were co-cultured with transgenic T cells that recognize OVA-derived peptides in the context of MHC I (OT-I) or MHC II (OT-II). This assay was performed in round-bottom plates to overcome possible defects of Cdc42-ko BMDCs in DC:T cell contact formation (92, 93). Interestingly, we found that Cdc42-ko BMDCs failed to effectively prime both OT-I and OT-II cells (Figure 7A), as concluded from frequencies (graphs) of dividing T cells. This result could simply be a direct consequence of reduced OVA uptake (see Figure 6A,B). Therefore, we sought to overcome the inability of Cdc42-ko BMDCs to take up OVA protein by adding pre-processed OVA peptide to mature, LPS-treated cells. These pre-processed peptides are readily loaded onto MHC molecules at the cell surface by competing for antigens that occupy the binding grooves of MHC molecules. Surprisingly, we found that peptide-pulsed Cdc42-ko BMDCs still failed to fully prime OT-I and OT-II cells (Figure 7B), as shown for frequencies (graphs) of dividing T cells. These results provide evidence that Cdc42 plays a role for both MHC I- and MHC II-restricted presentation of whole protein antigen and pre-processed antigenic peptides, indicating a function of Cdc42 in DC-mediated immune responses.

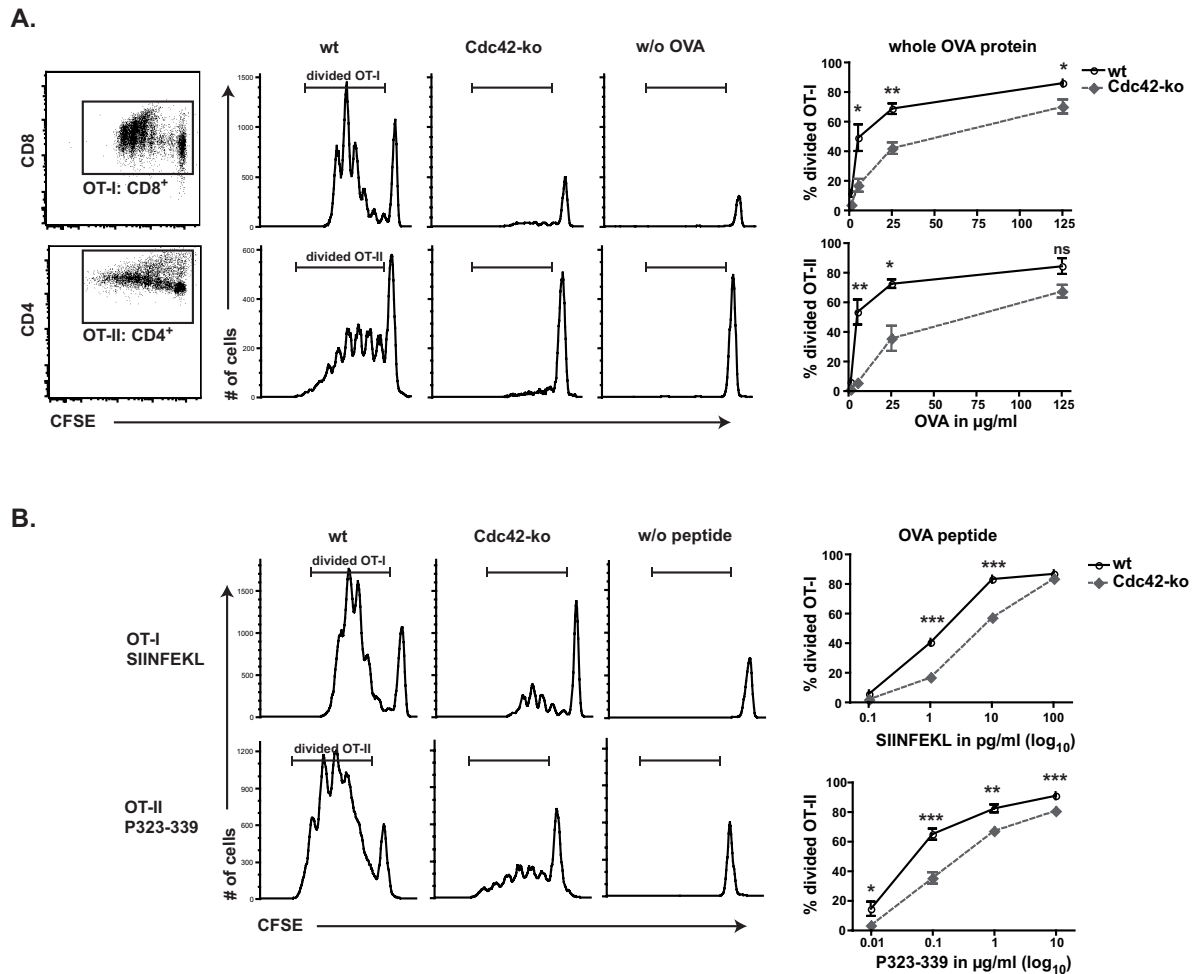


**Figure 7: Antigen presentation in the context of both MHC I and MHC II is impaired in Cdc42-ko BMDCs.**

(A) BMDCs were pulsed with the indicated concentrations of whole OVA protein (peptide-free), matured overnight in the presence of LPS and co-cultured with CD8<sup>+</sup> and CD4<sup>+</sup> OVA-specific CFSE-labeled T cells (OT-I or OT-II respectively). After 4 days of co-culture, T cell proliferation was determined as CFSE dilution. (B) For peptide presentation, BMDCs received LPS overnight and were then incubated with SIINFEKL or P323-339 pre-processed OVA peptides. After 3 hours, BMDCs were co-cultured with OT-I or OT-II cells. T-cells were harvested after 3 (OT-I) and 4 (OT-II) days of co-culture and proliferation was determined as CFSE dilution. (A, B) Diagrams show the percentage of divided T cells of one representative experiment carried out in triplicates.

## 5.2 The proteome of Cdc42-ko BMDCs

### 5.2.1 An unbiased proteomics screen

Having identified a role of Cdc42 in antigen presentation, we sought to determine factors responsible for the functional differences that occur upon Cdc42 knockout. Therefore, we analyzed the whole protein composition (proteome) of wt vs.

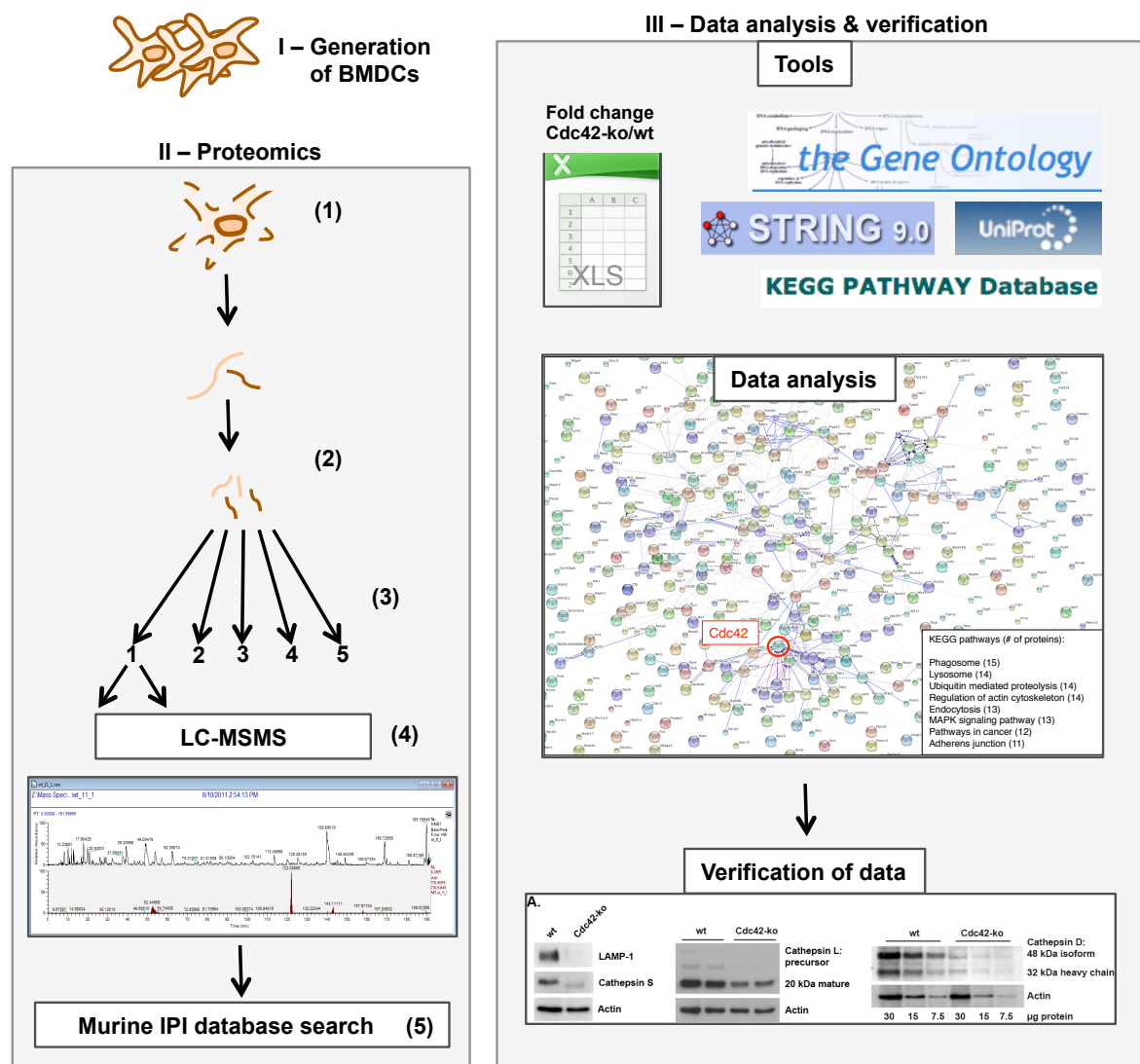


**Figure 8: Proteomics workflow.**

(I) BMDCs were generated In-house and subjected to proteomics (II). For a detailed description of the method, see (4.2.3). In brief, 20 million cells were lysed and proteins denatured using SDS (1). After detergent removal in the presence of Urea, Trypsin was used to digest the proteins (2). The resulting peptides were fractionated according to their ionic charge by anion-exchange fractionation SAX into 5 fractions (3). Two technical replicates of each fraction were measured by LC-MS/MS (4). Proteins were identified searching a murine IPI database (5) and quantification was performed on the basis of unique peptides. (III) Data analysis of proteins identified with at least 4 unique peptides was performed using the indicated online tools. Expression levels of selected proteins in wt vs. Cdc42-ko BMDCs were verified by Western blot or flow cytometry. The proteomics (part II of the experiment) were performed by Sebastian Höggl from Stefan Lichtenthaler's group at the DZNE Munich.

Cdc42-ko BMDCs by performing an unbiased quantitative proteomics screen. The workflow for this experiment is described in Figure 8. In brief, two biological replicates of wt and Cdc42-ko BMDCs were lysed and proteins digested using Trypsin. Resulting peptides were fractionated according to their ionic charge. Two technical replicates of each fraction were measured using a mass spectrometer (LC-MSMS) and the identified peptides were assigned to proteins by searching a murine IPI database on the basis of unique peptides. Wt and Cdc42-ko samples were analyzed separately from each other and resulting data sets were combined for label-free quantification as described in chapter 4.2.3.2. The final protein list contained fold change values for each identified protein as ratio of Cdc42-ko/wt, giving hints about which proteins were up- or downregulated in Cdc42 knockouts. A total of 2602 proteins could be identified from wt and Cdc42-ko BMDCs with a minimum of 4 unique peptides. This list was used for a web-based analysis of the data using the online tools shown in Figure 8 and listed in Table 9. These web pages contain information about proteins (UniProt), predicted and physical protein interactions (String database) and lists of proteins that are known to be part of a certain cellular component (the Gene Ontology) or a published pathway (KEGG PATHWAY database). Additionally, the screen was evaluated by verifying selected proteins that showed an altered abundance in Cdc42-ko BMDCs. We used both flow cytometry and Western blot analysis to verify the data set. Selected data of this verification procedure will be shown in chapter 5.3.

### 5.2.2 Pathways affected upon Cdc42 removal

To get an idea, which pathways might be affected in Cdc42-ko BMDCs, we first globally analyzed this proteomics data set. Therefore, we uploaded all proteins with fold change values (Cdc42-ko/wt)  $<-3.0$  (79 proteins) and  $>+3.0$  (475 proteins) into the String database to generate a network of known and predicted protein interactions (Figure 9). A total of 4 of these uploaded proteins were not included in this analysis, since they could not be identified by the String database. Cdc42 itself was decreased 16-fold, which matched the almost complete absence of Cdc42 from total cell lysates, as shown by Western blot in Figure 3B. Using data enrichment, the proteins were grouped according to their occurrence in the KEGG PATHWAY database, which contains a collection of pathways and associated proteins. Figure 9 shows the protein network generated by the String-database and lists the eight most affected KEGG entries in this experimental setup, and how

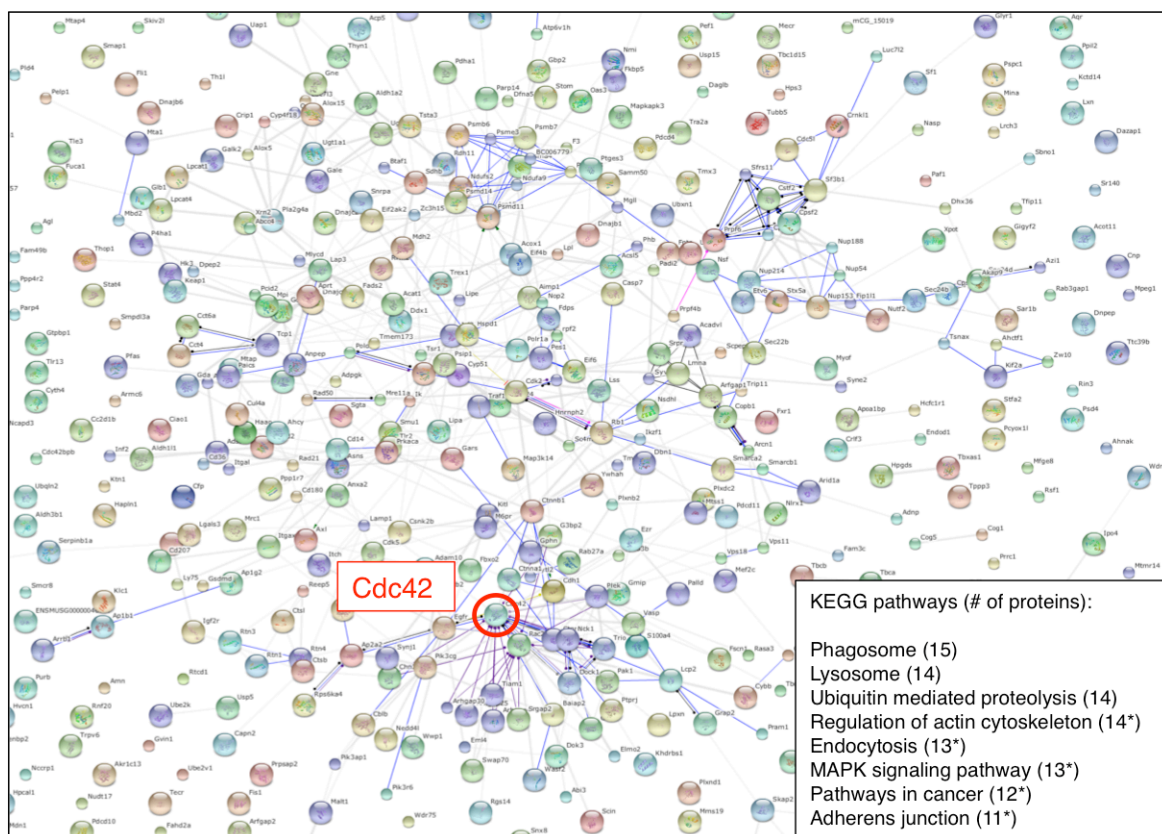


**Figure 9: Pathways affected upon Cdc42 removal.**

The diagram shows known and predicted interactions of proteins that were more than 3-fold up- or downregulated in Cdc42-ko as compared to wt BMDCs, and was generated using the String database ([www.string-db.org](http://www.string-db.org)). Each node represents one protein, lines represent direct binding of proteins (blue), catalysis (purple) or reactions (black). The 8 most abundant KEGG pathways were determined by data enrichment, which highlights the proteins that are listed in the above mentioned pathways in the KEGG database (<http://www.genome.jp/kegg/pathway.html>). For simplicity, only total numbers of input proteins matching the indicated pathways are shown in the figure. A full protein list is provided in Table 10 (see below). Pathways marked with an asterisk include Cdc42.

many of these 550 up- or downregulated proteins matched the respective KEGG entry (indicated by numbers in brackets). Interestingly, many of the identified pathways showed a clear connection to Cdc42 function. Furthermore, 5 of the 8 pathways were directly associated with Cdc42 protein. These KEGG entries were (1) Regulation of actin polymerization, (2) Endocytosis, (3) Mitogen-activated protein kinase (MAPK) signaling pathway, (4) Pathways in cancer and (5) Adherens junctions. Other pathways like Phagosome and Lysosome did not match Cdc42 itself, but proteins affected upon Cdc42 removal. Thus, removing Cdc42 from equation seemed to severely affect the lysosomal compartment of DCs, providing evidence for a previously unknown regulatory role of Cdc42 in maintaining lysosomal integrity. Table 10 provides a complete list of up- or downregulated proteins that matched the respective KEGG pathways.

**Table 10: Differentially regulated proteins in Cdc42-ko BMDCs matching the respective KEGG PATHWAY entry.**

Proteins were clustered by the String-database according to their occurrence within the respective KEGG pathway. Proteins are listed according to their gene names in alphabetical order. For more information on single proteins, see [www.uniprot.org](http://www.uniprot.org) (search: gene name and mus musculus), for their occurrence and function in the respective pathway see <http://www.genome.jp/kegg/pathway.html>.

Pathway (KEGG entry)	Differentially regulated proteins
Phagosome	Atp6v1e1, Atp6v1h, Cd14, Cd36, Ctsl, Cyba, Cybb, Lamp1, M6pr, Mrc1, Sec22b, Tap1, Tap2, TLR2, TUBB5
Lysosome	Acp5, Ap1b1, Asah1, Atp6v1h, Ctsb, Ctsl, DNase2a, Fuca1, Glb1, Igf2r, Lamp1, Lipa, M6pr, Man2b1
Ubiquitin mediated proteolysis	Birk6, Cblb, Cdc23, Cul4a, Fbxo2, Itch, Keap1, Nedd4l, Ppil2, Syvn1, Ube2k, Ube4a, Wwp1
Regulation of the actin cytoskeleton	Baiap2, Cd14, <u>Cdc42</u> , Dock1, Egfr, Git1, Itgal, Itgax, Pak1, Pik3cg, Rac2, Scin, Tiam1, Wasf2
Endocytosis	Apa2a2, Arfgap1, Arfgap2, Arrb1, Cblb, <u>Cdc42</u> , Egrf, Git1, Itch, Nedd4l, Psd4, Smap1, Wwp1
MAPK signaling pathway	Arrb1, Cd14, <u>Cdc42</u> , Egfr, Map3k14, Mapkapk3, Mef2c, Pak1, Pla2g4a, Prkaca, Ptpn7, Rac2, Rps6ka4
Pathways in cancer	Cblb, <u>Cdc42</u> , Cdh1, Cdk2, Cttna1, Ctnnb1, Egfr, Kitl, Pik3cg, Rac2, Rb1, Traf1
Adherens junctions	Baiap2, <u>Cdc42</u> , Cdh1, Csnk2b, Cttna1, Ctnnb1, Ctnnd1, Egfr, Fbxo2, Ftprj, Wasf2

### 5.2.3 Cdc42-ko DCs show abnormalities in lysosomal protein composition

The finding that the lysosome of DCs was affected upon removal of Cdc42 encouraged us to analyze the proteomics dataset with respect to lysosomal protein composition. The nature of the lysosome is crucial for antigen presentation since it contains proteases that degrade antigens and are involved in Ii processing and thus MHC II loading.

We used the Gene Ontology (GO) web site to obtain a complete list of proteins associated with the cellular component lysosome (GO:0005764). Of the 232 proteins listed under this term (as of September 2012), 82 could be identified in our screen. Of those 82 proteins, almost half (46 %) were more than 2 fold up- or downregulated in the absence of Cdc42. These changes in lysosomal protein composition were striking as compared to other GO terms analyzed in this

manner. A complete list of proteins that matched the GO term lysosome is provided in the Appendix (Chapter 7.1, Table 11).

While analyzing the GO term lysosome, we realized that besides the classical lysosomal proteins Lamp1 and Lamp2, many cathepsins were downregulated upon Cdc42 knockout (Figure 10). Interestingly, two of those, Cathepsin L (Ctsl) and Cathepsin S (Ctss), have roles for invariant chain (Ii) degradation and therefore MHC II loading. However, besides changes in the GO term lysosome there were also substantial changes in the GO term actin-binding proteins. Three interesting proteins with roles for actin-branching (Flna; Filamin a), filament capping (Capza1; F-actin capping protein subunit alpha1) and filament-severing (Scin; Adseverin) properties showed altered levels. Also, microtubule-binding proteins that play a role for actin-based cell motility (Myh10; Myosin heavy chain IIb), microtubule stability (Stmn; Stathmin) and microtubule assembly (Map4; Microtubule-associated protein 4) were affected. However, there were virtually no changes in MHC II (H2-Aa) expression and only a slight increase in the expression of the H2-M chaperone (H2-DMa/b), which functions in CLIP exchange for the antigenic peptide. Cdc42, which was decreased approximately 16-fold, is shown as positive control for the screen and Gapdh served as housekeeping protein with a normal, Cdc42-independent expression (Figure 10).

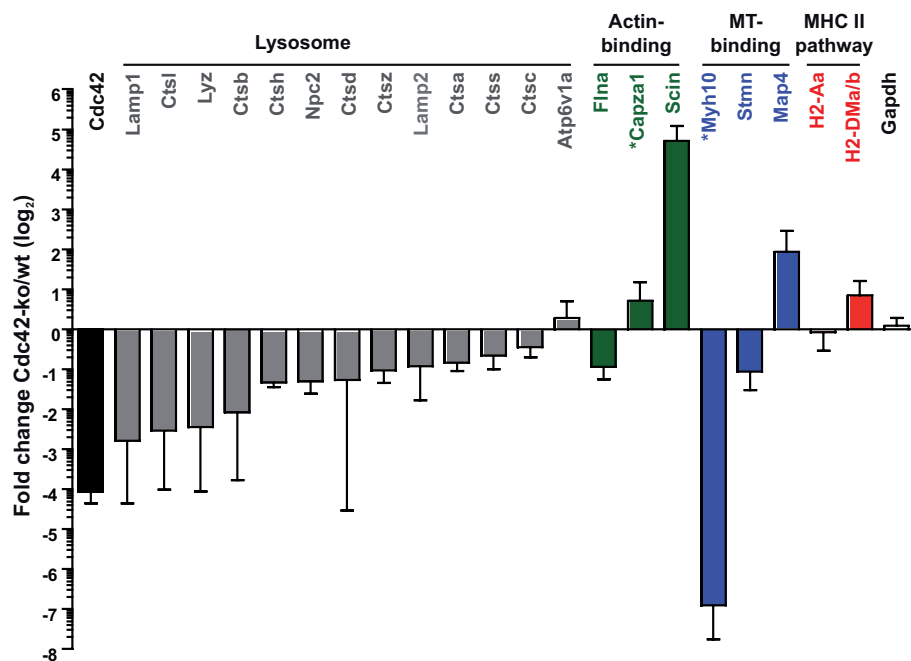


**Figure 10: Selected differentially regulated proteins in Cdc42-ko BMDCs .**

The bar graph shows fold change values (Cdc42-ko/wt) ± SEM of selected proteins that belong to the lysosomal compartment, have actin- or microtubule- (MT) binding properties, or are associated with the MHC II pathway. Proteins marked with an asterisk could not be detected with a minimum of 4 unique peptides. Data are depicted on a log<sub>2</sub>-scale.

### **5.3 Cdc42 controls invariant chain (Ii) processing and thus, MHC II loading in an actin-dependent manner**

Having performed these analyses we next sought to identify the mechanism by which Cdc42 controls MHC II antigen presentation. We have shown that Cdc42-deficient DCs, fail to present pre-processed OVA peptide in the context of MHC II (Figure 7B) despite of normal MHC II expression at the cell surface (Figure 4). Given the changes in lysosomal protein composition identified by the proteomics screen, we asked whether MHC II loading was functional.

#### **5.3.1 Confirmation of the proteomics screen: Cdc42-ko DCs lack lysosomal proteases**

To validate the proteomics screen, we performed Western blot analysis for selected lysosomal proteins. LAMP-1 (Lysosome-associated membrane glycoprotein 1) is present at lysosomal membranes and commonly used as a marker for late-endosomal/lysosomal compartments. Cathepsin D (Ctsd) is an aspartic protease that functions for protein breakdown in lysosomes, but in contrast to LAMP-1 is a soluble protein. Ctss and Ctsl are both cysteine proteases with high similarity, which can compensate for each other's loss to some extent (39). Both are active in lysosomes and especially Ctss has interesting functions for the processing of the invariant chain chaperone (Ii) that occupies the MHC II binding groove prior to antigen loading.

As shown in Figure 11A, the lysosomal proteins LAMP-1, Ctss, Ctsl and Ctsd were detected at very low amounts in Cdc42-ko BMDCs (Figure 11A). Interestingly, even the precursor forms of Ctsl and Ctsd, detected as higher molecular weight bands, were virtually absent in cells lacking Cdc42. This detail indicates that maturation of both Ctsl and Ctsd was not affected by the loss of Cdc42, as soon as their precursors entered the endocytic system. Low expression of LAMP-1 in Cdc42-ko cells was additionally confirmed by intracellular FACS analysis (Figure 11B). We tested, if the expression of these lysosomal proteins was normal at mRNA level, and performed qPCR from wt vs. Cdc42-ko BMDCs. We detected a non-significant reduction of LAMP-1, Ctsl and Ctsd mRNA in Cdc42-ko BMDCs, whereas the expression of Ctss mRNA was normal (Figure 11C). These data provide evidence that the Cdc42-dependent regulation of lysosomal protein contents most likely occurs at the protein level.

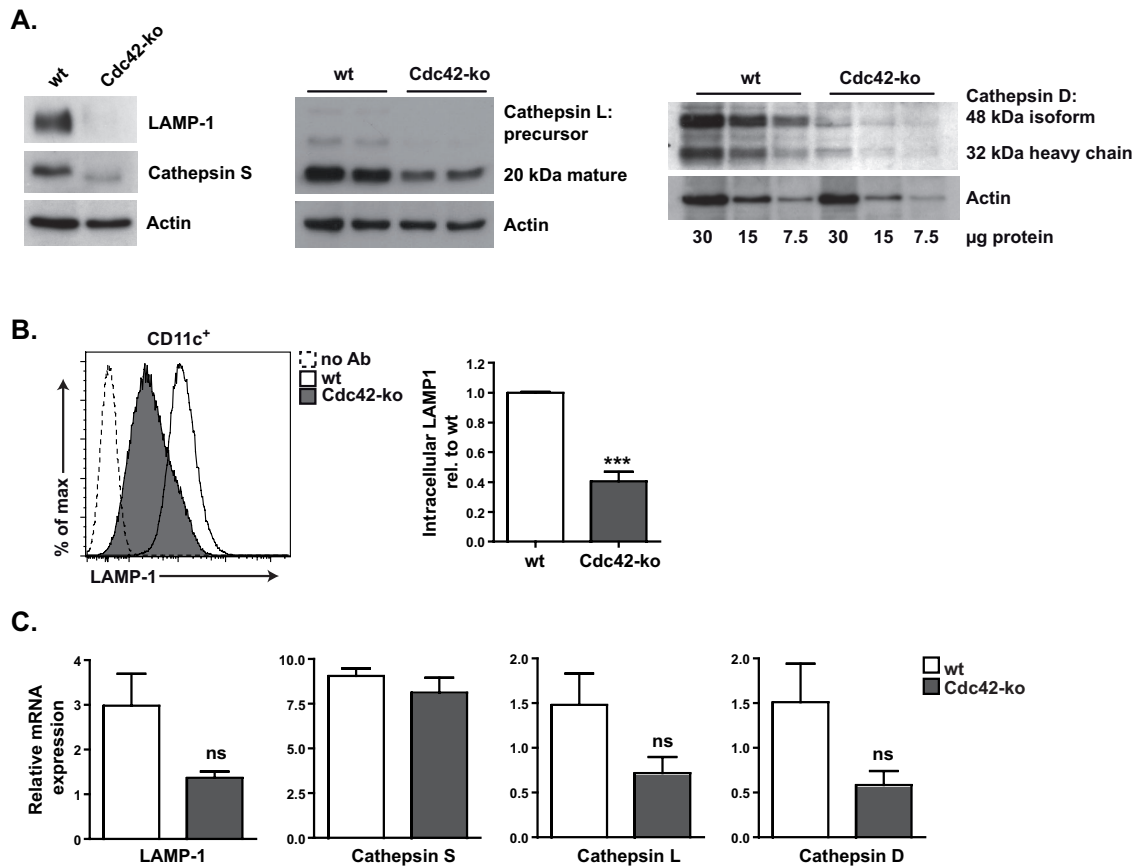


**Figure 11: Cdc42-ko BMDCs lack lysosomal proteins, which are expressed at normal amounts on mRNA level.**

(A) BMDC total cell lysates were analyzed by Western blot using specific antibodies for LAMP-1 and Cathepsin S, L and D. Actin was used as loading control. Each Western blot shows one representative out of at least three independent experiments. (B) Intracellular FACS analysis on fixed and permeabilized BMDCs confirms a downregulation of LAMP-1 protein. MFI are depicted as relative to wt gating on CD11c<sup>+</sup> cells. The histogram shows pooled data from two independent experiments (n=3). (C) mRNA expression of all lysosomal proteins shown in (A) was measured by qPCR. Data are from a single experiment carried out in triplicates.

### 5.3.2 The lack of Cathepsin S in Cdc42-ko BMDCs causes an MHC II loading defect by inhibiting Ii processing

Having shown that Cdc42-ko BMDCs express low levels of lysosomal enzymes including Ctss, we wondered whether MHC II loading was functional. MHC II occupied by Ii travels from the ER either directly to the MIIC, or via the plasma membrane. Therefore, Ii occupies a small portion of MHC II at the plasma membrane. This protein complex can be detected using an antibody (clone 15G4) that recognizes Ii in the context of MHC II with high affinity for the p12 fragment and low affinity for the p31 and p41 fragments of Ii.

We stained wt and Cdc42-ko BMDCs for surface-Ii and analyzed both groups by flow cytometry. Surprisingly, we could detect high levels of Ii at the cell surface of Cdc42-ko BMDCs (Figure 12A). Furthermore, Ii surface expression increased on

both wt and Cdc42-ko cells upon maturation, indicating that immature DCs possessed a large pool of intracellular Ii-bound MHC II that appeared only in parts at the plasma membrane. Next, we calculated a ratio between the MFI of Ii-bound MHC II (MFI clone 15G4) and total MHC II (MFI clone AF6-120.1,) and found that unstimulated as well as mature Cdc42-ko BMDCs expressed approximately 2-fold higher amounts of 15G4 epitopes relative to total MHC II epitopes (Figure 12B).

In immature DCs, Ii-bound MHC II molecules are quickly internalized from the plasma membrane and transported to MIICs. Therefore, we assessed internalization of Ii-bound MHC II, as a possible reason for its accumulation at the plasma membrane (Figure 12C). BMDCs were labeled for surface-Ii using antibody clone 15G4 (T=0) and internalization of the antibody was assessed after indicated times by detection of remaining antibody. Interestingly, Cdc42-ko BMDCs showed a much slower internalization rate of Ii as compared to wt cells, indicating that the expression of Ii-bound MHC II is stabilized at the cell surface of DCs in a Cdc42-dependent manner. However, also total MHC II was stabilized on the cell surface of Cdc42-ko BMDCs in a similar manner (data not shown), indicating a role of Cdc42 in MHC II trafficking as a general phenomenon upon Cdc42 knockout.

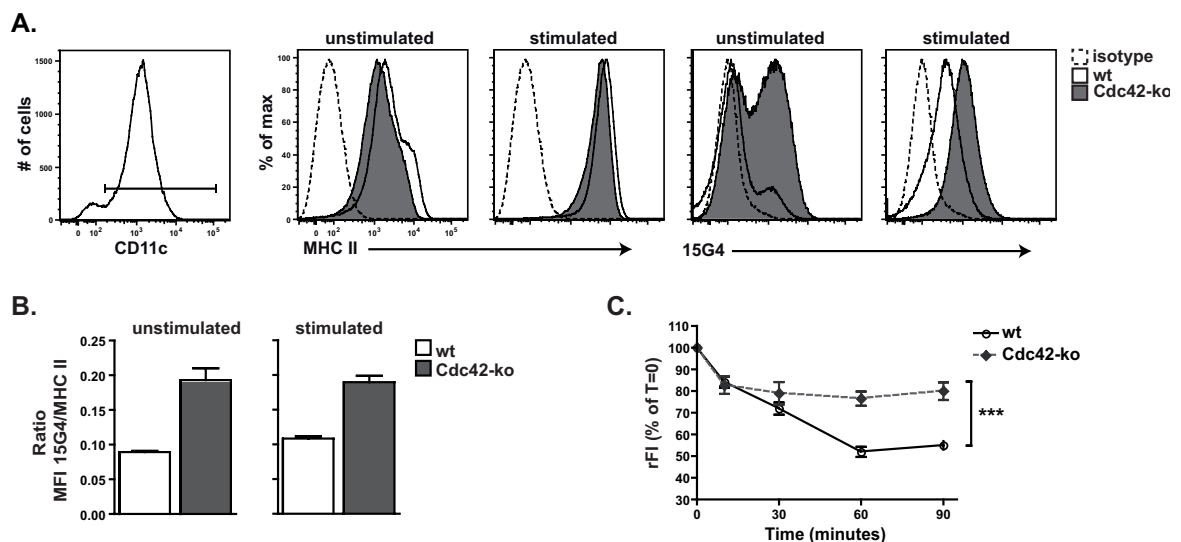


**Figure 12: Cdc42-ko BMDCs accumulate Ii-occupied MHC II molecules at the cell surface.**

(A) BMDCs were stained for total cell surface MHC II and 15G4 epitopes and analyzed by flow cytometry. Mature BMDCs were generated by overnight LPS treatment. (B) MFI values obtained from (A) were used to calculate the ratio of Ii-bound MHC II (clone 15G4) to total surface MHC II (clone AF6-120.1), which gives an indication about how much MHC II is occupied by Ii in wt vs. Cdc42-ko BMDCs. Bar graphs show one representative experiment out of 10 with 2 biological replicates. (C) Internalization of the 15G4 antibody was measured by detection of remaining 15G4 antibody at the indicated times. The graph shows relative fluorescence intensity (rFI) values on CD11c<sup>+</sup> cells as percentages of time zero. Data are from pooled experiments.

Having shown that Ctss is present at low concentrations (Figure 11A) and that Ii accumulates at the cell surface of *Cdc42*-ko BMDCs (Figure 12), we wondered whether Ii processing was functional in the absence of *Cdc42*. Figure 13A (94) summarizes Ii processing and the proteases involved. In brief, Ii processing proceeds from C-terminal to N-terminal direction along the endocytic route, including non-cysteine (purple fond) and cysteine (green fond) proteases. The non-cysteine protease asparagine endopeptidase (AEP) mediates the first processing step by degrading the 31kDa intermediate p31 of Ii (also expressed as 41kDa isoform p41) into a 22kDa fragment p22, which is then rapidly transformed into a 10kDa degradation intermediate p10 (also expressed as 12kDa isoform p12). Ii-p10/12 is the smallest fragment of Ii that still comprises its transmembrane domain and is further processed into CLIP. According to the literature Ctss conducts the final step of Ii-p12 degradation in DCs, separating the CLIP fragment at the luminal part of the protein, which occupies the MHC II binding groove,

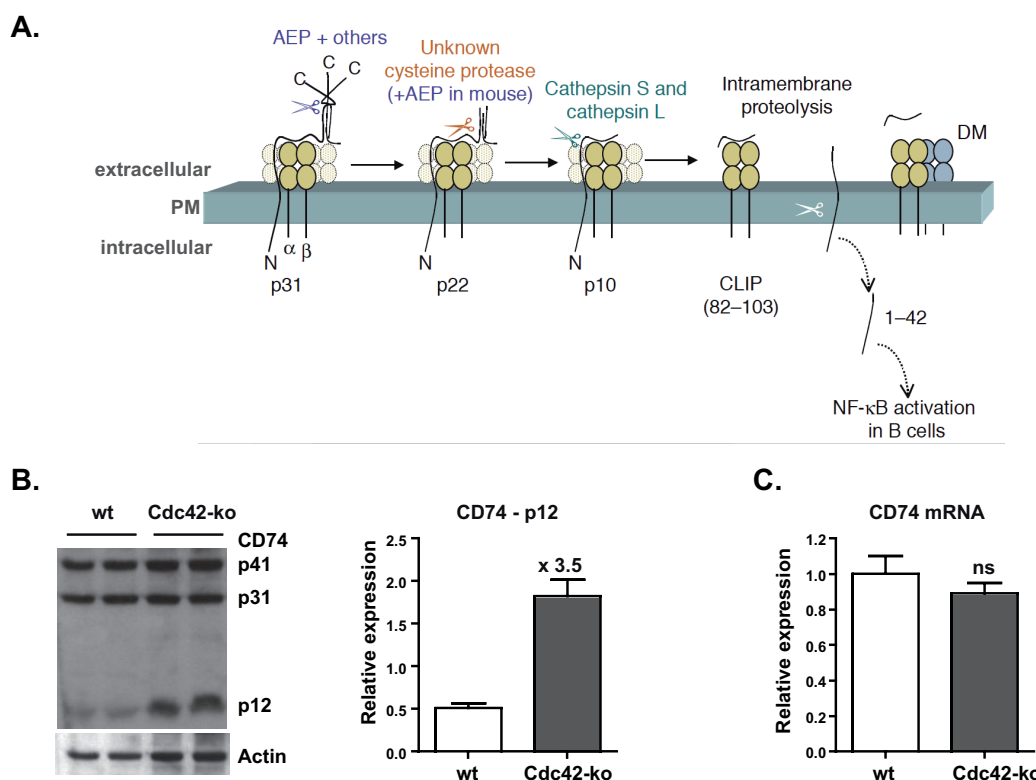


**Figure 13: The Ii degradation intermediate p12 accumulates in *Cdc42*-ko BMDCs.**

(A) Model of Ii processing published by Colin Watts, 2004 (94). For description, see text. (B) BMDC total cell lysates were analyzed by Western blot using a specific antibody for Ii (clone In-1) that recognizes a 41 and a 31kDa isoform as well as a 12kDa processing intermediate of Ii (termed p41, p31 and p12 of CD74). Actin was used as loading control. Bar graph shows a quantification of the Western blot (n=2). (C) To look at Ii message, RNA was isolated from unstimulated wt and *Cdc42*-ko BMDCs and qPCR was performed using CD74 specific primers. Relative expression levels of CD74 mRNA are from three combined experiments, each with a minimum of two mice per group.

from its transmembrane domain.

To study Ii degradation at the protein level, we used a CD74 antibody (clone In-1) that recognizes an epitope at the short N-terminal part of the Ii chaperone that faces the cytoplasm. Hence, the antibody recognizes all forms of Ii that still include the transmembrane domain, namely the p41, p31 and p12 degradation intermediates of Ii.

Indeed, we could detect all above mentioned degradation intermediates of Ii in total cell lysates from wt and Cdc42-ko BMDCs (Figure 13B). Notably, wt BMDCs expressed high amounts of 41 and 31kDa isoforms, whereas the 12kDa fragment was present at low abundance, due to its rapid degradation. In Cdc42-ko BMDCs, on the other hand, the 12kDa fragment accumulated more than three fold as compared to wt cells. This Ii degradation arrest in Cdc42-ko BMDCs would be in agreement with reduced Ctss levels in these cells as shown in Figure 11A. To exclude a regulation of Ii (CD74) expression on the mRNA level, we performed qPCR on total RNA from wt vs. Cdc42-ko BMDCs and found Ii message expressed at normal amounts (Figure 13C). This finding supports our interpretation that Cdc42-dependent Ii processing is regulated on the protein level.

### **5.3.3 Functional actin dynamics are required for both lysosomal integrity and Ii degradation**

We have shown that Cdc42 controls the expression of lysosomal proteases (Figure 11A,B) with effects on Ii degradation (Figure 13B) and MHC II loading (Figure 12). Ii-occupied MHC II molecules at the cell surface of Cdc42-ko BMDCs possibly hinder the presentation of pre-processed OVA peptides to OT-II cells (Figure 7B and Figure 12). However, the mechanism by which Cdc42 controls these processes remains unclear. Therefore, we studied actin and microtubule dynamics as well as endosomal acidification with respect to intracellular protease levels and Ii degradation.

Our approach was to target wt BMDCs with inhibitors that (i) globally inhibit actin polymerization through their direct interaction with the actin filament, (ii) inhibit microtubule dynamics or (iii) inhibit endosomal acidification. Latrunculin B (LatB) binds G-actin forming a 1:1 molar complex, thereby preventing monomers from re-polymerizing into filaments. Cytochalasin D (CytD), on the other hand, inhibits actin polymerization by capping filaments at their plus, fast growing barbed ends in a 1:1 stoichiometry. To discriminate

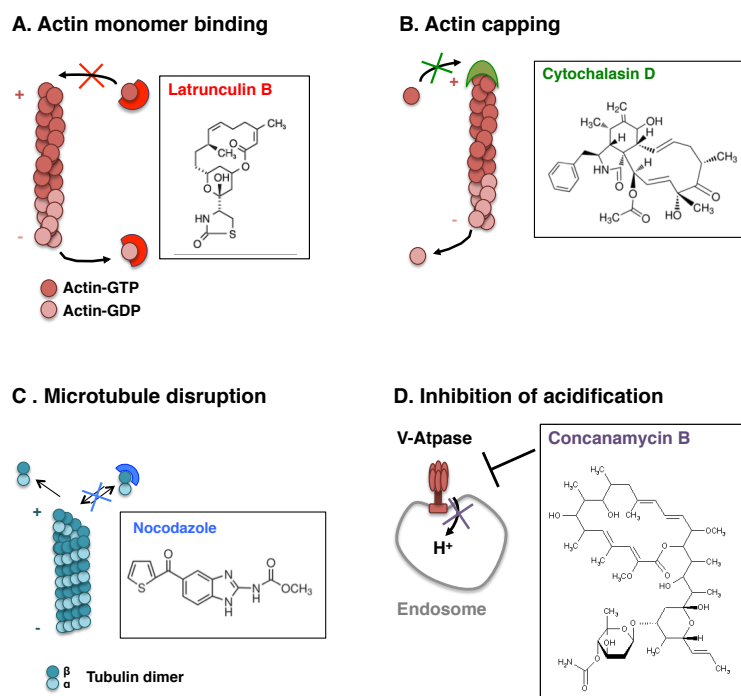


**Figure 14: Inhibitors used to disrupt actin, microtubules and endosomal acidification and modes of action.**

All above mentioned inhibitors are small molecules and freely permeable through cell membranes. For description, see text. Mechanisms of Latrunculin B (A) and Cytochalasin D (B) modes of action are based on Morton et al., 2000 (79) and John A. Cooper, 1987 (78) respectively. (C) Microtubule scheme is adapted from Conde & Caceres, 2009 (95). (D) V-ATPase functions were described by Michael Forgac (96).

between actin and microtubule dynamics, Nocodazole (Noco) was used as a microtubule-disrupting drug, which binds to both free and assembled tubulin causing conformational changes. Concanamycin B (ConB) was used to inhibit the V-ATPase proton pump, which is required for proton translocation into the vesicle and therefore endosomal acidification (see also Figure 14).

We treated BMDCs with these inhibitors overnight and looked for cell surface-Ii expression using antibody clone 15G4. Upon direct actin inhibition by either LatB or CytD, large amounts of both MHC II and Ii-bound MHC II (15G4) were transported to the cell surface of wt BMDCs, which resulted in an accumulation of MHC II molecules at the cell surface (Figure 15A, left panel). As for Cdc42-ko BMDCs (Figure 12B) we calculated the amount of Ii-bound MHC II as a ratio relative to total cell surface-MHC II expression of inhibitor-treated cells. Interestingly, specifically actin disruption, but not the inhibition of microtubules or V-ATPase mediated acidification of endosomes lead to an accumulation of Ii at the cell surface of wt BMDCs (Figure 15A, right panel).

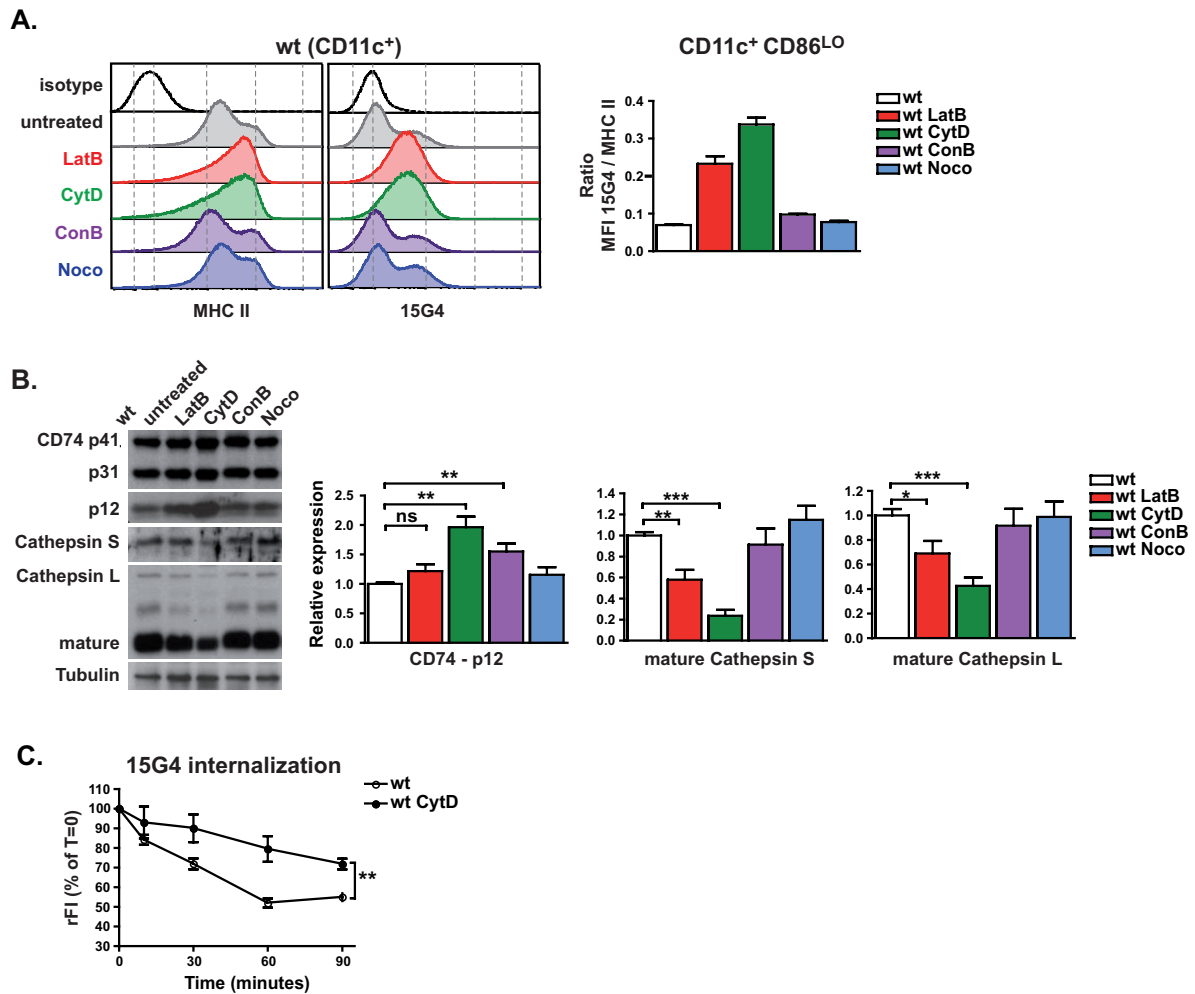


**Figure 15: MHC II loading and processing are impaired upon actin inhibition in wt BMDCs.**

(A) Wt BMDCs were incubated with the actin inhibitors LatB and CytD overnight or left untreated. The next day, total surface MHC II (clone AF6-120.1) and Ii bound to MHC II (clone 15G4) were analyzed by flow cytometry. The effects of V-ATPase inhibitor ConB and microtubule inhibitor Noco were also analyzed in this manner. Analysis was done gating on CD11c<sup>+</sup>CD86<sup>LO</sup> cells (not shown). Bar graphs show the ratio of MFI 15G4/total surface MHC II of one representative experiment out of 3 (n=2). (B) Wt BMDCs were treated with inhibitors as mentioned in (A) and total cell lysates were analyzed by Western blot. Membranes were probed for Cathepsin L, Cathepsin S and Ii (CD74). Tubulin served as loading control. Bar graphs show a quantification of protein expression levels from two independent experiments (n=2) normalized to actin or tubulin. (C) Internalization of the 15G4 antibody in untreated vs. CytD-treated wt BMDCs was assessed by detection of remaining antibody at the indicated times. The graph shows relative fluorescence intensity (rFI) values on CD11c<sup>+</sup> cells as percentages of time zero from pooled experiments.

DCs react strongly upon treatment with minimal doses of LPS or other bacteria-derived stimuli, which unfortunately often contaminate solutions. To exclude the possibility that the observed upregulation of MHC II on inhibitor-treated DCs simply represented a mature phenotype as a result of inhibitor-treatment, we analyzed BMDC supernatants for pro-inflammatory cytokines (Figure 16A); culture supernatants from LPS-treated BMDCs served as positive control. However, inhibitor-treated wt BMDCs neither showed elevated levels of pro-

inflammatory cytokines nor an increase in mRNA expression of CD86 and CD40 (Figure 16B), indicating that the upregulation of MHC II at the cell surface was not due to DC maturation, but specifically due to the inhibition of the actin cytoskeleton.

Next, we looked at Ii processing and intracellular Ctss and Ctsl expression by Western blot on inhibitor-treated wt BMDCs. We observed an accumulation of the smallest 12kDa fragment of Ii, similar to what was observed in DCs that lacked Cdc42 (Figure 15B and Figure 13B). Furthermore, actin inhibition lead to a substantial reduction of both Ctss and Ctsl levels from total cell lysates of inhibitor-treated wt BMDCs. Interestingly, also these effects could be dedicated specifically to the actin cytoskeleton, since disruption of microtubules using Noco did not show an effect. However, inhibition of V-ATPase using ConB also

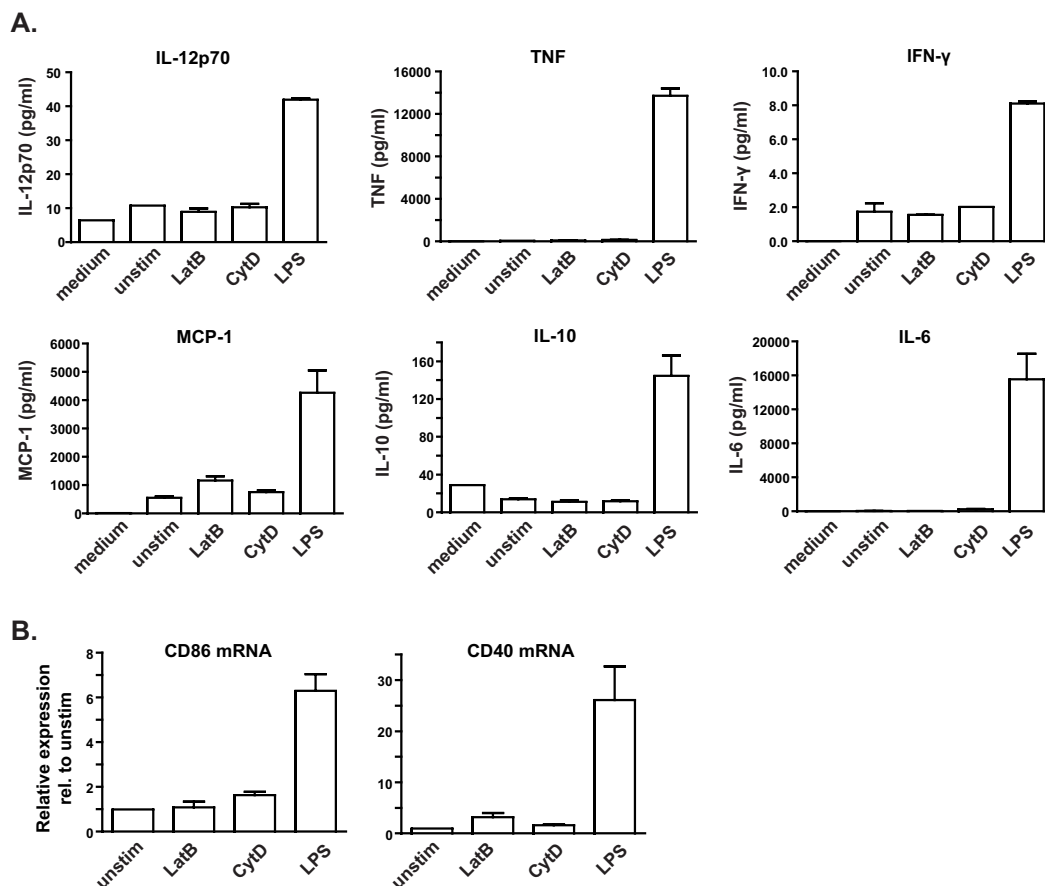


**Figure 16: Treatment with actin inhibitors does not induce maturation of BMDCs.**

(A) To exclude an effect on DC maturation, supernatants of wt DCs pulsed with LatB or CytD were analyzed using a cytometric bead array (CBA, Mouse Inflammation Kit). Supernatants were tested for pro-inflammatory cytokines; LPS-treated culture supernatants served as positive control. Bar graphs show one of two independent experiments carried out in duplicates. (B) mRNA transcription of co-stimulatory molecules was assessed to exclude the possibility that inhibitor treatment activates BMDCs. RNA from unstimulated and inhibitor-treated cells was isolated and CD86 and CD40 mRNA expression was analyzed by qPCR. HPRT was used as housekeeping gene. Data are from two experiments (n=4).

significantly increased p12 expression in inhibitor-treated wt BMDCs, which indicates that endosomal acidification might also be relevant for Ii degradation.

In immature DCs, Ii-bound MHC II is efficiently internalized from the plasma membrane by endocytosis and targeted to the MIIC. Inhibition of actin dynamics could thus, similar to the loss of Cdc42 from cells (see Figure 12C), lead to a retention of Ii at the plasma membrane. To evaluate, whether the surface accumulation of Ii upon actin inhibition was due to a decreased internalization rate of Ii-bound MHC II molecules, we tested the internalization of the 15G4 antibody and found that it was indeed stabilized on the cell surface of CytD treated wt cells (Figure 15C).

From this series of experiments we concluded that functional actin dynamics were definitely required for both Ii re-internalization from the plasma membrane and lysosome biogenesis as a prerequisite for functional Ii processing.

Since lysosomal proteins were present at low amounts in Cdc42-ko BMDCs and disappeared from wt cells upon actin inhibitor-treatment, we sought to determine the reason for this loss of lysosomal contents from cells that lacked Cdc42, or cells treated with actin inhibitors. One possibility of regulating intracellular protease content is secretion. Therefore, we wanted to know whether actin inhibition caused secretion and we tested if secreted proteins were detectable in the supernatant.

To evaluate CtSI levels in culture supernatants, equal amounts of protein were analyzed because this method lacks a loading control. Medium served as negative control and signals were quantified relative to supernatants from untreated wt BMDCs. As shown in Figure 17A actin inhibition by LatB and CytD indeed lead to an accumulation of mature CtSI in culture supernatants, whereas ConB and Noco treatment did not show an effect. Notably, also maturation of BMDCs using LPS did not alter extracellular CtSI levels significantly (data not shown), indicating that the export of CtSI was maturation-independent.

We used Western blot data from total cell lysates and supernatants and calculated the fold secretion of total mature CtSI contents, which visualizes the imbalance of intra- and extracellular CtSI levels upon actin inhibition or Cdc42 knockout (Figure 17B). CytD treatment of wt cells lead to an approximately 14-fold increase in secretion of total mature CtSI contents. The same tendency was observed for

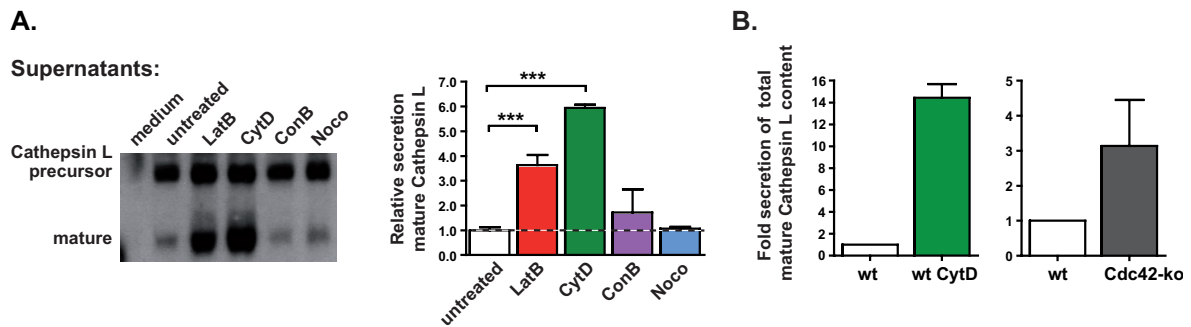


**Figure 17: Upon actin inhibition, lysosomal contents are secreted into culture supernatants.**

(A) Culture supernatants of inhibitor-treated wt BMDCs were analyzed by Western blot for Ctsl secretion. For this purpose, equal amounts of protein were loaded; medium was used as negative control. Bar graphs show a quantification of protein expression levels from one representative experiment (n=2) normalized to wt untreated. (B) Bar graphs show fold secretion of total 20kDa Cathepsin L (mature Ctsl) content taking into account intracellular and extracellular Ctsl. One representative experiment out of at least three with n=2 is shown.

untreated Cdc42-ko BMDCs, which secreted approximately three times more Ctsl as compared to untreated wt BMDCs (Figure 17B).

These results provide evidence that upon direct actin inhibition by LatB or CytD, DCs translocate mature Ctsl into culture supernatants, possibly as a default pathway. By treating DCs with actin inhibitors, we could therefore induce a phenotype similar to untreated Cdc42-deficient DCs. However, it may be noted here that Cdc42-deficient BMDCs showed a downregulation of lysosomal protein levels including Ctsl already in the steady-state (Figure 11A and B), whereas wt cells bore full stores of these proteins that could be secreted upon actin inhibition. Thus, inhibitor treated wt as well as untreated Cdc42-ko BMDCs both might secrete the amount of Ctsl at their disposal, which could explain the differences in the secretion of total Ctsl contents (Figure 17B).

### 5.3.4 Cdc42 acts via the Arp2/3 complex on the actin cytoskeleton, with no impact on li processing

Having shown in the previous chapter that global inhibition of the actin cytoskeleton had an impact on MHC II loading, we next wanted to investigate the mechanism Cdc42 might use to control actin dynamics. We used previously published inhibitors targeting protein complexes that, via Cdc42, lead to changes in the actin network. Figure 18 summarizes these inhibitors and their mode of action. In brief, CK-548 inhibits the Arp2/3 complex required for the branching of actin filaments. SMIFH2 inhibits a formin dimer important for the linear polymerization of filaments. Both CK-548 and SMIFH2 are drugs that inhibit

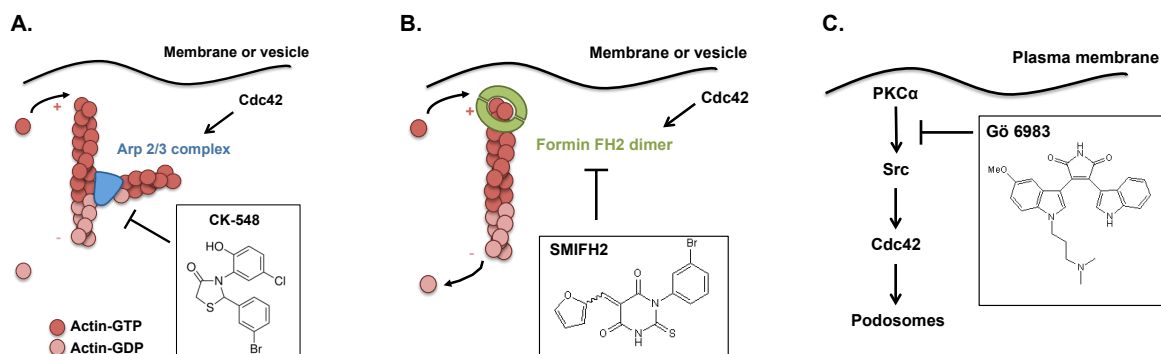


**Figure 18: Inhibitors used to target Cdc42-dependent actin polymerization and modes of action.**

(A) The Arp2/3 complex is required for the branching of actin filaments. CK-548 inhibits Arp2/3 binding to filaments and therefore filament branching. (B) Formins surround actin filaments at their plus end, thereby preventing binding of capping proteins. SMIFH2 inhibits the formin FH2 dimer required for a linear growth of the filament. (C) Protein kinase C (PKC $\alpha$ ) signaling is required for Cdc42-dependent podosome formation. The complex can be inhibited using Gö 6983. CK-548 and SMIFH2 target processes downstream of Cdc42, whereas Gö 6983 inhibits an upstream signaling cascade. All inhibitors are small molecules that are freely permeable through cell membranes. (A) and (B) were adapted from Campellone and Welch, 2010 (97). Model (C) was adapted from Tatin et al., 2006 (59).

complexes downstream of Cdc42 signaling required for functional actin dynamics.

The inhibitor Gö 6983, on the other hand, inhibits PKC $\alpha$  signaling upstream of Cdc42, which leads to an arrest of Cdc42-dependent podosome formation.

Figure 19A shows a titration of the Arp2/3 inhibitor CK-548 on wt BMDCs and its impact on Ii-bound MHC II complexes at the cell surface of these cells. Also the effects of SMIFH2 and Gö 6983 were analyzed in this manner. Upon treatment with the highest concentration of CK-548 over 80 % of cells died (gate R1). By gating on DAPI-CD11c<sup>+</sup> cells (gate R2) we could detect a slight upregulation of Ii at the cell surface using a high dose of CK-548, but this phenotype was modest as compared to unstimulated Cdc42-ko BMDCs (Figure 12). However, the effect was significant (Figure 19A), even though we could not observe a titration effect at lower concentrations of the inhibitor. The inhibitors SMIFH2 and Gö 6983 did not influence surface-Ii expression on wt BMDCs (Figure 19A). Furthermore, the treatment of wt BMDCs with CK-548, SMIFH2 or Gö 6983 had neither an effect on Ii processing nor intracellular protease expression, as observed by analyzing total cell lysates for the expression of Ii (CD74 p41, p31, p12) and Ctst1 by Western blot (Figure 19B). Due to dead cell contents in lysates at the highest concentration of CK-548 the signal obtained could not be quantified (Figure 19B, second lane).

We next investigated culture supernatants of inhibitor-treated cells for extracellular Ctst1 and found that specifically the mature form of Ctst1 accumulated upon CK-548 treatment (Figure 19C). Ctst1 precursor protein, which was expressed

at stable amounts upon inhibitor treatment, constitutes an internal control excluding an influence of dead cell contents on extracellular CtSI levels. Furthermore, we could detect a titration effect for secretion of mature CtSI that mirrors CK-548 titration. The inhibitors SMIFH2 and Gö 6983 showed no effect on CtSI secretion (Figure 19C). We concluded that specifically Arp2/3-mediated actin disruption resulted in an enhanced secretion of mature CtSI (Figure 19B) and an upregulation of surface-Ii expression at the highest concentration of CK-548 (Figure 19A, right bar graph).

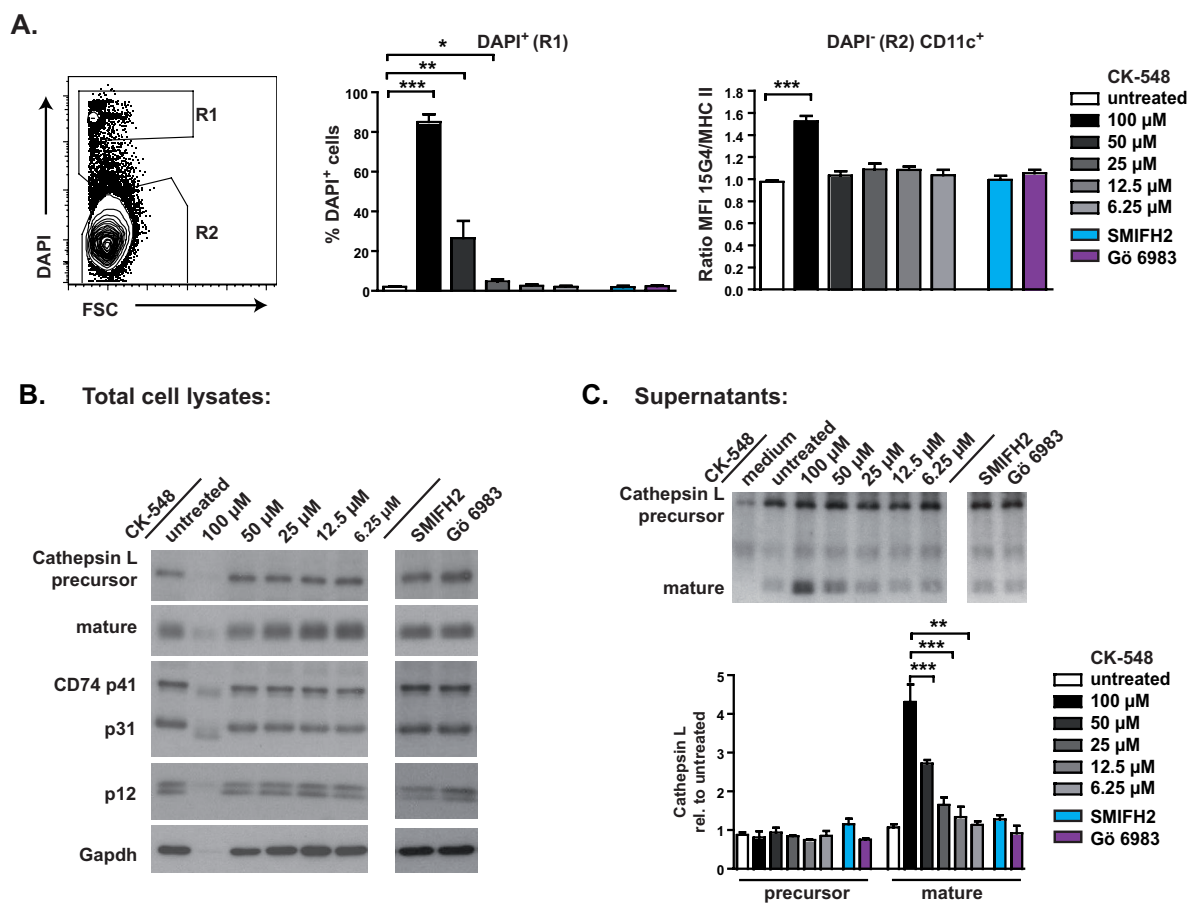


**Figure 19: Inhibition of the Arp2/3 complex has an impact on surface-Ii expression and influences CtSI secretion.**

(A) Wt BMDCs were treated with the indicated concentrations for CK-548, SMIFH2, Gö 6983 or left untreated. Analysis was done by flow cytometry based on DAPI staining for dead cell exclusion and surface-Ii expression (Ratio MFI 15G4/MHC II), the latter gating on DAPI<sup>-</sup>CD11c<sup>+</sup> cells. Bar graphs show two experiments (CK-548, n=4; SMIFH2, n=3) and three experiments (Gö 6983, n=6) with similar results. (B) Total cell lysates of inhibitor-treated wt BMDCs were analyzed for Cathepsin L and Ii (CD74) expression by Western blot. Gapdh served as loading control. One representative experiment out of two is shown. (C) Supernatants of inhibitor-treated wt BMDC cultures were analyzed by Western blot for Cathepsin L secretion. Medium served as negative control and signals were quantified relative to wt untreated. Bar graph shows one representative experiment (n=2) out of two with similar results.

### 5.3.5 BMDCs defective for clathrin-mediated vesicle budding secrete mature Ctsl into culture supernatants

Soluble lysosomal proteases exit the Golgi apparatus via clathrin-coated pits that bud off the trans-Golgi network (TGN) in an Arp2/3- and actin-dependent manner (26, 27). Therefore, we wondered whether clathrin-mediated vesicle budding played a role for Ctsl secretion.

We used the recently published inhibitor Pitstop 2, which inhibits clathrin-mediated endocytosis at the plasma membrane and possibly clathrin-dependent vesicle budding at the TGN (82). Interestingly, we observed that Pitstop 2-treated wt BMDCs secreted elevated amounts of mature Ctsl as compared to untreated wt cells, as shown by Western blot on inhibitor-treated culture supernatants (Figure 20). A quantification of both precursor and mature Ctsl protein expression visualized that predominantly the mature form of the protease was secreted—similar to what we observed upon Arp2/3 inhibition of wt cells (Figure 19C, Figure 20). However, there was no effect on either cell surface expression of Ii-bound MHC II, or Ii processing and intracellular protease levels (data not shown), which is therefore a rather mild phenotype with respect to MHC II loading as compared to the direct inhibition of actin (Figure 15B).

Clathrin coated pits and vesicles also contain Hip1r, which is thought to be a linker protein between the endocytic machinery and the actin cytoskeleton. Figure 21A (taken from (26)) shows the protein composition at clathrin coated vesicles (CCV) at both the plasma membrane and the TGN including actin nucleating and actin binding factors. In brief, F-Bar binding proteins (FCHO)

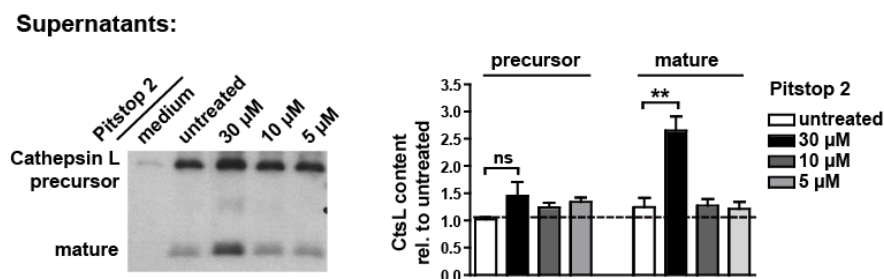


**Figure 20: Clathrin inhibition leads to an accumulation of mature Ctsl in culture supernatants.**

Wt BMDCs were treated with the indicated concentrations of Pitstop 2, an inhibitor for clathrin-mediated endocytosis, and supernatants were analyzed for Cathepsin L secretion by Western blot. Signals obtained from Western blot were quantified relative to wt untreated. Bar graph shows combined data of two independent experiments with similar results (n=3).

initially deform the membrane and, like clathrin, bind actin-nucleating factors. One of the proteins that connects the emerging vesicle with pre-existing F-actin filaments is Hip1r. Also, this protein might prevent actin polymerization at the coat surface of the vesicle and dissociate upon vesicle budding. Therefore, Hip1r might function as a negative regulator of vesicle scission. In order to release the vesicle from membranes actin nucleating factors like F-Bar domain proteins (BDPs), N-Wasp, Cdc42 and Arp2/3 provide the mechanical force to bend and push membranes.

To find out, whether Hip1r expression is affected upon Cdc42 knockout, we examined Hip1r protein expression in Cdc42-ko BMDCs (proteomics:  $4.6 \pm 1.64$  fold change Cdc42-ko/wt  $\pm$  SEM;  $\geq 2$  unique peptides). Interestingly, Hip1r was slightly upregulated in the absence of Cdc42, although not to an extent that was statistically significant ( $p=0.0732$ ,  $n=4$ ; Figure 21B). However, we concluded that vesicle coat components at both the plasma membrane and the TGN could be regulated in a Cdc42-dependent manner and might add up to their poor ability to provide functional vesicle transport.

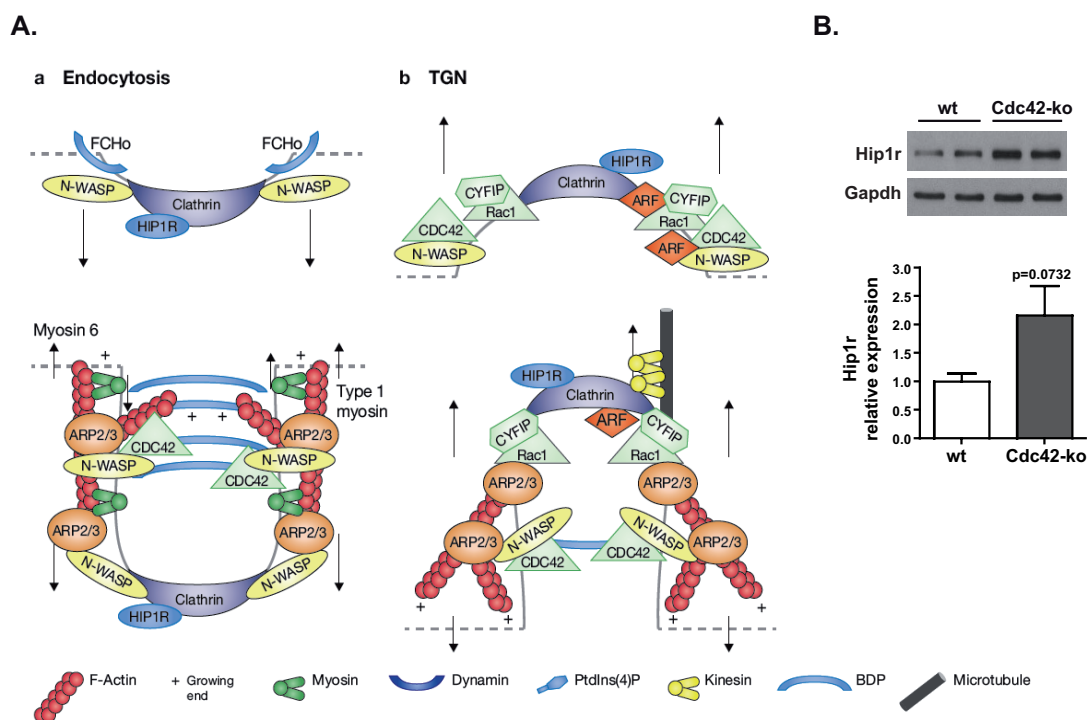


**Figure 21: Hip1r is slightly upregulated in Cdc42-ko BMDCs.**

(A) Model of clathrin carrier biogenesis at the plasma membrane (a) and the trans-Golgi network (b). For description see text. Figure from Anitei & Hoflack, 2012 (26) (B) Total cell lysates of wt and Cdc42-ko BMDCs were analyzed for the expression of Hip1r protein by Western blot; Gapdh served as loading control. The bar graph shows results from two experiments ( $n=4$ ). The difference in protein expression was not significant ( $p=0.0732$ ).

### **5.3.6 Summary of processes affected upon Cdc42 knockout with implications for MHC II loading**

In this chapter we provided evidence that Cdc42, possibly via its interaction with the actin cytoskeleton, interferes with lysosomal protease targeting to late endosomes. The inability to generate functional late endosomal compartments results in defective Ii processing and Ii-occupied MHC II molecules.

In brief, we showed that Cdc42-ko BMDCs failed to acquire sufficient amounts of antigens to induce proper immune responses. Furthermore, the composition of late endosomes was altered, resulting in a degradation arrest of Ii. Hence pre-occupied MHC II molecules accumulated at the plasma membrane as a result of their decreased re-internalization. This stabilization at the cell surface was actin-dependent, as was protease targeting to late endosomes, where Ii processing takes place. Altogether we describe a previously unknown role of Cdc42 that in an actin-dependent manner affects MHC II loading.

## 5.4 Phenotype of Cdc42-ko mice

### 5.4.1 DC subsets in spleen and lymph nodes of Cdc42-ko mice

The availability of Cdc42-ko mice gave us the possibility to study Cdc42 function *in vivo*. As described in our publication (Paper I) especially migratory DCs isolated from different organs of mice were strongly affected upon Cdc42 knockout. I would like to refer to the original publication for further detail on the migration of Langerhans cells, but will mention here selected findings published in this paper that are important for the current subject:

Spleen DCs were present at both normal frequencies and numbers in Cdc42-ko mice as compared to wt mice (Paper I, Supplementary Figure S1A), which also applied when CD8<sup>+</sup> and CD8<sup>-</sup> DC subsets were analyzed separately from each other (data not shown). The knockout in purified spleen DCs, analyzed as a representative *in vivo* DC subset, was not complete as judged from residual Cdc42 protein detected by Western blot (Paper I, Supplementary figure S1D). However, these cells were already devoid of functional Cdc42 mRNA (data not shown), indicating that their lifespan might be not long enough in order to metabolize 100 % of remaining Cdc42 protein.

In contrast, in skin-draining lymph nodes we observed substantial changes. Both frequencies and numbers of CD11c<sup>+</sup>MHC II<sup>HI</sup> migratory DCs were dramatically reduced (\*\*p<0.0001), whereas CD11c<sup>+</sup>MHC II<sup>IM</sup> resident DCs, represented in significantly elevated frequencies (\*p=0.0189), seemed to compensate for this loss to some extent (Paper I, Figure 1A).

In order to investigate, if there is a similar contribution of Cdc42 to MHC II loading in DCs *in vivo*, we investigated P323-339 peptide presentation in spleens and Ii expression on both spleen and lymph node DCs from Cdc42-ko as compared to wt mice.

### 5.4.2 Antigen presentation of OT-II peptide is impaired *in vivo*

In previous chapters, we clearly identified a role of Cdc42 in MHC II antigen presentation in DCs using *in vitro* generated BMDCs. However, we had an animal model at hand that allowed us to study the function of Cdc42 *in vivo*.

We started our investigation with a transfer of a single dose of P323-339 peptide plus LPS to wt and Cdc42-ko mice that had received OT-II cells the previous day. Five days after immunization, spleens of immunized mice were analyzed for transgenic T cells. CD4<sup>+</sup>CD90.1<sup>+</sup> transferred OT-II cells were clearly present at both reduced frequencies and numbers in spleens from immunized Cdc42-ko mice (Figure 22A), indicating defective CD4<sup>+</sup> T cell stimulation by Cdc42-ko DCs *in vivo*. Downregulation of CD62L and up-regulation of CD44 were used as markers for T cell activation. Interestingly, CD90.1<sup>+</sup> OT-II cells in Cdc42-ko mice were less activated (Figure 22B), as indicated by a reduced downregulation of CD62L. However, CD44 upregulation was normal on OT-II cells isolated from immunized Cdc42-ko mice, indicating that the activation of T cells was probably delayed in these mice.

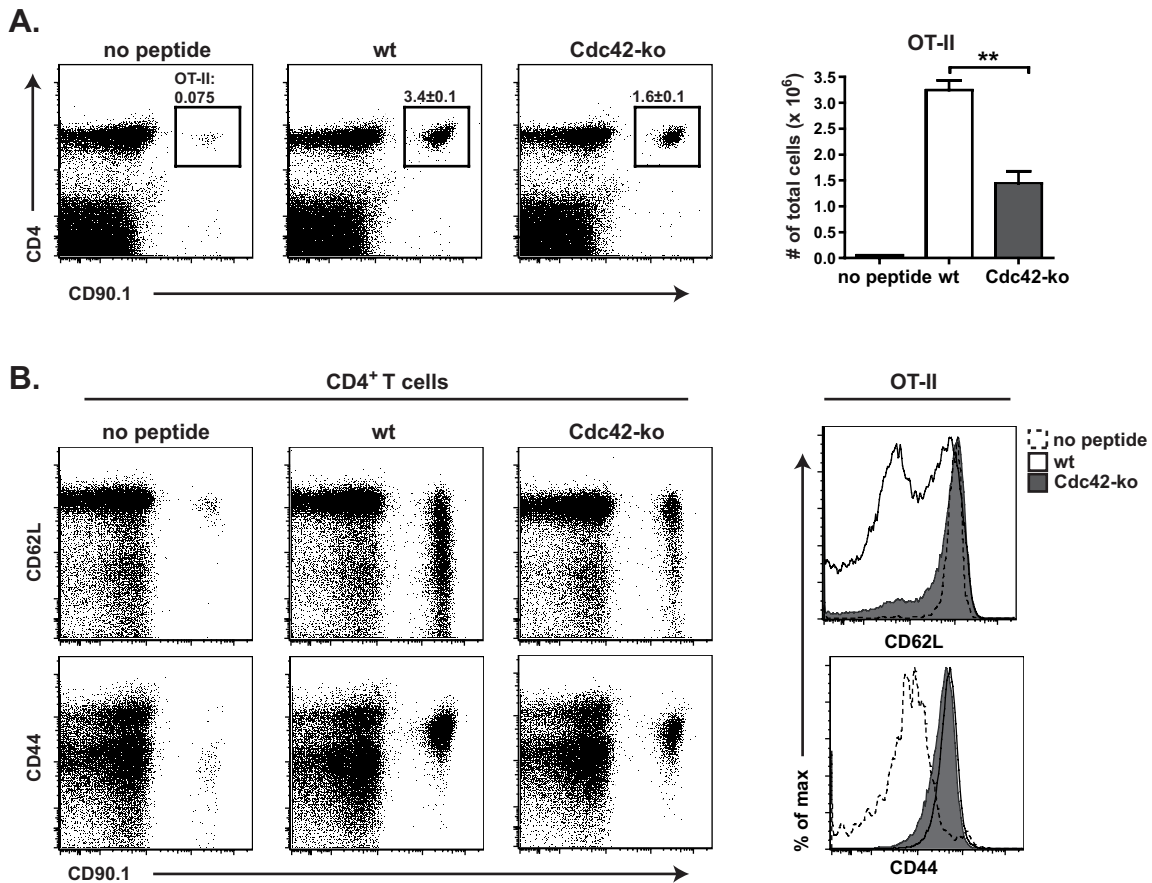


**Figure 22: Cdc42-ko mice exhibit an impaired T cell response upon P323-339 peptide transfer.**

(A) CD4<sup>+</sup> OT-II cells (CD90.1<sup>+</sup>) were enriched by negative selection and transferred into wt or Cdc42-ko mice. The next day, mice were challenged with a single dose of LPS plus P323-339 peptide, or LPS alone (no peptide control). Spleens were harvested after five days and T cells were analyzed based on the expression of CD4 and CD90.1. Numbers in FACS blots indicate frequencies and bar graph shows cell numbers. (B) CD4<sup>+</sup> T cells from immunized mice were analyzed for CD62L and CD44 expression. Histograms show CD62L and CD44 expression specifically on CD4<sup>+</sup>CD90.1<sup>+</sup> cells (OT-II). The data shown in this figure are from one representative experiment out of three, which was carried out in triplicates.

### 5.4.3 DC subsets in Cdc42-ko mice differentially regulate Ii expression

We next sought to take a closer look at the spleen and lymph node DC populations in Cdc42-ko mice. From our studies using *in vitro* generated DCs we know that Ii accumulates at the cell surface of Cdc42-ko BMDCs, thereby possibly preventing peptide exchange. Therefore, we characterized CD11c<sup>+</sup>MHC II<sup>+</sup> spleen DCs with respect to Ii surface expression. We made the interesting observation that despite of equal MHC II expression at the cell surface of CD8<sup>+</sup> and CD8<sup>-</sup> wt spleen DCs, Ii-bound to MHC II (15G4) expression was substantially reduced on CD8<sup>+</sup> as compared to CD8<sup>-</sup> DCs (Figure 23A, left and middle panel). The ratio of 15G4 and MHC II fluorescence was accordingly much higher in CD8<sup>+</sup> spleen DCs isolated from wt mice (Figure 23A, right panel, white bars). However, when we investigated Cdc42-ko spleen DCs we could detect neither stronger 15G4 fluorescence, nor an increased ratio on CD8<sup>+</sup> and CD8<sup>-</sup> Cdc42-ko spleen DCs as compared to wt cells, indicating that Ii surface expression was not elevated on Cdc42-ko spleen DC subsets. Notably, the knockout was not complete in sorted Cdc42-ko spleen DCs (Paper I, Supplementary Figure S1D), indicating that there might be remaining Cdc42 protein in these cells analyzed.

In order to characterize other *in vivo* DC subsets, we analyzed migratory DCs (mDCs) and resident DCs (rDCs) from cutaneous draining lymph nodes. Whereas the MFI of Ii-bound MHC II (15G4) was normal on both cutaneous lymph node DC subsets, the MFI of total MHC II was decreased on Cdc42-ko mDCs (Figure 23B, middle panel). Hence we observed an increased Ii surface expression relative to total MHC II, as indicated by the ratio MFI 15G4/MHC II (Figure 23B, right panel). This observation was interesting, because mDCs from Cdc42-ko mice were present at low frequencies and numbers and seem to be severely affected upon Cdc42 knockout (Paper I, Figure 1A (gate R2)).

Since mDCs from cutaneous draining lymph nodes cannot be analyzed by Western blot due to very low cell numbers, we instead analyzed Ii processing in purified MHC II<sup>+</sup>CD11c<sup>+</sup>CD8<sup>+</sup> and CD8<sup>-</sup> spleen DCs. Interestingly, CD8<sup>+</sup> wt spleen DCs showed higher amounts of intracellular Ii and accumulated the smallest p12 fragment, as compared to CD8<sup>-</sup> wt spleen DCs (Figure 23C). This differential Ii expression pattern in CD8<sup>+</sup> vs. CD8<sup>-</sup> spleen DCs surprisingly does not correlate with surface-Ii levels: CD8<sup>+</sup> spleen DCs expressed high intracellular Ii and are low

in 15G4 epitopes at the cell surface, whereas CD8<sup>-</sup> spleen DCs show the opposite phenotype. At the same time, Ctstl levels were reduced in CD8<sup>-</sup> DCs. However, spleen DCs from Cdc42-ko mice showed both, an accumulation of the smallest p12 fragment of Ii and a reduced expression of Ctstl protein in both DC subsets (Figure 23C), as compared to their wt counterparts, which matches the Ii processing pattern observed in Cdc42-ko BMDCs (see Figure 13).

Taken together, we could confirm a role for Cdc42 in MHC II antigen presentation *in vivo* (Figure 22), but detected normal expression of Ii at the cell surface of Cdc42-ko spleen DCs, despite of an altered Ii processing pattern (Figure 23). However, mDCs from cutaneous draining lymph nodes showed an increased expression of Ii at the cell surface as compared to rDCs, indicating that DC subsets from different organs might display altered Ii processing patterns and/or turnover rates at the cell surface.

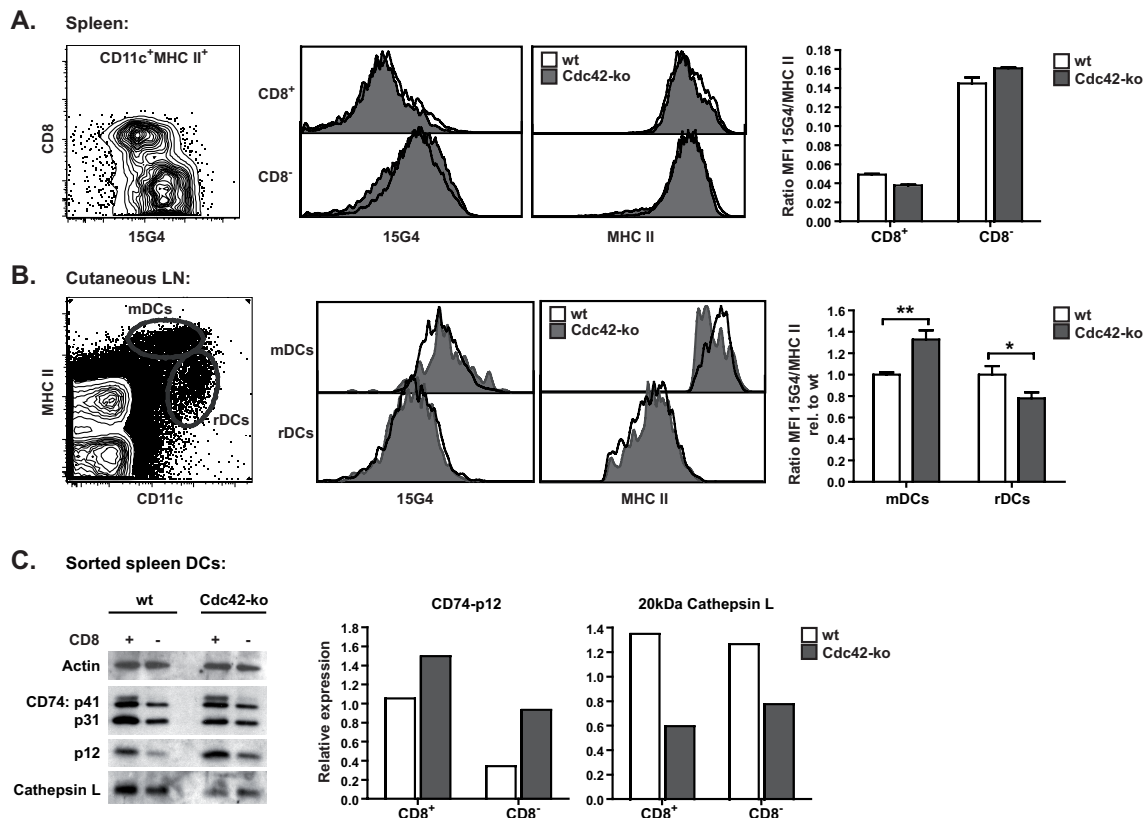


**Figure 23: DC subsets differentially regulate Ii expression.**

(A) Spleen DCs (CD11c<sup>+</sup>MHC II<sup>+</sup>) were analyzed for Ii surface expression; CD8 was additionally used to discriminate between DC subsets. Bar graph shows the amount of Ii (Ratio MFI 15G4/MHC II) expressed on CD8<sup>+</sup> and CD8<sup>-</sup> spleen DCs. Data are from one experiment (n=3) out of three. (B) Migratory and resident DCs (mDCs and rDCs) in skin-draining lymph nodes were analyzed for surface Ii expression. Bar graph shows surface-Ii expression (Ratio MFI 15G4/MHC II) relative to wt. Data are combined from three independent experiments (n=6). (C) Spleen DCs were sorted on a FACSARIA instrument based on the expression of CD11c, MHC II and CD8. Total cell lysates from CD8<sup>+</sup> and CD8<sup>-</sup> DCs were analyzed by Western blot for Ii degradation intermediates and Cathepsin L protein levels. Bar graphs show signals normalized to actin.

## 6 DISCUSSION

### 6.1 Cdc42 controls DC-mediated immunity

Silencing of Cdc42 impairs the DC's potential to take up antigens and delays immune responses, which are fundamental DC functions required for effective onset of immunity. In brief, we showed that cells deficient for Cdc42 were inefficient in antigen uptake, possibly through their inability to re-shape the plasma membrane to engulf the antigen. Furthermore, Cdc42-ko DCs not only express low levels of MHC I, but also high levels of immature MHC II still occupied by Ii at the cell surface and deficiently primed both the CD8<sup>+</sup> and CD4<sup>+</sup> T cell responses.

DCs are important immune cells, since they are amongst the first cells in contact with a pathogen. Upon encounter of bacterial or viral antigens, DCs obtain a mature phenotype that fully enables them to induce specific immune responses by their interactions with T cells. Interestingly, bacteria as well as viruses have found ways to influence the DC's potential to become fully activated and/or obtain all defense mechanisms required for the induction of antigen-specific immune responses. As a matter of fact, many of these mechanisms include the regulation of Rho GTPase activities by bacterial or viral products. For example, many bacterial virulence factors either activate or inactivate the Rho GTPases Rac1, Cdc42 or RhoA. One virulence factor that co-activates Rac1 and Cdc42 by its GEF activity is the Salmonella protein SopE. SopE-induced over-activation of these Rho GTPases causes a massive production of lamellipodia and filopodia around cell edges, provoking cell spreading, but inhibiting motility, thereby inducing local bacterial cell invasiveness (67).

Interestingly, the viral human immunodeficiency virus (HIV-1) accessory protein Nef, produced early after infection, also triggers mechanisms that make cells non-responsive promoting HIV's evasion of the cellular immune response:

First, Nef induces an accelerated internalization of MHC I protein from the plasma membrane, resulting in low MHC I surface expression on lymphoid, monocytic and epithelial cells (98) and immature PBMC-derived DCs (99). This down-regulation of MHC I protects the infected cells from cytotoxic T lymphocyte killing (100) and delays an immune response. In this study we show that Cdc42-ko

BMDCs display a reduced expression of MHC I at the cell surface (Figure 4B and C). The reason for this phenotype is unclear and has not fully been uncovered. The internalization of MHC I could be one factor leading to reduced MHC I surface levels, but was not tested in this study. Instead, we studied intracellular MHC I protein expression and found it slightly reduced (Figure 5A). This reduction was, however, not statistically significant. It has to be noted here that increasing the number of biological replicates for this experiment might confirm this downregulation and should be subject of future experiments.

Second, in human PBMCs the HIV-1 protein Nef induces Vav phosphorylation, which leads to an increase of both Rac1 and Cdc42 activities, the latter to a lesser extent. Activation of Rac1 by Nef triggered rearrangements of actin filaments, the formation of uropods and ruffles and an increase of the DC's ability to form clusters with allogeneic CD4<sup>+</sup> T cells (101), fostering virus dissemination through activation of these T cells. In cells deficient for Cdc42 we did not investigate the amount of activated Rac1. However, it may be noted here that feedback mechanisms triggering GEFs that target both Rac1 and Cdc42 (e.g. proto-oncogene Vav) could indeed change the expression levels of total and GTP-bound Rac1 in the absence of Cdc42 and thus, induce cytoskeletal changes and surface marker expression in a Nef-similar fashion as secondary effects of Cdc42 removal. Indeed, in our proteomics screen p95vav (Vav1) protein was present at slightly elevated amounts in Cdc42-ko BMDCs (mean fold change value (FC) Cdc42-ko/wt±SEM: 1.4±0.46), and could possibly, in the absence of Cdc42, target Rac1 (FC Cdc42-ko/wt±SEM: 1.3±0.43) instead. However, an effect of Cdc42-removal on Rac1 activation can only be speculated and might be unraveled in future experiments.

Third, another study showed that Nef stabilizes Ii-bound MHC II at the cell surface of infected HeLa-CIITA cells, while reducing surface levels of mature, peptide-loaded MHC II (102, 103), affecting MHC II function and peptide presentation. Ii-bound "immature" MHC II molecules were also stabilized on the cell surface of Cdc42-ko BMDCs (Figure 12A and B), due to a decreased internalization (Figure 12C). However, although the amount of peptide-loaded MHC II was not determined in this study, we observed a low expression of total MHC II molecules on immature BMDCs deficient for Cdc42 (Figure 4B and C).

These studies provide evidence, that studying Cdc42 function in DCs could give promising insights in the DC's exact mechanisms to fight viral transmission. Indeed, a study using immature DCs elegantly showed that cell-to-cell

transmission of HIV-1 was Cdc42-dependent: DCs silenced for Cdc42 lacked membrane protrusions induced by the virus to facilitate the transfer of viral particles to CD4<sup>+</sup> T cells (104).

The present study aimed at understanding the mechanisms regulated by Cdc42 in immature and mature DCs and which influence Cdc42 has on basic DC functions such as the presentation of exogenously derived antigens.

### **Phenotype of Cdc42-ko BMDCs**

Immature Cdc42-ko BMDCs express low levels of MHC I as well as MHC II molecules (discussed below) that mediate the presentation of antigens to T cells. DC maturation can be induced by LPS treatment, which enables their priming ability required for the initiation of immune responses. This process is accompanied by substantial rearrangements of the actin cytoskeleton (105), leading to a shutdown of endocytosis of soluble antigens and a transport of MHC molecules to the cell surface (72). However, Cdc42-ko BMDCs normally responded to LPS and were able to upregulate MHC I as well as MHC II cell surface expression (Figure 4B and C), indicating that TLR4 signaling was still functional. Indeed, it has been reported that Cdc42 activity did not increase in BMDCs treated with LPS (106), but rather gradually decreased upon DC maturation, as also described by Mellman's group (72). As a result, Cdc42 activity was high in immature DCs resulting in a high potential of endocytosis, and downregulated in mature DCs in order to shut down this process. As opposed to Mellman's observations, human LC-type DCs show a different phenotype regarding the regulation of Cdc42 activity upon maturation: these human DCs treated with LPS did upregulate Cdc42 activity, which resulted in an activated DC phenotype (69). The authors claim that active Cdc42 is required for "the maintenance of a typical actin cytoskeleton" of mature DCs. This study suggests that Cdc42 might be differentially regulated during DC development in DC subsets in mice and humans, or different DC subsets.

In our system unstimulated Cdc42-ko BMDCs lack Cdc42 protein, whereas wt BMDCs should, according to Mellman's observations, express high amounts of active Cdc42. This deficiency in unstimulated Cdc42-deficient cells causes malfunctions concerning MHC expression, antigen uptake and antigen presentation. Upon treatment with LPS these knockout BMDCs became activated

and upregulated MHC and costimulatory molecules, indicating that a deficiency of Cdc42 in immature DCs does not inhibit the onset of DC maturation. This would be in agreement with Mellman's observations that Cdc42 activity is required for basic DC functions such as antigen uptake in immature DCs, and downregulated upon maturation. Thus, our results support the notion that Cdc42 might have prevalent functions in immature DCs.

In addition to a decreased expression of MHC I and MHC II, immature Cdc42-ko BMDCs express low levels of CCR7 (Figure 4B). This decrease in CCR7 expression on Cdc42-ko BMDCs could indicate a functional relationship between CCR7 signaling and Cdc42 activation. A recent study in spleen DCs showed that cross-linking of CCR7 with its ligand CCL19 increased the amount of active, GTP-bound Cdc42, which lead to an increased endocytic capacity of these cells (107). Besides endocytosis, CCR7 signaling was shown to be important for skin-DC migration to draining lymph nodes (108), which is a prerequisite for antigen transport from sites of infection to sites of T cell activation. Because of reduced CCR7 surface levels, CCR7 signaling might therefore not be functional in DCs deficient for Cdc42- with fundamental consequences for the initiation of immune responses requiring both functional antigen uptake and its transport. This might be of interest for future *in vivo*-studies with Cdc42-ko mice.

### **Antigen uptake and processing**

Cdc42 controls the acquisition of soluble antigens, as shown in Figure 6. Our results are in agreement with previous studies using BMDCs showing that macropinocytosis, receptor-mediated uptake and pinocytosis (71, 72) required functional Cdc42 protein. However, a study using spleen DCs challenged the concept that these processes are conserved between DC subsets, by showing that cultured N17Cdc42-transfected spleen DCs did not show a significant defect in the uptake of soluble dextran (109). The authors argued that BMDCs and spleen DC populations might differentially express Rho GTPases and/or their effectors, which could possibly account for differences in regulation. Therefore, DC subsets might use different strategies to regulate endocytosis in response to environmental stimuli. Thus, Cdc42 might have altered, extenuated functions in spleen DCs *in vivo* as compared to *in vitro* generated BMDCs, where the strong GM-CSF stimulus might additionally influence DC-functions of GTPase-regulation. Interestingly,

our own results also point towards the possibility that endocytosis in DC subsets might be differently affected upon Cdc42-knockout. Cdc42-ko CD8<sup>+</sup> spleen DCs were fully capable of taking up soluble OVA, which was true for both *ex vivo* (data not shown) as well as *in vivo* OVA uptake (Céline Leroy, personal communication). Additionally, LCs isolated from the epidermis of Cdc42-ko mice were capable of taking up comparable amounts of OVA protein *ex vivo* (data not shown), suggesting that also LCs might regulate OVA uptake differently, as compared to *in vitro* generated BMDCs. However, to fully address these differences and the specific contribution of Cdc42 to endocytosis within different (wt-) DC subsets, further studies are required that would ideally correlate antigen uptake capacity with protein levels of active, GTP-bound Cdc42.

Interestingly, OVA that was taken up with reduced efficacy was nevertheless efficiently degraded by Cdc42-ko BMDCs (Figure 6C). Hence, we could exclude a role of Cdc42 in OVA processing. However, given the multiple pathways by which OVA protein can be degraded, this finding might not only account for proteins that are presented via MHC II and are destined for proteolytic degradation in lysosomes. In fact there is emerging evidence that, depending on their intrinsic properties, DC subtypes take up soluble antigens via different routes that selectively trigger intracellular pathways of peptide generation promoting either CD4<sup>+</sup> or CD8<sup>+</sup> T cell activation. For example, a study showed that mannose receptor (MR)-dependent OVA uptake in CD8<sup>+</sup> spleen DCs introduced OVA into stable early endosomal compartments, from where it entered the cross-presentation pathway. This pathway also includes protein degradation by the proteasome complex, generating peptides that are loaded onto MHC I molecules and then presented to CD8<sup>+</sup> T cells (110). CD8<sup>-</sup> DCs, on the other hand, take up OVA via pinocytosis and directly conveyed the protein to lysosomes for MHC II-restricted antigen presentation to CD4<sup>+</sup> T cells. Also, OVA targeting with antibodies that triggered receptor-mediated uptake in CD8<sup>+</sup> ( $\alpha$ DEC205-OVA) or pinocytosis in CD8<sup>-</sup> DCs ( $\alpha$ 33D1-OVA), subjected OVA for presentation to CD8<sup>+</sup> or CD4<sup>+</sup> T cells respectively (111). However, since we did not target a specific route of OVA uptake but rather used unconjugated OVA protein, our experimental setup did not allow the discrimination between proteasome-dependent and -independent mechanisms of antigen processing, and thus, only provides quantitative rather than qualitative evidence. Furthermore, for both MHC I as well

as MHC II antigen presentation, cells possess a variety of proteases with broad specificities, as reviewed for the MHC I pathway (31), that might already process OVA in Cdc42-ko DCs before it actually reaches lysosomal compartments. To improve the experimental setup, a negative control for OVA processing (e.g. ConB) could be included that blocks acidification of the endosome and thus, might result in attenuated OVA-degradation. Also, antibody-tagged latex beads could trigger a specific pathway of entry.

### **Antigen presentation**

We next studied the functional consequences of Cdc42-depletion in BMDCs for T cell priming. Cdc42-ko DCs failed to prime CD8<sup>+</sup> as well as CD4<sup>+</sup> T cells when pulsed with whole protein antigen or pre-processed antigenic peptides (Figure 7). While it was expected that reduced antigen uptake might lead to the generation of fewer antigenic peptides presented in the context of MHC I and MHC II in Cdc42-ko DCs (Figure 7A), this defect could interestingly not be overcome by loading MHC molecules of activated DCs with pre-processed antigenic peptides (Figure 7B). Our results concerning the presentation of whole protein antigen are in agreement with previous studies showing that BMDCs deficient for functional Cdc42 protein fail to induce proper immune responses to CD4<sup>+</sup> T cells, when pulsed with whole OVA protein (71). Also, a study using human LC-type DCs showed an impaired CD8<sup>+</sup> T cell response, after pre-processed OVA peptide was applied to the cells (69), which was due to low surface expression of MHC I and costimulation on mature DCs deficient for functional Cdc42.

To overcome a possible inability of Cdc42-ko BMDCs to form functional DC:T cell synapses due to cytoskeletal defects possibly caused by the loss of Cdc42, we performed the antigen presentation assay in round-bottom plates that, as opposed to flat-bottom plates, force DCs and T cells to fall in close proximity to each other (93). However, a recent study showed that DCs transfected with Cdc42-siRNA were in fact able to form DC:T cell contacts, thereby inducing OT-I cells to enter division, which, however, did not accumulate due to reduced T cell survival. Rather than being important for DC:T cell contact formation, in DCs Cdc42 was shown to mediate the polarization of intracellular stores of IL-12 towards the immunological synapse (61); IL-12 release by DCs constitutes a third signal promoting full activation and survival of activated T cells. Interestingly, own data also showed that IL-12 secretion indeed was significantly reduced upon Cdc42-

removal ( $60 \pm 7.2$  % of wt,  $n=8$ ,  $**p < 0.001$ ; data not shown), as measured by CBA (see 4.2.1.7) on supernatants of LPS-treated Cdc42-ko BMDCs. In this regard, also the pro-inflammatory cytokines IL-6 and TNF were highly significant reduced in supernatants of LPS-treated Cdc42-ko BMDCs ( $39 \pm 5.8$  % and  $44 \pm 5.4$  % of wt respectively,  $n=8$ ,  $***p < 0.0001$ ; data not shown). These results suggest that in DCs lacking Cdc42 multiple pathways including the release of inflammatory cytokines might be affected, adding up to their inability to fully activate T cells.

## **6.2 Loss of Cdc42 affects actin dynamics and vesicle trafficking**

Having identified a function of Cdc42 in cellular processes tightly associated with antigen presentation we wondered, which pathways might be affected upon Cdc42 knockout that add up to their inability to fully prime T cells. Using proteomics we determined changes in the whole proteome composition of DCs deficient for Cdc42. We were surprised by the fact that Cdc42 seemed to be a rather global player for important DC immune functions. The global analysis of up- and downregulated proteins upon Cdc42 removal revealed known interactions, but also unknown functions, for example the general involvement of Cdc42 in controlling the DC's lysosomal protein composition (Table 11). Gene Ontology (GO) term analysis of proteins grouped according to their molecular function, biological process or cellular component was used to reveal novel candidates with novel functions of Cdc42 in DCs. As an example, a GO term that was substantially affected in Cdc42-ko BMDCs was the molecular function Actin-binding Proteins (GO:0003779, Table 12). Interestingly, few proteins (Arpc2, Vasp) were mentioned as directly associated with Cdc42 function, whereas others represent novel candidates that have not been directly associated with Cdc42 before. For example Palladin (FC  $0.002 \pm 0.0017$ ), a protein that localized to actin-containing podosomes of immature human monocyte-derived DCs and along actin filaments upon maturation (112), was virtually absent from Cdc42-ko BMDCs. Another GO term substantially affected was the Biological Process intracellular protein transport (GO:0006886, Table 13), showing also known, and novel relationships. However, in order to prove, whether these theoretical changes in protein composition are valid, confirmation of data would be required for each protein, as we did for selected proteins using biochemical methods like Western blot or flow cytometry.

### 6.3 MHC II loading requires Cdc42 and a functional actin network

Having identified a function of Cdc42 in the induction and control of DC-mediated immune responses, we sought to determine the mechanism, by which Cdc42 specifically affects MHC II antigen presentation. Until now, a regulation of MHC II expression on the cell surface of DCs has not been connected with Cdc42 function so far. However, using a literature-based model Paul et al. propose an influence of Cdc42 protein on the MHC II pathway via its role for endocytosis of exogenous antigens (31). In our study we suggest a previously unknown role for Cdc42 in MHC II loading based on three observations: Cdc42-ko BMDCs (i) accumulated Ii-bound MHC II at the plasma membrane, (ii) accumulated the smallest degradation intermediate of Ii, Ii-p12, intracellular and (iii) expressed low levels of the protease Ctss that conducts the final step of Ii-p12 processing. These processes contribute to pre-occupied MHC II molecules at the cell surface of Cdc42-ko BMDCs, which are not susceptible for loading with antigenic peptides. Moreover, we found that these processes were also actin-dependent and conclude that Cdc42 might trigger MHC II loading by influencing actin-dynamics.

#### **Accumulation of Ii-bound MHC II at the plasma membrane**

Ii-occupied MHC II heterodimers travel from the ER to MIICs, either directly through the endocytic pathway, or indirectly via the plasma membrane and subsequent endocytosis. However, in immature DCs only a small fraction of Ii-occupied MHC II at the plasma membrane is detectable due to fast internalization rates. Hence, an unexpected and fundamental finding was that "immature", Ii-pre-occupied MHC II molecules were stabilized at the plasma membrane of Cdc42-ko BMDCs (Figure 12) and actin-inhibitor treated wt BMDCs (Figure 15A and C).

Trafficking of nonameric Ii-bound MHC II molecules depends on two dileucine-based sorting motifs integrated in the cytoplasmic part of the Ii chaperone. Ii-associated MHC II is endocytosed predominantly through the interactions of these sorting motifs with the clathrin-adaptor protein AP-2 (113, 114), which is part of the clathrin coat required for vesicle budding. An explanation for the stabilization of Ii at the plasma membrane of Cdc42-ko BMDCs could be altered cell surface dynamics upon the loss of active Cdc42 protein. Interestingly, we could also define a contribution of the actin cytoskeleton in the turnover of Ii-bound MHC II,

which was stabilized upon global inhibition of actin-polymerization on the cell surface of wt cells (Figure 15A). The contributions of Cdc42 on cell surface dynamics are multi-faceted, but all of them include actin polymerization as a downstream signaling event upon Cdc42 activation (reviewed in (51)). In this regard, clathrin-mediated vesicle budding at the plasma membrane is Arp2/3- and actin-dependent and could be impaired in the absence of Cdc42 despite a functional interaction of the Ii cytoplasmic tail with adaptor protein AP-2.

Cdc42-ko BMDCs also showed a reduced internalization, hence stabilization of total MHC II molecules at the cell surface (data not shown). A study showed that quick internalization of mature CLIP- or peptide-loaded MHC II molecules from the plasma membrane in immature DCs depended on oligoubiquitination of the MHC II  $\beta$ -chain, which was, however, suppressed in LPS-activated, mature DCs, triggering MHC II stabilization at the cell surface. Interestingly, ubiquitination of MHC II- $\beta$  was dependent on Ii processing: quick internalization of ubiquitinated MHC II proteins and targeting to multi vesicular bodies (MVBs) was only observed after Ii was fully processed by lysosomal proteases (19). Thus, in Cdc42-ko BMDCs Ii-p12, which might not have been fully processed into CLIP, may prevent the premature exposure of MHC II- $\beta$  to the ubiquitination machinery, thereby stabilizing MHC II at the cell surface in a maturation-independent manner. This finding somehow contradicts the low expression of MHC II observed at the cell surface of immature Cdc42-ko BMDCs and indicates that a certain proportion of MHC II molecules might be retained in intracellular compartments of the cell, when Cdc42 is not functional. However, also actin inhibition in wt BMDCs by CytD lead to a decreased internalization of MHC II (data not shown), indicating that both Cdc42 and functional actin dynamics are important for the internalization of MHC II from the plasma membrane.

### **Intracellular accumulation of Ii-p12**

Intracellular Ii-p12 processing in DCs depends on the protease Ctss (37, 38). However, in some cell types, e.g. cTECs, the structurally very similar protease Ctst1 is the enzyme that conducts this final step of Ii processing (35). Accumulation of CLIP- or Ii-p12-bound MHC II at the cell surface has been reported for HIV-infected HeLa-CIITA cells (discussed above), Ctst1-deficient cortical thymic epithelial cells (cTEC) (35), Ctss and Ctst1-deficient fibroblasts using clone 15G4 antibody (39), Ctss-deficient murine intestinal epithelial cells (IEC) using clone

15G4 (40) and H2-M-deficient lymph node cells using clone 15G4 (36); a phenotype that was accompanied with an intracellular Ii-p12 degradation arrest in these knockout cells. Indeed, the loss of Cdc42 protein and the inhibition of actin in DCs both resulted in an accumulation of the smallest, Ii-p12 processing intermediate (Figure 15B), possibly as a direct consequence of the absence of Ctss, as also described for Ctss-deficient DCs (37, 38). However, even though intracellular Ii-p12 accumulation correlated with Ii-stabilization on the cell surface of Cdc42-ko BMDCs, the latter might not be a direct consequence of defective Ii processing, but rather a secondary effect caused by the inhibition of actin dynamics by Cdc42.

Both Cdc42-ko BMDCs and wt BMDCs treated with the actin-inhibitors CytD or LatB expressed low intracellular levels of Ctss (Figure 11A and Figure 15B, respectively). Consistent with the finding that Ctss was lost from cells treated with actin inhibitors, CytD and LatB treated cells accumulated Ii-p12 intracellularly (Figure 15B), which was possibly due to poorly equipped late endosomes, where Ii processing into CLIP occurs. These results clearly point towards a contribution of the actin cytoskeleton in Ii processing. Interestingly, our results are in agreement with a study showing that CytD-treated B cells accumulated Ii-p12 intracellularly (115). However, this study did not address a role of actin dynamics in Ctss expression, but rather showed that CytD interfered with MHC II targeting to lysosomes, thereby blocking the access of Ii to lysosomal proteases.

Ii expression at the cell surface was, however, neither microtubule-, nor Arp2/3 and clathrin-dependent (Figure 15B and data not shown), indicating that inhibition of neither of these processes was sufficient to cause this severe phenotype. Notably, ConB-treatment also caused a slight but significant accumulation of Ii-p12 in inhibitor-treated wt BMDCs (Figure 15B). ConB delays endosomal and phagosomal acidification (77) by inhibition of V-ATPase, which could possibly result in reduced Ctss activity at high pH. However, Ctss, as opposed to most endosomal hydrolases, has been shown to survive and maintain enzymatic activity at even a slightly basal pH (116) with approximately 25 % remaining activity at pH 7.0-8.0 (117), indicating that a pH above 8.0 might be required to fully suppress its activity. Taken together we could define a microtubule-independent role of actin dynamics in Ii processing through the regulation of lysosomal Ctss levels.

**Regulation of lysosomal protein contents**

Besides the lack of Ctss, Cdc42-ko BMDCs expressed low levels of many other lysosomal proteins (Figure 10 and Figure 11). Interestingly, these changes comprised lysosomal membrane proteins as well as soluble proteins; both protein groups require different modes of vesicle transport to reach their final destination, the lysosome. For example, one of the most abundant lysosomal membrane proteins is LAMP-1, which was virtually absent in Cdc42-ko BMDCs, is transported in an M6pr-independent manner in AP1<sup>+</sup>clathrin<sup>+</sup> vesicles positive for AP1 and clathrin. Cathepsins on the other hand, which are soluble proteases also reduced upon Cdc42 knockout, require both M6pr and clathrin to enter the endocytic system. Cdc42-ko cells did not accumulate cathepsin precursors, neither intracellular nor extracellular, as shown for Ctss in M6pr-deficient mouse embryonic fibroblasts (MEF) (41). This supports the theory that in Cdc42-deficient DCs lysosomal proteases might be able to enter the endocytic system independently of Cdc42, and are processed into their mature forms. Thus, rather than playing a role in the delivery of selected proteins to the lysosome, Cdc42 seemed to affect a general mechanism leading to the loss of lysosomal proteins from cells.

But which mechanism might cause this phenotype? Besides entering the endosomal pathway directly, a small fraction of lysosomal proteases is first transported to the plasma membrane and then re-internalized- a pathway of minor importance in wt cells. This secretion-recapture pathway is sensitive to mannose-6-phosphate in the medium, hence M6pr dependent. Two types of M6pr are ubiquitously expressed: a 46 kDa cation-dependent (CD-M6pr) and a 300 kDa cation-independent (CI-M6pr, Igf2r) receptor. Both function in transport of lysosomal proteases from the TGN and the plasma membrane to lysosomes (27). Fibroblasts deficient for both mannose-phosphate receptors (MPR64/CD-M6pr and MPR300/Igf2r) missorted the majority ( $\geq 85\%$ ) of lysosomal proteins into culture supernatants (41). Both mannose receptors were expressed at slightly elevated amounts in Cdc42-ko BMDCs (FC (Igf2r) Cdc42-ko/wt  $25.8 \pm 24.14$ ; FC (CD-M6pr) Cdc42-ko/wt  $4.4 \pm 1.91$ ), indicating that the machinery at both the TGN and the plasma membrane might be able to “use” these important sorting receptors. However, whether the receptors were efficiently internalized from the plasma membrane in the absence of Cdc42 was not assessed in this study.

To study protease secretion from cells into culture supernatants, we used Ctstl as an example lysosomal protein since this enzyme was highly expressed in BMDCs and thus, well detectable. Taken both intracellular and extracellular Ctstl expression into account, Cdc42-ko BMDCs secreted approximately three fold more mature Ctstl protein than their wt counterparts (Figure 17B) irrespective of its stability in the medium. Interestingly, actin-inhibition (Figure 17A) and more specifically, inhibition of the Arp2/3 complex (Figure 19C) and clathrin (Figure 20) in wt BMDCs also resulted in enhanced secretion of mature 20kDa Ctstl protein, but not its 37kDa precursor. This result suggests that the pro-enzyme entered the endocytic system, matured upon acidification of the vesicle, and was possibly finally secreted from a late endocytic compartment upon inhibitor-treatment. Consistent with this conclusion was also the preliminary finding that CytD and LatB actin-inhibitor treated wt BMDCs lost their lysosomal contents, as measured by LysoTracker staining, which is a probe that accumulates in vesicles with low pH (data not shown). However, LysoTracker staining was normal in Cdc42-ko BMDCs as compared to wt cells as measured from MFI (data not shown), indicating that DCs devoid of Cdc42 still expressed acidic, albeit possibly not fully functional lysosomes. It has to be noted here that LysoTracker staining examined by flow cytometry measures lysosomal contents in quantitative rather than qualitative terms. Therefore, future experiments are needed to characterize LysoTracker<sup>+</sup> vesicles in terms of pH, size and/or distribution within Cdc42-ko cells.

Actin-dynamics are important for both short-range transport and the recently discovered collective vesicle movement, which depends on the actin-nucleating factors Spire-1, Spire-2 and Formin-2 (64). In brief, short filaments surround the vesicle surface, thereby facilitating a connection of the vesicle with the pre-existing actin network, inducing its long-range transport via the actin lattice. Interestingly, both inhibition of Formin-2 and inhibition of actin by CytD in mouse oocytes utilized in this study (64) lead to the loss of both transport directionality and vesicle speed, and therefore, drastically decreased actin-dependent vesicle transport. Interestingly, the treatment of mouse oocytes with an Arp2/3 inhibitor only slightly interfered with vesicle dynamics, indicating that mostly linear, formin-mediated actin polymerization played a role for this mechanism of vesicle movement along the actin cytoskeleton. Interestingly, not only vesicle speed was

affected upon CytD-treatment, but also vesicle convergence (vesicle movement towards neighboring vesicles), which increased the number of vesicles per cell while their average size significantly decreased (64).

In wt BMDCs, only the inhibition of Arp2/3, but not the inhibition of formins lead to an accelerated Ctsl translocation into supernatants (Figure 19B), indicating that specifically actin-branching played a role for Ctsl transport. In addition both vesicle convergence and localization could be affected in the absence of functional actin dynamics and upon Cdc42 knockout, and impaired Arp2/3 and formin-signaling could result in smaller lysosomes of higher abundance that cannot release their contents due to their inability to fuse with MIICs.

The inhibitor Pitstop 2 is a recently published small molecule that, based on its interaction with the amino terminal domain of clathrin heavy chain, was thought to inhibit specifically clathrin-mediated endocytosis, while leaving clathrin-independent endocytosis intact (82). Clathrin-mediated endocytosis occurs at the plasma membrane, when specific cargo or transmembrane proteins are endocytosed in a clathrin-dependent manner. However, another area of clathrin-dependent vesicle budding is the TGN, where AP-1 and GGA proteins maintain bidirectional traffic between TGN and endosomes (118, 119). Therefore, it was to be expected that Pitstop 2 also inhibited clathrin-dependent movement at the TGN and therefore the supply of endosomes with protease precursors. Wt BMDCs treated with Pitstop 2 showed an accumulation of Ctsl in supernatants (Figure 20). However, this phenotype was neither accompanied with a loss of lysosomal contents from total cell lysates, nor a defect in MHC II loading, hence constitutes a rather mild phenotype as compared to the amounts secreted upon direct actin inhibition or knockout of Cdc42. This result might point towards a contribution of clathrin to protease secretion, but interestingly, the specificity of Pitstop 2 has recently been challenged. As discussed by Lemmon and Traub (120), its mode of action could not clearly be defined, since clathrin coated vesicles still budded from the plasma membrane. However, these vesicles were not efficiently transported to the interior of the cells, so simply seemed to be stabilized and less dynamic (82). Furthermore, Pitstop 2 was shown to not only inhibit clathrin-mediated endocytosis, but also clathrin-independent endocytosis of the transmembrane protein MHC I (121). Therefore, it is currently unresolved whether the inhibitor, even though it binds specifically to the clathrin terminal domain, might also bind

to a second site of action and hence, might lack specificity. Thus, our effects observed upon Pitstop 2 treatment might not be caused specifically by the inhibition of clathrin. Future research will be of importance to clearly identify underlying mechanism of Pitstop 2 treatment.

The contribution of Cdc42 to clathrin-mediated endocytosis is unclear. We examined the expression of Hip1r, a clathrin-coat component that connects emerging vesicles to pre-existing actin filaments and found it slightly upregulated in Cdc42-ko BMDCs (Figure 21B). However, which effect this overexpression might have on clathrin vesicle budding at the TGN can only be speculated. Interestingly, a study in HeLa cells showed that Hip1r was present at CCVs emerging on the TGN in vesicles positive for M6pr and the Arp2/3 complex (122). Furthermore, silencing of Hip1r resulted in Golgi disruption, stabilization of actin structures associated with CCVs and impaired Cathepsin D exit from the TGN. The authors suggested that Hip1r might negatively regulate actin polymerization at the TGN, thereby facilitating the release of CCVs from the TGN (122). Therefore we could speculate that in DCs Hip1r-expression could be negatively regulated by Cdc42, in order to promote (Arp2/3-dependent) actin polymerization at the TGN, required for efficient vesicle release and subsequent vesicle movement. However, this effect might be DC-specific since silencing of Cdc42 using the drug Secramine A did not arrest pit formation of apical or basolateral pits in polarized epithelial cells (123).

#### **6.4 *In vivo* DC subsets differentially regulate MHC II loading**

The examination of *in vivo* DC subsets uncovered that Ii processing and thus MHC II loading might be differentially regulated in DC subsets. This observation is not surprising given the fact that DC subsets differentially express MHC II at the cell surface and also show preferences for one or another mechanism of antigen presentation. As already introduced in chapter 6.1 DCs display different specifications regarding MHC I or MHC II antigen presentation (favored by e.g. CD8<sup>+</sup> and CD8<sup>-</sup> spleen DCs, respectively (124)). Interestingly, despite of comparable MHC II expression at the cell surface of CD8<sup>+</sup> and CD8<sup>-</sup> DCs, these two spleen DC subsets expressed Ii-bound to MHC II (Figure 23A) at different amounts: CD8<sup>+</sup> DCs displayed less Ii-bound MHC II molecules at the cell surface

as compared to CD8<sup>-</sup> DCs. This is surprising given their preferences for MHC I or MHC II antigen presentation (124). One would think that DCs that express high level of Ii at the cell surface would be inferior at MHC II antigen presentation as compared to DCs expressing high amounts of peptide-loaded MHC II molecules, but this reasoning might not to be true for every DC subset. Apparently, the quality of MHC II loading is also regulated by factors other than Ii processing; the best example are CD8<sup>-</sup> spleen DCs as very good MHC II presenters despite of their high expression of Ii-bound MHC II molecules at the cell surface (Figure 23A, left panel). How Cdc42 might be regulated in CD8<sup>+</sup> vs. CD8<sup>-</sup> spleen DCs has not been studied so far, but the specialization of endocytosing different kinds of antigens points towards a differential regulation of Cdc42 activity in these two DC subsets. However, we did not observe a difference regarding Ii expression on Cdc42-ko spleen DCs (Figure 23A, right panel) as we see in BMDCs (Figure 12A and B), which can be interpreted in different ways. Cdc42-ko spleen DCs are devoid of functional Cdc42 message, but express low amounts of residual Cdc42 protein (Paper I, Supplementary Figure S1D). Thus, the knockout was not as efficient as observed for BMDCs (Figure 3B, right panel). An explanation might be the relatively short 3-day lifespan of spleen DCs (125), which could simply be too short to degrade 100 % of the remaining Cdc42 protein (half-life of Cdc42 protein is approximately 15 h in macrophages (126)). Thus, the attenuated phenotype of Cdc42-ko spleen DCs, as compared to BMDCs, could be due to either remaining Cdc42 activity in this *in vivo* DC subset or differential regulation of Cdc42 activity by other, subset-specific factors.

DC subsets affected most upon Cdc42 depletion are migratory DCs of all kinds, mostly the ones found in cutaneous (Paper I, Figure 1A) or mesenteric (Paper I, Figure 2C and D) lymph nodes of Cdc42-ko mice. Also, in absence of inflammation spontaneously migrated LCs can be found in reduced numbers in the dermis of Cdc42-ko mice (Paper I, Figure 1C). We investigated Ii expression on MHC II<sup>HI</sup> CD11c<sup>IM</sup> migratory DCs in cutaneous lymph nodes of Cdc42-ko mice and found a significantly increased ratio of Ii expression on MHC II molecules (Figure 23B, right panel), indicating that these highly affected DCs might regulate Cdc42 similar to our BMDC model, or might as well be completely devoid of any residual Cdc42 protein. However, due to technical constraints such as very low

DC numbers in cutaneous lymph nodes we were not able to study either Cdc42 protein expression, or Ii processing by Western blot in this migratory DC subset.

We were, however, able to study Ii processing in spleen DCs and made the interesting observation that CD8<sup>-</sup> wt DCs, showing low CD74 expression as compared to CD8<sup>+</sup> wt DCs, seemed to process Ii more efficiently than their CD8<sup>+</sup> counterparts (Figure 23C, left panel, see wt only). In Cdc42-ko spleen DCs both the CD8<sup>+</sup> and the CD8<sup>-</sup> DC subset showed an Ii-p12 degradation arrest as compared to wt cells. This result was consistent to what we observed in Cdc42-ko BMDCs (Figure 13), indicating that Cdc42 might, also in spleen DCs, regulate some aspects of MHC II loading. Why inefficient intracellular processing of Ii-p12 did not correlate with an increased surface expression of Ii-occupied MHC II molecules on Cdc42-ko spleen DCs can only be speculated. Cdc42 might simply be still expressed at low amounts sufficient to mediate efficient turnover of cell surface proteins, or might account for a partial defect on secretion vs. lysosomal loading. Interestingly, spleen DCs of Cdc42-ko mice were not able to fully activate OT-II cells, as judged from the reduced downregulation of CD62L on those T cells (Figure 22B). As a result, Cdc42-ko spleen DCs could not promote sufficient stimulation to induce proliferation *in vivo*, as observed upon P323-339 peptide transfer (Figure 22A). Since we could not control the quality of MHC II peptide loading, but have to assume that similar amounts of peptides can be loaded onto MHC II molecules on Cdc42-ko spleen DCs (due to similar surface MHC II and Ii expression, Figure 23A), there might also other factors account for this phenotype. These factors might include DC polarization, the secretion of pro-inflammatory cytokines and/or poor DC migration within the spleen after LPS-treatment and could be subject of future studies.

## 6.5 Conclusion & Outlook

In this study we wanted to address the role of Cdc42 in DC-mediated immunity and, more specific, its contribution to MHC II-restricted antigen presentation.

We could show that Cdc42 controls fundamental aspects of DC biology such as the surface expression of MHC molecules, antigen acquisition and antigen presentation. We used a conditional knockout lacking Cdc42 in DCs only, leaving other Rho GTPases in DCs and other cell types in the mouse unaffected. Using *in vitro*-generated DCs from these mice we not only confirmed previous studies

regarding Cdc42 functions, but also propose a novel Cdc42 and actin-dependent mechanism for MHC II loading in DCs. Furthermore, in Cdc42-ko mice we uncovered a contribution of Cdc42 to the MHC II-mediated antigen presentation and T cell priming functions of DCs using pre-processed antigenic peptide *in vivo*. This study contributes to our understanding of the complicated process of MHC II antigen presentation, which is relevant for effective immune responses towards extracellular antigens and thus, the induction of adaptive immune responses. Our findings help to fully unravel this process. Infection models for viral or bacterial diseases may uncover a role of Cdc42 in infected DCs for pathogen recognition and clearance. This knowledge could reveal therapeutic strategies to modulate DC function in order to support an effective pathogen clearance in DC-mediated immunity and could contribute to vaccine improvement.

## 7 APPENDIX

### 7.1 Gene Ontology (GO) term analyses

**Table 11: GO analysis CC Lysosome (GO:0005764, 82 of 232 proteins detected)**

Proteins are grouped according to their degree of up- and downregulation in Cdc42-ko BMDCs as compared to wt cells. Within these groups, proteins are listed in alphabetical order. As an example, a fold change value of 0.007 for Acp5 (first row) indicates that only 0.7 % of this protein was detectable in Cdc42-ko BMDCs, as compared to Acp5 protein expression in wt cells.

Gene name	UniProt	Fold change (Cdc42-ko/wt)	Stabw	SEM
> 3 fold downregulated				
Acp5	Q05117	0.007	0.007	0.005
Asah1	Q9WV54	0.150	0.084	0.060
Ctsb	P00787	0.237	0.233	0.165
Ctsl	P07154	0.173	0.157	0.111
Dnase2a	P56542	0.092	0.009	0.006
Lamp1	P11279	0.144	0.135	0.096
Lipa	Q64194	0.207	0.066	0.047
Man2b1	O09159	0.272	0.063	0.044
Tpcn1	Q9ULQ1	0.122	0.166	0.117
> 2 fold downregulated				
Acp2	P11117	0.490	0.133	0.094
Ctsd	P24268	0.416	0.527	0.372
Ctsz	Q9WUU7	0.490	0.134	0.094
Fnbp1	Q80TY0	0.368	0.107	0.076
Ggh	Q9Z0L8	0.368	0.047	0.033
Glb1	P23780	0.408	0.129	0.091
Gm2a	Q60648	0.352	0.223	0.157
Manba	Q8K2I4	0.442	0.112	0.079
Npc2	P61916	0.406	0.112	0.079
Plbd2	Q3TCN2	0.495	0.153	0.108
Tpp1	O14773	0.354	0.054	0.038
between 2 fold down- and upregulated				
Ada	P00813	0.525	0.443	0.313
Arl8a	Q8VEH3	0.520	0.146	0.103
Arl8b	Q9CQW2	1.359	0.726	0.513
Arsa	P50428	0.785	0.096	0.068
Cat	P04762	1.497	0.228	0.161
Cst3	P14841	1.493	1.229	0.869
Ctsa	P16675	0.559	0.103	0.073
Ctsc	P80067	0.736	0.170	0.120
Ctss	O70370	0.633	0.191	0.135
Galns	Q571E4	1.314	0.036	0.025
Gba	Q69ZF3	0.626	0.086	0.061
Gla	P06280	0.726	0.345	0.244
Gns	Q8BFR4	0.629	0.600	0.424
Got1	P13221	0.580	0.114	0.081
Gusb	P06760	0.951	0.130	0.092

The table continues on the next page.

Gene name	UniProt	Fold change (Cdc42-ko/wt)	Stabw	SEM
between 2 fold down- and upregulated				
H2-Aa	P14434	0.950	0.364	0.258
H2-DMa	P28078	1.799	0.712	0.504
H2-Eb1	P01911	1.504	0.284	0.201
Hexb	P20060	0.508	0.073	0.052
Ifi30	P13284	1.877	0.028	0.020
Il4i1	O09046	1.311	1.208	0.854
Lamp2	P13473	0.529	0.335	0.237
Mtor	P42345	1.109	0.635	0.449
Naaa	Q9D7V9	0.833	0.332	0.235
Naga	Q9QWR8	1.573	0.067	0.047
Ncstn	P57716	1.655	0.814	0.576
Npc1	O35604	0.829	1.161	0.821
Pcyox1	Q9UHG3	1.869	1.587	1.122
Pla2g15	Q8VEB4	1.562	1.946	1.376
Pon2	Q62086	0.837	0.866	0.612
Ppt1	P50897	1.519	0.399	0.282
Prcp	Q7TMR0	0.733	0.058	0.041
Prdx6	O08709	0.971	0.012	0.009
Psap	P07602	1.827	2.087	1.476
Rab14	P61107	1.164	0.466	0.330
Rab7	P51149	1.554	0.435	0.307
Rab9	P51151	1.288	1.293	0.914
Rraga	Q7L523	0.897	0.516	0.365
Rragc	Q9HB90	1.221	0.905	0.640
Snap23	O00161	0.783	0.103	0.073
Stx7	O70257	0.646	0.025	0.018
Stxbp2	Q15833	1.211	0.496	0.351
Vps36	Q91XD6	1.581	0.186	0.132
Vps4b	O75351	1.237	0.028	0.020
> 2 fold upregulated				
Adam8	P78325	2.547	2.514	1.778
Sphk2	Q9JIA7	2.105	0.463	0.327
Stx8	O88983	2.528	0.398	0.282
Unc13d	Q70J99	2.364	0.149	0.106
Vamp7	Q9JHW5	2.551	1.608	1.137
Vps39	Q8R5L3	2.867	2.548	1.802
> 3 fold upregulated				
Anxa11	P50995	3.521	0.724	0.512
Ass1	P09034	5.692	1.375	0.973
Fuca1	P17164	54.831	1.280	0.905
Igf2r	Q07113	25.807	34.145	24.144
Kif2a	P28740	3.788	3.298	2.332
Lrba	Q9ESE1	4.983	0.965	0.682
M6pr	P24668	4.411	2.705	1.913
Rab27a	P51159	3.708	0.322	0.227
Tm9sf1	Q9DBU0	4.310	4.493	3.177
Vps11	Q91W86	3.375	3.377	2.388
Vps18	Q8R307	4.083	3.648	2.580
Vps33b	Q9H267	3.845	3.950	2.793

Table 12: Selected ACTIN-BINDING PROTEINS (grouped as Molecular Function GO:0003779).

Protein Name	Gene Name	Function (from www.uniprot.org)	Ratio Cdc42-ko/wt	SEM (n=2)
Downregulated in Cdc42-ko BMDCs				
Palladin	Palld	Organization of normal actin cytoskeleton into higher order structures; roles in establishing cell morphology, adhesion and DC maturation	0.002	0.0017
Destrin	Dstin	Actin-depolymerizing protein; severs F-actin and binds to actin monomers	0.375	0.0466
Actin-related protein 2/3 complex, subunit 2	Arpc2	Actin-binding component of the Arp2/3 complex; mediates formation of branched filaments; <b>acts downstream of Cdc42</b>	0.409	0.0594
Actin-related protein 2/3 complex, subunit 3	Arpc3	Component of the Arp2/3 complex; involved in actin polymerization	0.534	0.0501
Supervillin	Svil	Forms a high affinity link between actin and membranes; isoform-1 involved in myosin II regulation through MLCK during cell spreading	0.475	0.1808
Upregulated in Cdc42-ko BMDCs				
FH1/FH2 domain-containing protein 1	Fhod1	Assembly of F-actin structures, such as stress fibers; contributes to the coordination of microtubules with actin	2.523	0.4758
Vasodilator-stimulated phosphoprotein	Vasp	Promotes actin filament elongation by promoting transfer of profilin-bound actin monomers to barbed end of growing filaments; <b>acts downstream of Cdc42</b>	4.910	2.6326
Wiskott-Aldrich syndrome protein family member 2	Wasp2	Promotes formation of actin filaments; part of the WAVE complex regulating actin filament reorganization via its interaction with the Arp2/3 complex	5.662	2.6314
Catenin	Ctnna1	Associates with Cadherins; homodimeric form might compete with the Arp2/3 complex and inhibit branching of filaments	6.631	0.9662
Scinderin	Scin	Ca <sup>2+</sup> -dependent actin filament severing protein; barbed end capping and nucleating activities in the presence of Ca <sup>2+</sup>	26.161	7.7361

Table 13: Selected proteins involved in INTRACELLULAR PROTEIN TRANSPORT (grouped as Biological Process GO:0006886).

Protein Name	Gene Name	Function (from www.uniprot.org)	Ratio Cdc42-ko / wt	SEM (n=2)
Downregulated in Cdc42-ko BMDCs				
Sortin nexin-9	Snx9	Involved in actin-dependent endocytosis and macropinocytosis; promotes Arp2/3 activation via Wasl	0.417	0.0079
Upregulated in Cdc42-ko BMDCs				
46kDa mannose 6-phosphate receptor	M6pr	Transport of phosphorylated lysosomal enzymes from the Golgi and the cell surface to lysosomes	4.411	1.9129
Sortin nexin-8	Snx8	Involved in intracellular protein trafficking	6.436	0.0683
Syntaxin 5	Stx5	Mediates ER to Golgi transport	17.652	7.3735
Coatamer complex subunits:		Required for the budding of non-clathrin coated vesicles from the Golgi and for retrograde transport from Golgi to ER		
gamma 2	Copg2	<b>Binds to Cdc42 (by similarity)</b>	3.323	0.5415
gamma 1	Copg1	Interacts with Copb1	2.940	2.2046
beta 1	Copb1	Interacts with Copg1	3.564	1.3453
Adapter-related protein complex 1/2 subunits:		Vesicle coat components involved in intracellular protein transport, assembles at clathrin coat; AP2 at the plasma membrane is involved in receptor-mediated endocytosis; AP1 may function in protein sorting in late endosomes or MVBs		
AP2 subunit alpha 2	Ap2a2	Interacts with Hip1 (by similarity) and FCHo1	3.479	1.9107
AP2 subunit beta 1	Ap2b1	Binds clathrin heavy chain	2.682	1.6727
AP1 subunit gamma 2	Ap1g2	Adaptin and part of the heterotetramer AP-1	3.573	2.6900
AP1 subunit beta 1	Ap1b1	Adaptin and part of the heterotetramer AP-1	8.200	5.5730
Clathrin heavy chain	Cltc	Part of the clathrin triskelion composed of 3 heavy and 3 light chains; cytoplasmic face of coated pits and vesicles; interacts with Hip1	1.169	0.1836

## 8 REFERENCES

1. Steinman, R. M., D. Hawiger, and M. C. Nussenzweig. 2003. Tolerogenic dendritic cells. *Annual review of immunology* 21: 685-711.
2. Reis e Sousa, C. 2006. Dendritic cells in a mature age. *Nat Rev Immunol* 6: 476-483.
3. Ohnmacht, C., A. Pullner, S. B. King, I. Drexler, S. Meier, T. Brocker, and D. Voehringer. 2009. Constitutive ablation of dendritic cells breaks self-tolerance of CD4 T cells and results in spontaneous fatal autoimmunity. *The Journal of experimental medicine* 206: 549-559.
4. Merad, M., and M. G. Manz. 2009. Dendritic cell homeostasis. *Blood* 113: 3418-3427.
5. Naik, S. H., P. Sathe, H. Y. Park, D. Metcalf, A. I. Proietto, A. Dakic, S. Carotta, M. O'Keeffe, M. Bahlo, A. Papenfuss, J. Y. Kwak, L. Wu, and K. Shortman. 2007. Development of plasmacytoid and conventional dendritic cell subtypes from single precursor cells derived in vitro and in vivo. *Nat Immunol* 8: 1217-1226.
6. Steinman, R. M., and J. Idoyaga. 2010. Features of the dendritic cell lineage. *Immunol Rev* 234: 5-17.
7. Hashimoto, D., J. Miller, and M. Merad. 2011. Dendritic cell and macrophage heterogeneity in vivo. *Immunity* 35: 323-335.
8. Colonna, M., G. Trinchieri, and Y. J. Liu. 2004. Plasmacytoid dendritic cells in immunity. *Nat Immunol* 5: 1219-1226.
9. Pulendran, B., H. Tang, and T. L. Denning. 2008. Division of labor, plasticity, and crosstalk between dendritic cell subsets. *Current opinion in immunology* 20: 61-67.
10. Alvarez, D., E. H. Vollmann, and U. H. von Andrian. 2008. Mechanisms and consequences of dendritic cell migration. *Immunity* 29: 325-342.
11. Forster, R., A. C. Davalos-Misslitz, and A. Rot. 2008. CCR7 and its ligands: balancing immunity and tolerance. *Nat Rev Immunol* 8: 362-371.
12. Villadangos, J. A., and P. Schnorrer. 2007. Intrinsic and cooperative antigen-presenting functions of dendritic-cell subsets in vivo. *Nat Rev Immunol* 7: 543-555.
13. Romani, N., B. E. Clausen, and P. Stoitzner. 2010. Langerhans cells and more: langerin-expressing dendritic cell subsets in the skin. *Immunol Rev* 234: 120-141.
14. Bogunovic, M., F. Ginhoux, J. Helft, L. Shang, D. Hashimoto, M. Greter, K. Liu, C. Jakubzick, M. A. Ingersoll, M. Leboeuf, E. R. Stanley, M. Nussenzweig, S. A. Lira, G. J. Randolph, and M. Merad. 2009. Origin of the lamina propria dendritic cell network. *Immunity* 31: 513-525.

15. Kurts, C., B. W. Robinson, and P. A. Knolle. 2010. Cross-priming in health and disease. *Nat Rev Immunol* 10: 403-414.
16. Mellman, I., and R. M. Steinman. 2001. Dendritic cells: specialized and regulated antigen processing machines. *Cell* 106: 255-258.
17. Pierre, P., S. J. Turley, E. Gatti, M. Hull, J. Meltzer, A. Mirza, K. Inaba, R. M. Steinman, and I. Mellman. 1997. Developmental regulation of MHC class II transport in mouse dendritic cells. *Nature* 388: 787-792.
18. Platt, C. D., J. K. Ma, C. Chalouni, M. Ebersold, H. Bou-Reslan, R. A. Carano, I. Mellman, and L. Delamarre. 2010. Mature dendritic cells use endocytic receptors to capture and present antigens. *Proceedings of the National Academy of Sciences of the United States of America* 107: 4287-4292.
19. van Niel, G., R. Wubbolts, T. Ten Broeke, S. I. Buschow, F. A. Ossendorp, C. J. Melief, G. Raposo, B. W. van Balkom, and W. Stoorvogel. 2006. Dendritic cells regulate exposure of MHC class II at their plasma membrane by oligoubiquitination. *Immunity* 25: 885-894.
20. Heath, W. R., G. T. Belz, G. M. Behrens, C. M. Smith, S. P. Forehan, I. A. Parish, G. M. Davey, N. S. Wilson, F. R. Carbone, and J. A. Villadangos. 2004. Cross-presentation, dendritic cell subsets, and the generation of immunity to cellular antigens. *Immunol Rev* 199: 9-26.
21. Schmid, D., M. Pypaert, and C. Munz. 2007. Antigen-loading compartments for major histocompatibility complex class II molecules continuously receive input from autophagosomes. *Immunity* 26: 79-92.
22. Mayor, S., and R. E. Pagano. 2007. Pathways of clathrin-independent endocytosis. *Nat Rev Mol Cell Biol* 8: 603-612.
23. Sandvig, K., S. Pust, T. Skotland, and B. van Deurs. 2011. Clathrin-independent endocytosis: mechanisms and function. *Curr Opin Cell Biol* 23: 413-420.
24. Traub, L. M. 2009. Tickets to ride: selecting cargo for clathrin-regulated internalization. *Nat Rev Mol Cell Biol* 10: 583-596.
25. Sorkin, A., and M. von Zastrow. 2009. Endocytosis and signalling: intertwining molecular networks. *Nat Rev Mol Cell Biol* 10: 609-622.
26. Anitei, M., and B. Hoflack. 2012. Bridging membrane and cytoskeleton dynamics in the secretory and endocytic pathways. *Nature cell biology* 14: 11-19.
27. Saftig, P., and J. Klumperman. 2009. Lysosome biogenesis and lysosomal membrane proteins: trafficking meets function. *Nature Reviews Molecular Cell Biology* 10: 623-635.
28. Underhill, D. M., and H. S. Goodridge. 2012. Information processing during phagocytosis. *Nat Rev Immunol* 12: 492-502.

29. Compeer, E. B., T. W. Flinsenbergh, S. G. van der Grein, and M. Boes. 2012. Antigen processing and remodeling of the endosomal pathway: requirements for antigen cross-presentation. *Frontiers in immunology* 3: 37.
30. Joffre, O. P., E. Segura, A. Savina, and S. Amigorena. 2012. Cross-presentation by dendritic cells. *Nat Rev Immunol* 12: 557-569.
31. Neefjes, J., M. L. Jongsma, P. Paul, and O. Bakke. 2011. Towards a systems understanding of MHC class I and MHC class II antigen presentation. *Nat Rev Immunol* 11: 823-836.
32. Lotteau, V., L. Teyton, A. Peleraux, T. Nilsson, L. Karlsson, S. L. Schmid, V. Quaranta, and P. A. Peterson. 1990. Intracellular transport of class II MHC molecules directed by invariant chain. *Nature* 348: 600-605.
33. Odorizzi, C. G., I. S. Trowbridge, L. Xue, C. R. Hopkins, C. D. Davis, and J. F. Collawn. 1994. Sorting signals in the MHC class II invariant chain cytoplasmic tail and transmembrane region determine trafficking to an endocytic processing compartment. *J Cell Biol* 126: 317-330.
34. Pond, L., L. A. Kuhn, L. Teyton, M. P. Schutze, J. A. Tainer, M. R. Jackson, and P. A. Peterson. 1995. A role for acidic residues in di-leucine motif-based targeting to the endocytic pathway. *J Biol Chem* 270: 19989-19997.
35. Nakagawa, T. 1998. Cathepsin L: Critical Role in Ii Degradation and CD4 T Cell Selection in the Thymus. *Science (New York, N.Y.)* 280: 450-453.
36. Liljedahl, M., O. Winqvist, C. D. Surh, P. Wong, K. Ngo, L. Teyton, P. A. Peterson, A. Brunmark, A. Y. Rudensky, W. P. Fung-Leung, and L. Karlsson. 1998. Altered antigen presentation in mice lacking H2-O. *Immunity* 8: 233-243.
37. Driessen, C., R. A. Bryant, A. M. Lennon-Dumenil, J. A. Villadangos, P. W. Bryant, G. P. Shi, H. A. Chapman, and H. L. Ploegh. 1999. Cathepsin S controls the trafficking and maturation of MHC class II molecules in dendritic cells. *J Cell Biol* 147: 775-790.
38. Nakagawa, T. Y., W. H. Brissette, P. D. Lira, R. J. Griffiths, N. Petrushova, J. Stock, J. D. McNeish, S. E. Eastman, E. D. Howard, S. R. Clarke, E. F. Rosloniec, E. A. Elliott, and A. Y. Rudensky. 1999. Impaired invariant chain degradation and antigen presentation and diminished collagen-induced arthritis in cathepsin S null mice. *Immunity* 10: 207-217.
39. Hsieh, C. S., P. deRoos, K. Honey, C. Beers, and A. Y. Rudensky. 2002. A role for cathepsin L and cathepsin S in peptide generation for MHC class II presentation. *J Immunol* 168: 2618-2625.
40. Beers, C., A. Burich, M. J. Kleijmeer, J. M. Griffith, P. Wong, and A. Y. Rudensky. 2005. Cathepsin S controls MHC class II-mediated antigen presentation by epithelial cells in vivo. *J Immunol* 174: 1205-1212.
41. Kasper, D., F. Dittmer, K. von Figura, and R. Pohlmann. 1996. Neither type of mannose 6-phosphate receptor is sufficient for targeting of lysosomal enzymes along intracellular routes. *J Cell Biol* 134: 615-623.

42. Sohar, I., D. Sleat, C. Gong Liu, T. Ludwig, and P. Lobel. 1998. Mouse mutants lacking the cation-independent mannose 6-phosphate/insulin-like growth factor II receptor are impaired in lysosomal enzyme transport: comparison of cation-independent and cation-dependent mannose 6-phosphate receptor-deficient mice. *The Biochemical journal* 330 ( Pt 2): 903-908.
43. Futter, C. E., A. Pearse, L. J. Hewlett, and C. R. Hopkins. 1996. Multivesicular endosomes containing internalized EGF-EGF receptor complexes mature and then fuse directly with lysosomes. *J Cell Biol* 132: 1011-1023.
44. Heasman, S. J., and A. J. Ridley. 2008. Mammalian Rho GTPases: new insights into their functions from in vivo studies. *Nat Rev Mol Cell Biol* 9: 690-701.
45. Wennerberg, K., K. L. Rossman, and C. J. Der. 2005. The Ras superfamily at a glance. *J Cell Sci* 118: 843-846.
46. Guilluy, C., R. Garcia-Mata, and K. Burridge. 2011. Rho protein crosstalk: another social network? *Trends Cell Biol* 21: 718-726.
47. Jaffe, A. B., and A. Hall. 2005. Rho GTPases: biochemistry and biology. *Annu Rev Cell Dev Biol* 21: 247-269.
48. Ridley, A. J. 2001. Rho family proteins: coordinating cell responses. *Trends Cell Biol* 11: 471-477.
49. Raftopoulou, M., and A. Hall. 2004. Cell migration: Rho GTPases lead the way. *Dev Biol* 265: 23-32.
50. Bokoch, G. M. 2005. Regulation of innate immunity by Rho GTPases. *Trends Cell Biol* 15: 163-171.
51. de Curtis, I., and J. Meldolesi. 2012. Cell surface dynamics - how Rho GTPases orchestrate the interplay between the plasma membrane and the cortical cytoskeleton. *J Cell Sci*.
52. Voth, D. E., and J. D. Ballard. 2005. Clostridium difficile toxins: mechanism of action and role in disease. *Clin Microbiol Rev* 18: 247-263.
53. Wang, L., and Y. Zheng. 2007. Cell type-specific functions of Rho GTPases revealed by gene targeting in mice. *Trends Cell Biol* 17: 58-64.
54. Chen, F., L. Ma, M. C. Parrini, X. Mao, M. Lopez, C. Wu, P. W. Marks, L. Davidson, D. J. Kwiatkowski, T. Kirchhausen, S. H. Orkin, F. S. Rosen, B. J. Mayer, M. W. Kirschner, and F. W. Alt. 2000. Cdc42 is required for PIP(2)-induced actin polymerization and early development but not for cell viability. *Curr Biol* 10: 758-765.
55. Lee, S. H., and R. Dominguez. 2010. Regulation of actin cytoskeleton dynamics in cells. *Molecules and cells* 29: 311-325.

56. Carlier, M. F., A. Ducruix, and D. Pantaloni. 1999. Signalling to actin: the Cdc42-N-WASP-Arp2/3 connection. *Chem Biol* 6: R235-240.
57. Miki, H., and T. Takenawa. 2003. Regulation of actin dynamics by WASP family proteins. *J Biochem* 134: 309-313.
58. Block, J., D. Breitsprecher, S. Kuhn, M. Winterhoff, F. Kage, R. Geffers, P. Duwe, J. L. Rohn, B. Baum, C. Brakebusch, M. Geyer, T. E. Stradal, J. Faix, and K. Rottner. 2012. FMNL2 drives actin-based protrusion and migration downstream of Cdc42. *Curr Biol* 22: 1005-1012.
59. Tatin, F., C. Varon, E. Genot, and V. Moreau. 2006. A signalling cascade involving PKC, Src and Cdc42 regulates podosome assembly in cultured endothelial cells in response to phorbol ester. *J Cell Sci* 119: 769-781.
60. Etienne-Manneville, S. 2004. Cdc42--the centre of polarity. *J Cell Sci* 117: 1291-1300.
61. Pulecio, J., J. Petrovic, F. Prete, G. Chiaruttini, A. M. Lennon-Dumenil, C. Desdouets, S. Gasman, O. R. Burrone, and F. Benvenuti. 2010. Cdc42-mediated MTOC polarization in dendritic cells controls targeted delivery of cytokines at the immune synapse. *The Journal of experimental medicine* 207: 2719-2732.
62. Kardon, J. R., and R. D. Vale. 2009. Regulators of the cytoplasmic dynein motor. *Nat Rev Mol Cell Biol* 10: 854-865.
63. Hirokawa, N., Y. Noda, Y. Tanaka, and S. Niwa. 2009. Kinesin superfamily motor proteins and intracellular transport. *Nat Rev Mol Cell Biol* 10: 682-696.
64. Schuh, M. 2011. An actin-dependent mechanism for long-range vesicle transport. *Nature cell biology* 13: 1431-1436.
65. Steele-Mortimer, O., L. A. Knodler, and B. B. Finlay. 2000. Poisons, ruffles and rockets: bacterial pathogens and the host cell cytoskeleton. *Traffic (Copenhagen, Denmark)* 1: 107-118.
66. Sansonetti, P. 2002. Host-pathogen interactions: the seduction of molecular cross talk. *Gut* 50 Suppl 3: III2-8.
67. Boquet, P., and E. Lemichez. 2003. Bacterial virulence factors targeting Rho GTPases: parasitism or symbiosis? *Trends Cell Biol* 13: 238-246.
68. Swetman, C. A., Y. Leverrier, R. Garg, C. H. Gan, A. J. Ridley, D. R. Katz, and B. M. Chain. 2002. Extension, retraction and contraction in the formation of a dendritic cell dendrite: distinct roles for Rho GTPases. *Eur J Immunol* 32: 2074-2083.
69. Jaksits, S., W. Bauer, E. Kriehuber, M. Zeyda, T. M. Stulnig, G. Stingl, E. Fiebiger, and D. Maurer. 2004. Lipid raft-associated GTPase signaling controls morphology and CD8+ T cell stimulatory capacity of human dendritic cells. *J Immunol* 173: 1628-1639.

70. Burns, S., A. J. Thrasher, M. P. Blundell, L. Machesky, and G. E. Jones. 2001. Configuration of human dendritic cell cytoskeleton by Rho GTPases, the WAS protein, and differentiation. *Blood* 98: 1142-1149.
71. Shurin, G. V., I. L. Tourkova, G. S. Chatta, G. Schmidt, S. Wei, J. Y. Djeu, and M. R. Shurin. 2005. Small rho GTPases regulate antigen presentation in dendritic cells. *J Immunol* 174: 3394-3400.
72. Garrett, W. S., L. M. Chen, R. Kroschewski, M. Ebersold, S. Turley, S. Trombetta, J. E. Galan, and I. Mellman. 2000. Developmental control of endocytosis in dendritic cells by Cdc42. *Cell* 102: 325-334.
73. Benninger, Y., T. Thurnherr, J. A. Pereira, S. Krause, X. Wu, A. Chrostek-Grashoff, D. Herzog, K. A. Nave, R. J. M. Franklin, D. Meijer, C. Brakebusch, U. Suter, and J. B. Relvas. 2007. Essential and distinct roles for cdc42 and rac1 in the regulation of Schwann cell biology during peripheral nervous system development. *J Cell Biol* 177: 1051-1061.
74. Wu, X., F. Quondamatteo, T. Lefever, A. Czuchra, H. Meyer, A. Chrostek, R. Paus, L. Langbein, and C. Brakebusch. 2006. Cdc42 controls progenitor cell differentiation and beta-catenin turnover in skin. *Genes Dev* 20: 571-585.
75. Nolen, B. J., N. Tomasevic, A. Russell, D. W. Pierce, Z. Jia, C. D. McCormick, J. Hartman, R. Sakowicz, and T. D. Pollard. 2009. Characterization of two classes of small molecule inhibitors of Arp2/3 complex. *Nature* 460: 1031-1034.
76. Drose, S., and K. Altendorf. 1997. Bafilomycins and concanamycins as inhibitors of V-ATPases and P-ATPases. *J Exp Biol* 200: 1-8.
77. Savina, A., C. Jancic, S. Hugues, P. Guermonprez, P. Vargas, I. C. Moura, A. M. Lennon-Dumenil, M. C. Seabra, G. Raposo, and S. Amigorena. 2006. NOX2 controls phagosomal pH to regulate antigen processing during crosspresentation by dendritic cells. *Cell* 126: 205-218.
78. Cooper, J. A. 1987. Effects of cytochalasin and phalloidin on actin. *J Cell Biol* 105: 1473-1478.
79. Morton, W. M., K. R. Ayscough, and P. J. McLaughlin. 2000. Latrunculin alters the actin-monomer subunit interface to prevent polymerization. *Nature cell biology* 2: 376-378.
80. Coue, M., S. L. Brenner, I. Spector, and E. D. Korn. 1987. Inhibition of actin polymerization by latrunculin A. *FEBS Lett* 213: 316-318.
81. Lee, J. C., D. J. Field, and L. L. Lee. 1980. Effects of nocodazole on structures of calf brain tubulin. *Biochemistry* 19: 6209-6215.
82. von Kleist, L., W. Stahlschmidt, H. Bulut, K. Gromova, D. Puchkov, M. J. Robertson, K. A. MacGregor, N. Tomilin, A. Pechstein, N. Chau, M. Chircop, J. Sakoff, J. P. von Kries, W. Saenger, H. G. Krausslich, O. Shupliakov, P. J. Robinson, A. McCluskey, and V. Haucke. 2011. Role of the clathrin terminal domain in regulating coated pit dynamics revealed by small molecule inhibition. *Cell* 146: 471-484.

83. Rizvi, S. A., E. M. Neidt, J. Cui, Z. Feiger, C. T. Skau, M. L. Gardel, S. A. Kozmin, and D. R. Kovar. 2009. Identification and characterization of a small molecule inhibitor of formin-mediated actin assembly. *Chem Biol* 16: 1158-1168.
84. Klein, E. 2005. CD83 localization in a recycling compartment of immature human monocyte-derived dendritic cells. *International Immunology* 17: 477-487.
85. Shimada, I., K. Matsui, R. Iida, E. Tsubota, and T. Matsuki. 2009. Time course of housekeeping gene expression changes in diffuse alveolar damage induced by hyperoxia exposure in mice. *Leg Med (Tokyo)* 11 Suppl 1: S151-154.
86. Abramoff, M. D., P. J. Magalhaes, and S. J. Ram. 2004. Image Processing with ImageJ. *Biophotonics International* 11: 36-42.
87. Wisniewski, J. R., A. Zougman, and M. Mann. 2009. Combination of FASP and StageTip-based fractionation allows in-depth analysis of the hippocampal membrane proteome. *J Proteome Res* 8: 5674-5678.
88. Wisniewski, J. R., A. Zougman, N. Nagaraj, and M. Mann. 2009. Universal sample preparation method for proteome analysis. *Nat Methods* 6: 359-362.
89. Cox, J., and M. Mann. 2008. MaxQuant enables high peptide identification rates, individualized p.p.b.-range mass accuracies and proteome-wide protein quantification. *Nat Biotechnol* 26: 1367-1372.
90. Cox, J., N. Neuhauser, A. Michalski, R. A. Scheltema, J. V. Olsen, and M. Mann. 2011. Andromeda: a peptide search engine integrated into the MaxQuant environment. *J Proteome Res* 10: 1794-1805.
91. Caton, M. L., M. R. Smith-Raska, and B. Reizis. 2007. Notch-RBP-J signaling controls the homeostasis of CD8- dendritic cells in the spleen. *The Journal of experimental medicine* 204: 1653-1664.
92. Yuseff, M. I., A. Reversat, D. Lankar, J. Diaz, I. Fanget, P. Pierobon, V. Randrian, N. Larochette, F. Vascotto, C. Desdouets, B. Jauffred, Y. Bellaiche, S. Gasman, F. Darchen, C. Desnos, and A. M. Lennon-Dumenil. 2011. Polarized secretion of lysosomes at the B cell synapse couples antigen extraction to processing and presentation. *Immunity* 35: 361-374.
93. Benvenuti, F., S. Hugues, M. Walmsley, S. Ruf, L. Fetler, M. Popoff, V. L. Tybulewicz, and S. Amigorena. 2004. Requirement of Rac1 and Rac2 expression by mature dendritic cells for T cell priming. *Science (New York, N.Y.)* 305: 1150-1153.
94. Watts, C. 2004. The exogenous pathway for antigen presentation on major histocompatibility complex class II and CD1 molecules. *Nat Immunol* 5: 685-692.
95. Conde, C., and A. Caceres. 2009. Microtubule assembly, organization and dynamics in axons and dendrites. *Nat Rev Neurosci* 10: 319-332.

96. Forgac, M. 2007. Vacuolar ATPases: rotary proton pumps in physiology and pathophysiology. *Nat Rev Mol Cell Biol* 8: 917-929.
97. Campellone, K. G., and M. D. Welch. 2010. A nucleator arms race: cellular control of actin assembly. *Nat Rev Mol Cell Biol* 11: 237-251.
98. Schwartz, O., V. Marechal, S. Le Gall, F. Lemonnier, and J. M. Heard. 1996. Endocytosis of major histocompatibility complex class I molecules is induced by the HIV-1 Nef protein. *Nature medicine* 2: 338-342.
99. Shinya, E., A. Owaki, M. Shimizu, J. Takeuchi, T. Kawashima, C. Hidaka, M. Satomi, E. Watari, M. Sugita, and H. Takahashi. 2004. Endogenously expressed HIV-1 nef down-regulates antigen-presenting molecules, not only class I MHC but also CD1a, in immature dendritic cells. *Virology* 326: 79-89.
100. Collins, K. L., B. K. Chen, S. A. Kalams, B. D. Walker, and D. Baltimore. 1998. HIV-1 Nef protein protects infected primary cells against killing by cytotoxic T lymphocytes. *Nature* 391: 397-401.
101. Quaranta, M. G., B. Mattioli, F. Spadaro, E. Straface, L. Giordani, C. Ramoni, W. Malorni, and M. Viora. 2003. HIV-1 Nef triggers Vav-mediated signaling pathway leading to functional and morphological differentiation of dendritic cells. *FASEB journal : official publication of the Federation of American Societies for Experimental Biology* 17: 2025-2036.
102. Stumptner-Cuvelette, P., S. Morchoisne, M. Dugast, S. Le Gall, G. Raposo, O. Schwartz, and P. Benaroch. 2001. HIV-1 Nef impairs MHC class II antigen presentation and surface expression. *Proceedings of the National Academy of Sciences of the United States of America* 98: 12144-12149.
103. Toussaint, H., F. X. Gobert, M. Schindler, C. Banning, P. Kozik, M. Jouve, F. Kirchhoff, and P. Benaroch. 2008. Human immunodeficiency virus type 1 nef expression prevents AP-2-mediated internalization of the major histocompatibility complex class II-associated invariant chain. *J Virol* 82: 8373-8382.
104. Nikolic, D. S., M. Lehmann, R. Felts, E. Garcia, F. P. Blanchet, S. Subramaniam, and V. Piguet. 2011. HIV-1 activates Cdc42 and induces membrane extensions in immature dendritic cells to facilitate cell-to-cell virus propagation. *Blood* 118: 4841-4852.
105. West, M. A., R. P. Wallin, S. P. Matthews, H. G. Svensson, R. Zaru, H. G. Ljunggren, A. R. Prescott, and C. Watts. 2004. Enhanced dendritic cell antigen capture via toll-like receptor-induced actin remodeling. *Science (New York, N.Y.)* 305: 1153-1157.
106. Kamon, H., T. Kawabe, H. Kitamura, J. Lee, D. Kamimura, T. Kaisho, S. Akira, A. Iwamatsu, H. Koga, M. Murakami, and T. Hirano. 2006. TRIF-GEFH1-RhoB pathway is involved in MHCII expression on dendritic cells that is critical for CD4 T-cell activation. *The EMBO journal* 25: 4108-4119.

107. Yanagawa, Y., and K. Onoe. 2003. CCR7 ligands induce rapid endocytosis in mature dendritic cells with concomitant up-regulation of Cdc42 and Rac activities. *Blood* 101: 4923-4929.
108. Ohl, L., M. Mohaupt, N. Czeloth, G. Hintzen, Z. Kiafard, J. Zwirner, T. Blankenstein, G. Henning, and R. Forster. 2004. CCR7 governs skin dendritic cell migration under inflammatory and steady-state conditions. *Immunity* 21: 279-288.
109. West, M. A., A. R. Prescott, E. L. Eskelinen, A. J. Ridley, and C. Watts. 2000. Rac is required for constitutive macropinocytosis by dendritic cells but does not control its downregulation. *Curr Biol* 10: 839-848.
110. Burgdorf, S., A. Kautz, V. Bohnert, P. A. Knolle, and C. Kurts. 2007. Distinct pathways of antigen uptake and intracellular routing in CD4 and CD8 T cell activation. *Science (New York, N.Y.)* 316: 612-616.
111. Dudziak, D., A. O. Kamphorst, G. F. Heidkamp, V. R. Buchholz, C. Trumfheller, S. Yamazaki, C. Cheong, K. Liu, H. W. Lee, C. G. Park, R. M. Steinman, and M. C. Nussenzweig. 2007. Differential antigen processing by dendritic cell subsets in vivo. *Science (New York, N.Y.)* 315: 107-111.
112. Mykkanen, O. M., M. Gronholm, M. Ronty, M. Lalowski, P. Salmikangas, H. Suila, and O. Carpen. 2001. Characterization of human palladin, a microfilament-associated protein. *Mol Biol Cell* 12: 3060-3073.
113. Dugast, M., H. Toussaint, C. Dousset, and P. Benaroch. 2005. AP2 clathrin adaptor complex, but not AP1, controls the access of the major histocompatibility complex (MHC) class II to endosomes. *J Biol Chem* 280: 19656-19664.
114. McCormick, P. J., J. A. Martina, and J. S. Bonifacino. 2005. Involvement of clathrin and AP-2 in the trafficking of MHC class II molecules to antigen-processing compartments. *Proceedings of the National Academy of Sciences of the United States of America* 102: 7910-7915.
115. Barois, N., F. Forquet, and J. Davoust. 1998. Actin microfilaments control the MHC class II antigen presentation pathway in B cells. *J Cell Sci* 111 ( Pt 13): 1791-1800.
116. Bromme, D., A. Steinert, S. Friebe, S. Fittkau, B. Wiederanders, and H. Kirschke. 1989. The specificity of bovine spleen cathepsin S. A comparison with rat liver cathepsins L and B. *The Biochemical journal* 264: 475-481.
117. Shi, G. P., J. S. Munger, J. P. Meara, D. H. Rich, and H. A. Chapman. 1992. Molecular cloning and expression of human alveolar macrophage cathepsin S, an elastinolytic cysteine protease. *J Biol Chem* 267: 7258-7262.
118. Bonifacino, J. S., and L. M. Traub. 2003. Signals for sorting of transmembrane proteins to endosomes and lysosomes. *Annual review of biochemistry* 72: 395-447.

119. Hirst, J., D. A. Sahlender, M. Choma, R. Sinka, M. E. Harbour, M. Parkinson, and M. S. Robinson. 2009. Spatial and functional relationship of GGAs and AP-1 in *Drosophila* and HeLa cells. *Traffic (Copenhagen, Denmark)* 10: 1696-1710.
120. Lemmon, S. K., and L. M. Traub. 2012. Getting in Touch with the Clathrin Terminal Domain. *Traffic (Copenhagen, Denmark)*.
121. Dutta, D., C. D. Williamson, N. B. Cole, and J. G. Donaldson. 2012. Pitstop 2 is a potent inhibitor of clathrin-independent endocytosis. *PLoS One* 7: e45799.
122. Carreno, S., A. E. Engqvist-Goldstein, C. X. Zhang, K. L. McDonald, and D. G. Drubin. 2004. Actin dynamics coupled to clathrin-coated vesicle formation at the trans-Golgi network. *J Cell Biol* 165: 781-788.
123. Boulant, S., C. Kural, J. C. Zeeh, F. Ubelmann, and T. Kirchhausen. 2011. Actin dynamics counteract membrane tension during clathrin-mediated endocytosis. *Nature cell biology* 13: 1124-1131.
124. Kamphorst, A. O., P. Guermonprez, D. Dudziak, and M. C. Nussenzweig. 2010. Route of antigen uptake differentially impacts presentation by dendritic cells and activated monocytes. *J Immunol* 185: 3426-3435.
125. Kamath, A. T., S. Henri, F. Battye, D. F. Tough, and K. Shortman. 2002. Developmental kinetics and lifespan of dendritic cells in mouse lymphoid organs. *Blood* 100: 1734-1741.
126. Backlund, P. S., Jr. 1997. Post-translational processing of RhoA. Carboxyl methylation of the carboxyl-terminal prenylcysteine increases the half-life of RhoA. *J Biol Chem* 272: 33175-33180.

## 10 PUBLICATIONS

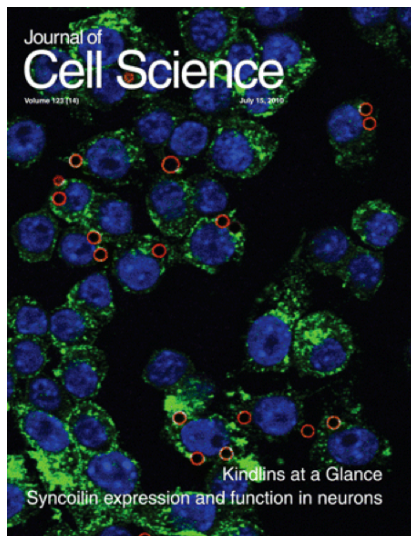
**Schulz, A.** et al. Rho GTPase Cdc42 controls invariant chain processing and MHC II loading in Dendritic Cells. Manuscript in preparation.

Luckashenak, N.\*, **Wähe, A.\***, Breit, K., Brakebusch, C., Brocker, T. 2013. Rho-family GTPase Cdc42 controls migration of Langerhans cells *in vivo*. *J Immunol.* 190:27-35. \*equal contribution

**Obtained during master thesis at the EMBL in Heidelberg, Germany:**

**Wähe, A.**, Kasmapour, B., Schmaderer, C., Liebl, D., Sandhoff, K., Nykjaer, A., Griffiths, G., Gutierrez, M.G. 2010. Golgi-to-phagosome transport of acid sphingomyelinase and prosaposin is mediated by sortilin. *J Cell Sci.* 123:2502-11.

**Including Cover**



## 11 ACKNOWLEDGMENTS

Prof. Dr. Thomas Brocker danke ich für die Bereitstellung des Projektes, sowie zahlreiche Gespräche und Diskussionen, die neue Denkanstöße gaben und oft richtungsweisend waren. Gleichzeitig danke ich ihm für sein Vertrauen in meine wissenschaftliche Arbeit und die finanzielle Freiheit, wodurch ein selbstständiges und kreatives Arbeiten ermöglicht wurde.

Prof. Dr. Stefan Lichtenthaler und Sebastian Hogl vom *German Center for Neurodegenerative Diseases (DZNE)* in München danke ich für die Zusammenarbeit und die tollen Ergebnisse, die im Rahmen unserer Kooperation entstanden sind. Auch möchte ich Prof. Dr. Axel Imhof und Dr. Ignasi Forné danken für eine anfängliche Analyse des Proteoms unserer Zellen.

Jan Kranich danke ich für die Korrektur meiner Arbeit, sowie seine konstruktiven Verbesserungsvorschläge.

Special thanks go to Nancy Luckashenak, who supported me during the first year and contributed to my project by teaching me methods and sharing her scientific ideas. Also, I thank her for critically reading and correcting the manuscript.

Andrea Bol danke ich für die exzellente Pflege der Tiere, Christine Ried für den reibungslosen Ablauf im Labor und ihre Hilfe wann immer sie benötigt wurde. Katharina Breit danke ich für ihre Unterstützung bei zahlreichen Experimenten und dem Genotypisieren der Mäuse. Auch Céline Leroy danke ich für ihre Unterstützung und für informative Gespräche über DC Subtypen in der Haut.

Ganz besonders danke ich Stefan Schulz dafür, dass er mir den Rücken freigehalten hat und immer für mich da war.